Dissertation

EVALUATION AND COUNTERMEASURE EFFECTIVENESS OF CONCRETE STRUCTURES DETERIORATED BY ALKALI-SILICA REACTION AND DE-ICING SALTS

Graduate School of

Natural Science & Technology

Kanazawa University

Division of Environmental Design

Student ID No. 1624052007

Name: Ho Hong Sao

Chief advisor: Assoc. Prof. Yoshimori Kubo

Date of Submission: January, 2019

AKNOWLEDGEMENTS

The author wishes to thank the people, who directly or indirectly contributed to research in this dissertation. Firstly, I want to express my appreciation to my academic supervisor Assoc. Prof. Kubo Yoshimori, who spent countless hours of his working time with me to do research and sole may academic problems with his ample knowledge. Not only in research, but also in daily life, our family was full-filled with the warmest concern.

Secondly, my thesis would be unable to complete without many experiments by cooperating companies and distinguished researchers. I would like to thank my colleagues, other students in my laboratory who help me to do experiments.

Thirdly, I want to thank the Vietnamese Government for financial support in spite of many difficulties. During the period of 3 years living and studying in Japan, many Japanese people and friends have indicated that my choice in Kanazawa city and study in Kanazawa University could not be better. I appreciate their support and share all the unforgettable memory.

Last, but not least, I want to thank my family for their endless love and support, especially, my beloved daughter.

CONTENTS

FIGURES

TABLES

ABSTRACT

Currently, in Japan, many concrete structures that had been constructed during the high economic growth period (from the 1960s to the 1980s) are being deteriorated or damaged due to the Alkali-Silica Reaction (ASR). In particular, many concrete works such as roads, bridges, tunnels, etc., along the highway, which are located in snowy areas, are often affected by de-icing salts sprayed in the winter to ensure the safety of vehicles. As a result, many reinforced concrete structures have been suffering from ASR and chloride attack due to de-icing salts. This combined deterioration mechanism is complicated and influenced by many factors such as the quantity of reactive aggregates, sufficient content of alkali in cement, moisture of concrete, content of water leakage included de-icing salts, etc. Therefore, the standard of repair and maintenance for this combined deterioration of concrete structure has not been established yet.

From the practical point of view, this study was conducted to evaluate the actual stage of concrete members, the effectiveness of applied countermeasures for ASR-deteriorated concrete structures affected by de-icing salts (chloride attack). Several road bridges are located in the Hokuriku region in Japan, which have been affected significantly by ASR and de-icing salts, are selected as target subjects of this study.

The main result of this study shows that the risk of steel corrosion tends to increase when concrete structures have been deteriorated by ASR and de-icing salts because cracking caused by ASR expansion becomes a significant reason for the penetration of chloride, moisture, and oxygen. Furthermore, steel corrosion could occur when the countermeasures such as patching and surface treatment were conducted. The evaluation of the steel corrosion risk regarding surface moisture and surface chloride ions contents of concrete showed reliable results.

CHAPTER 1 INTRODUCTION

1.1 The deterioration of concrete structures and present maintenance methods

Through the period of high economic growth (from the 1960s to the 1980s) in Japan, an enormous number of works had been constructed such as roads, tunnels and bridges. These structures were considered durable and maintenance-free at that time. However, many concrete structures were deteriorated due to chloride-induced corrosion, alkali-silica reaction (ASR), carbonation, frost attack, etc. Therefore, appropriate maintenances are necessary applied to satisfy the economic and performance requirements during the service period of these structures. The diagnosis and prediction of deterioration mechanisms are essential for application of appropriate maintenance. The deterioration mechanisms, factors, phenomena and indexes of concrete structures are shown in **Table 1.1** (JSCE. 2010).

Effective repair methods can be changed due to various deterioration mechanisms, thus, it is necessary to assess accurately the factors and degree of deterioration when applying remedial measures. **Table 1.2** shows principles, components of repair or strengthening methods and factors to be considered for required performance of each deterioration mechanism (JSCE. 2010).

Depending on properties of materials and/or working conditions, environmental factors that cause combined deterioration of concrete structures, the deterioration mechanism becomes complicated and causes of this phenomenon are diversified. Although many researchers are being studied in concrete structures affected by a combination of two or more deterioration mechanisms, repair and strengthening methods to deal with these phenomena have not been established at present.

Table 1.1 Mechanism, causes, phenomena and indexes of deterioration (JSCE. 2010)

Deterioration mechanism	Deterioration factor	Phenomenon of deterioration	Examples of deterioration index
Carbonation	Carbon dioxide	The decrease of pH in pore solution due to the chemical reaction between carbon dioxide and cement hydrate induces the corrosion of steel and it causes the cracking or peeling of concrete or reducing the cross-section of steel	Depth of carbonation Amount of steel corrosion Corrosion - crack
Chloride-induced corrosion	Chloride ions	Corrosion of steel in concrete is induced by chloride ions and it causes the cracking or peeling of concrete or reducing the cross-section of steel	The concentration of chloride ion Amount of steel corrosion Corrosion - crack
Frost attacks	Freezing and thawing	Freezing and thawing of water in concrete causes deterioration of the concrete surface, e.g., scaling, micro cracks and pop-outs	Depth of frost deterioration Amount of steel corrosion
Chemical attacks	Acidic substances Sulfate ions	Hardened concrete in contact with acidic substances or sulfate ions is dissolved, or concrete deteriorates due to the expansion pressure due to the formation of chemical substances	Depth of penetration of deleterious substances Depth of carbonation Amount of steel corrosion
Alkali-silica reaction	Reactive aggregates	Reactive silicate minerals contained in aggregates or carbonate rocks chemically combine with pore solution whose pH is high and it causes irregular expansion or cracking in concrete	Degree of expansion (cracking)
Fatigue of deck slab	Volume of traffic of large vehicles	Cycle wheel loading on highway bridge decks causes cracking or caving-in of reinforced concrete	Density of cracks Deflection
Fatigue of beam member	Cyclic loading	Cyclic loading on railway bridge causes cracking in tensile steel reinforcements in beams and it leads to fracture of steel reinforcement	Cumulative damage Lengths of cracks in steel
Abrasion	Wearing	Wearing by flowing water or wheel causes the loss of concrete gradually with time	Amount of abrasion Rate of abrasion

Table 1.2 Principles of repair methods due to deterioration mechanism (JSCE. 2010)

Deterioration mechanism	Principle of repair	Components of repair methods	Factors to be considered for meeting required performances
Carbonation	-Remove concrete in which carbonation occurred -Control the infiltration of CO^2 and water after repair	-Patching -Surface treatment -Re-alkalization	-Degree of removal of sections of concrete in which carbonation occurred -Prevention of corrosion of reinforcing bars -Quality of minerals for patching -Quality and thickness of materials for surface treatment -Alkali amount in concrete
Chloride attack	-Remove Cl- that intruded -Control the permeation of Cl-, water, and oxygen after repair	-Patching -Surface treatment -Desalination	-Degree of removal of sections subjected to permeation -Prevention of corrosion of reinforcing bars -Quality of materials for patching -Quality and thickness of materials for surface treatment
	Potential control for reinforcing bars	-Anode materials -Electric power unit	-Quality of anode materials -Amount of polarization
Frost attacks	-Remove deteriorated concrete -Control water infiltration after repair -Improve the resistance of concrete to freezing and thawing	-Patching -Crack injection -Surface treatment	-Resistance of patching materials to freezing and thawing -Prevention of corrosion of reinforcing bars -Materials and method for crack injection -Quality and thickness materials for surface treatment
Chemical attacks	-Remove deteriorated concrete -Control the permeation of hazardous substances	-Patching -Surface treatment	-Quality of materials for patching -Quality and thickness materials for surface treatment -Degree of removal of deteriorated concrete
Alkali-silica reaction	-Control water supplies -Accelerating the diffusion of internal water -Control alkali supplies -Control expansion -Restore member stiffness	-Water treatment (starling and drainage) -Crack injection -Surface treatment -Jacketing	-Materials and method for crack injection -Quality and thickness materials for surface treatment
Fatigue of deck slab	-Control the progress of cracking -Restore member stiffness -Restore shearing load bearing capacity	-Water treatment (drainage) -Waterproofing of deck slabs -Adhesion -Increase of thickness	-Integration with existing concrete members
Abrasion	- Restore lost cross section - Restore or improve roughness coefficient	- Patching - Surface treatment	-Quality of materials for patching -Bond -Resistance to abrasion -Roughness coefficient

1.2 Alkali-silica reaction (ASR) and countermeasures for ASR in concrete

1.2.1 ASR deterioration mechanism

Alkali-silica reaction is a chemical reaction between the alkali present (Na_2O and K_2O) in pore solution of concrete that reacts with reactive silica minerals in some types of fine and/or coarse aggregates and produces the alkali-silica gel in concrete (Bauer et al. 2006). This gel can absorb moisture and swell inside concrete, which results in the expansion of hardened concrete and the mechanical deterioration of concrete materials. ASR process can be summarized in two main steps:

Step 1: Alkali + Silica → ASR gel product

Step 2: Gel product + Moisture → ASR expansion

About the chemistry of this reaction, the presence of a high concentration of hydroxyl ions (OH-), silanol groups ($\equiv$Si-OH) and siloxane groups ($\equiv$Si-O-Si$\equiv$) tend to dissolve by neutralization reaction, then the silanol and siloxane bridges are broken. The negative charges Si-O- ions attract positive charges such as sodium (Na+) and potassium (K+) which are abundant in concrete pore solution. The reactions can be summarized as follows (Glasser and Kataoka. 1981):

$$\equiv Si\text{-}OH + OH^- + Na^+ \rightarrow Si\text{-}O\text{-}Na + H_2O \qquad\qquad Eq\ 1.1$$

$$\equiv Si\text{-}O\text{-}Si \equiv\ + 2OH^- + 2Na^+ \rightarrow 2(Si\text{-}O\text{-}Na) + H_2O \qquad\qquad Eq\ 1.2$$
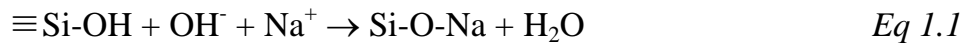
Figure 1.1 shows an illustration of alkali-silica reaction sequence (FHWA. 2013). The concrete pore solution is dominated by mainly of Na, K, and OH (minor amount of Ca). If silica in aggregate is reactive, the OH and then the Na, K will react with the SiO_2. A product of this reaction is the alkali-silica gel combined of Na, K, Ca and Si, and this gel forms around and within aggregates. Then, this gel absorbs water (moisture) from surrounding cement paste and expands. When the swelling pressure may exceed the tensile strength of the surround cement paste, it causes expansion and cracking of concrete.

According to the reaction mechanism described above, ASR can occur in concrete due to three major conditions (FHWA. 2013):

- A sufficient quantity of reactive silica (within aggregates)

- A sufficient concentration of alkali (primarily from Portland cement)

- Sufficient moisture

Thereby, based on specific conditions affected to ASR mechanism, the following proposals have been suggested as measures to suppress ASR expansion for concrete structures such as control the total amount of alkali in concrete, use of blended cement that has a suppressing effect, use of aggregate that is recognized safety, etc. (MLIT. 2002).
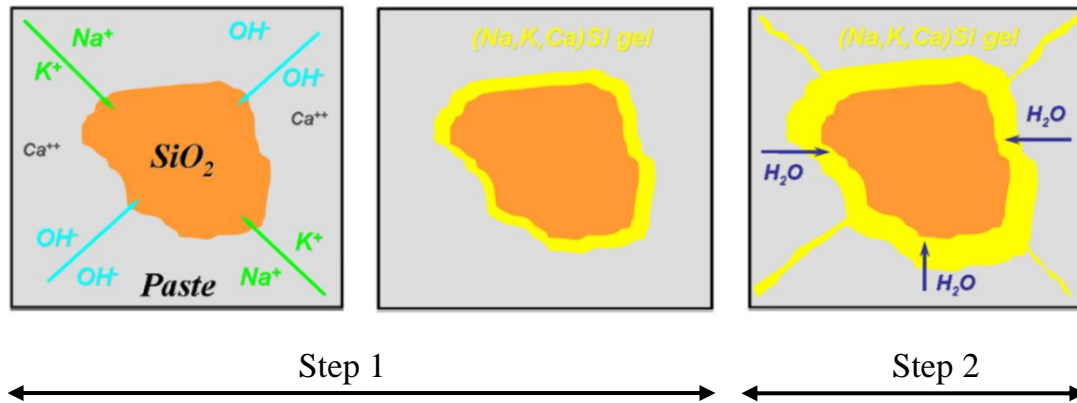
Figure 1.1 Alkali-Silica Reaction sequence (FHWA. 2013)

In Japan, many concrete structures such as tunnels and road bridges were built in the period of high economic growth and were deteriorated by alkali-silica reaction. The reason for ASR occurred in many regions could be considered by using reactive aggregate in the past. **Figure 1.2** shows the distribution of reactive aggregate in Japan. Some types of rock are reactive that could be used in concrete such as andesite, dacite, rhyolite, sandstone, chert, quartz schist, etc. (Wakizaka. 1999).
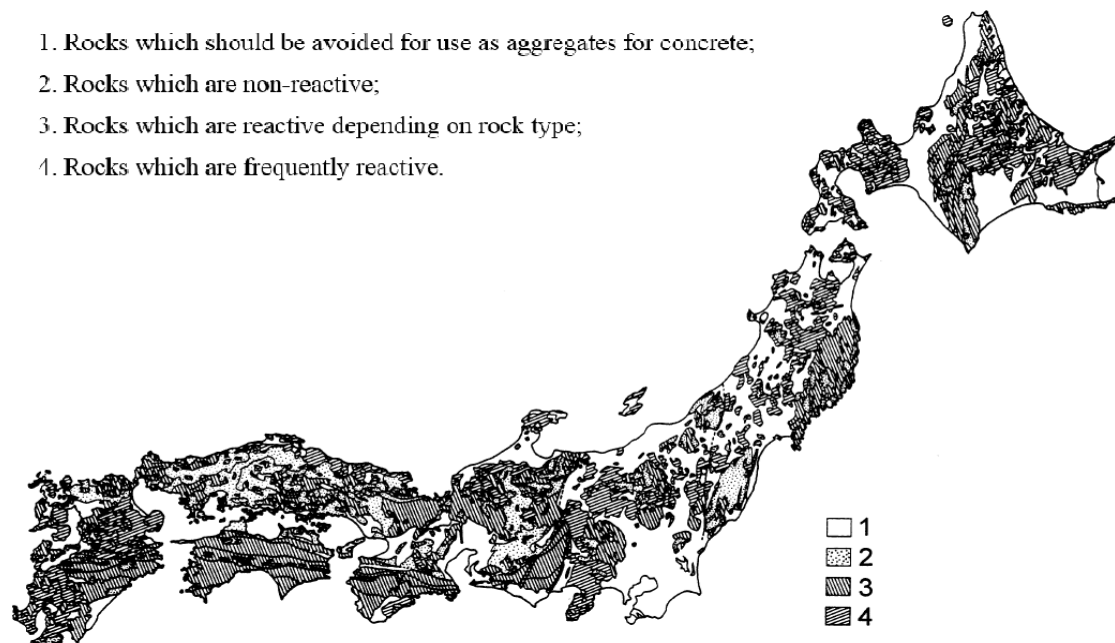
Figure 1.2 Distribution of reactive rocks in Japan (Wakizaka. 1999)

In addition, the complicated reaction mechanism and expansion progress depend on environmental conditions such as humidity, temperature, time of sunshine, moisture supply conditions, etc. For these reasons, it is difficult to predict the progress of expansion precisely, and at present, effective countermeasures that ensure sufficient effect for a long-term are not established. The ASR expansion causes cracks inside and on surface of concrete. When ASR expansion occurs and it is restrained properly, the load carrying capacity of concrete structures has not reduced significantly. However, many concrete structures suffered from remarkable deterioration due to excessive expansion of ASR have been reported (JSCE 2005). The deterioration or degradation caused by ASR requires detailed assessments about the performance of concrete structures and necessitates establish appropriate countermeasures for this deterioration. Therefore, many studies are being conducted to evaluate mechanical performance of reinforced concrete members and to establish diagnostic technical measures related to concrete structures deteriorated by ASR.

1.2.2 Countermeasures against ASR

The "countermeasures" in this dissertation refers to the repair and strengthening methods that are applied to ASR deteriorated concrete structures. When concrete structures have been affected by ASR, applied countermeasures should be decided based on the deteriorating state of concrete members and life cycle cost. Regarding the expected effects for ASR-deteriorated concrete, suitable countermeasures can be selected and classified as shown in **Table 1.3** (JSCE. 2010).

Table 1.3 Expected effects and countermeasures for ASR deteriorated concrete

Expected effect	Examples of countermeasures
Control of progress of ASR	Water control (cutoff, drainage), crack injection, surface treatment (covering, impregnation)
Retraining of ASR-induced expansion	Prestressing, steel/PC/FRP jacketing
Removal of the deteriorated portion	Cross-sectional restoration (Patching method)
Steel corrosion control	Crack injection, crack filling, surface treatment (covering, impregnation)
Elimination of third-party impact	Prevention of spalling
Restoration/enhancement of load-carrying capacity	Steel plate/FRP sheet bonding, prestressing, overlay, steel/PC/FRP jacketing, external tendon

For structures that have been deteriorating due to ASR, it is difficult to predict exactly ASR deterioration progress. Hence, the effective countermeasures for a long-term have not been established yet. The countermeasures commonly applied to concrete structures affected by ASR are crack injection, surface coating and patching, etc. These repair methods are primarily to prevent ASR expansion by restriction of moisture from the outside. However, ASR may still proceed even if moisture is blocked. In concrete structures such as bridge abutments, wing walls, etc., reinforcing bars inside may restrain somewhat the expansion. Nevertheless, these structures are normally affected by water leakage from expansion joints or water supplied from the backside of structures. In addition, depending on quantity of reactive silica in aggregate, the content of alkali in concrete and the water supply condition, expansion of concrete could continue for a long time and excessive expansion could occur.

Practically, appropriate method applied for ASR deteriorated concrete should be decided based on the current deteriorating state of structures due to ASR progress. The applicable countermeasures, which correspond with deterioration grades, are shown in **Table 1.4** (JSCE. 2010). Currently, some methods have been carried out on ASR-affected concrete structures. However, some of them might insufficient or fail to prevent the deterioration of structures due to some effective factors that cannot comprehend quite deeply. Therefore, the in-situ surveys are needed to assess actual situation and to consider the effectiveness of countermeasures after being applied to concrete structures.

Table 1.4 Degradation grade caused by ASR and examples of countermeasures

Grade of structural appearance	Stage of deterioration	Expected expansion	Standard countermeasures
I (initiation stage)	ASR-induced expansion and resultant cracking have not yet occurred, and there is no anomaly in appearance.	-	Water control (cutoff, drainage)
II (propagation stage)	Expansion occurs continuously in the presence of moisture and alkali, cracking occurs, and discoloration and alkali-silica gel bleeding can be seen. There is no rust water due to steel corrosion.	Small	Water control, crack injection, surface treatment (covering, impregnation), spalling prevention.
III (acceleration stage)	This is the stage which the rate of expansion due to ASR is maximized. Cracking occurs and cracks width and density increase. Rusty water due to steel corrosion may be seen.	Large	Water control, crack injection, surface treatment, prevention of spalling, cross-sectional restoration (patching), prestressing, steel plate/FRP sheet bonding, overlay, steel/PC/FRP jacketing, external tendon.
IV (deterioration stage)	Crack width and density increase further, and localized surface unevenness, displacement and localized scaling and spalling occur. Steel corrosion continues and rusty water can be seen. Cracks or steel damage due to environmental deterioration factors may be seen. Displacement and deformation increase.	Small	Water control, surface treatment (covering), prevention of spalling, cross-sectional restoration (patching), prestressing, steel plate/FRP sheet bonding, overlay, steel/PC/FRP jacketing, external tendon.

1.3 Chloride attack and its countermeasures

1.3.1 Deterioration due to chloride attack

Chloride attack is a deterioration phenomenon that occurs in reinforced concrete structures. Steel corrosion has been progressing in concrete due to the existence of chloride ions. This phenomenon causes the cracking or spalling in concrete or the reduction of steel bar section. Chloride ions are mainly supplied from external environments such as seawater and de-icing salt sprayed in snowy areas or from material used in concrete. In Japan, all sides are surrounded by the ocean and many regions are located in snowy areas. Thus, chloride attack is considered as one of common deterioration phenomena in concrete structures.

Normally, reinforcing steel bar in concrete is embedded in the passive state due to high alkalinity of the pore solution (pH is about 12 or higher) which enables for the formation of a protective passivity layer (passive film) on steel surface. However, corrosion of steel occurs if this passive film is destroyed due to the decrease in pH values of concrete, the increase in chloride ion concentration and the presence of water and oxygen. In addition, the corrosion products (brown/red rust) occupy a volume several times larger than original steel. The resulted expansive stresses in concrete can cause cracking, spalling, or delamination. Then, the cross-sectional area of steel bars can be reduced as the corrosion proceeds. This phenomenon results in a significant reduction of load carrying capacity of concrete structures.

1.3.2 Mechanism of chloride-induced corrosion

In general, the passive film strongly adheres to embedded steel and prevents it from corrosion in the highly alkaline environment condition. Therefore, if concrete structures have a good quality without cracks, the steel corrosion does not occur even in a marine environment. However, depending on the quality of concrete structures and the impact of the surrounding environment, chloride ions (Cl-) content of the vicinity of reinforcing bars could reach or exceed the threshold limit of corrosion occurrence. Hence, this passive film existed on the surface of reinforcing bars is damaged and the corrosion occurs.

The process of chloride-induced corrosion phenomenon can be described as follows. An electrochemical cell is established when the difference of electrical potential occurs along reinforcing bars in concrete. This cell includes anodic,

cathodic parts and they are connected by the electrolyte in pore water in hardened cement paste. The reactions of steel corrosion are shown as follows (Neville. 1995):

+ <u>Anode reaction</u>: $Fe \rightarrow Fe^{2+} + 2e^-$ (*oxidation*)   *Eq 1.3*

$Fe^{2+} + 2OH^- \rightarrow Fe(OH)_2$ (*ferrous hydroxide*)   *Eq 1.4*

$4Fe(OH)_2 + 2H_2O + O_2 \rightarrow 4Fe(OH)_3$ (*ferric hydroxide*)   *Eq 1.5*

+ <u>Cathodic reaction</u>: $4e^- + O_2 + 2H_2O \rightarrow 4OH^-$ (*reduction*)   *Eq 1.6*

Then, the ferric hydroxide is converted by further oxidation to form the rust ($Fe_2O_3.3H_2O$). These reactions indicate that steel corrosion can occur when a large content of oxygen and moisture permeated into concrete. The relative humidity (RH), that is the most susceptible to corrosion, is from 70% to 80%. Corrosion could be limited in dry concrete that had RH less than 60% and concrete was immersed fully in water that resulted in the lack of oxygen (Neville. 1995).

Chloride ions in reinforced concrete structures can be supplied from two main sources that incorporated in mixing concrete due to contaminated aggregate, seawater, admixtures containing chlorides and/or penetrated into concrete from outside such as seawater, de-icing salt spraying, etc. Corrosion can be occurred due to the breakdown of passive film surrounded reinforcing bars. Chloride ions become a factor to activate the surface of steel bars to form an anode and passive film is being the cathode. This reaction can be described as follows (Neville. 1995):

$Fe^{2+} + 2Cl^- \rightarrow FeCl_2$ *Eq 1.7*

$FeCl_2 + 2H_2O \rightarrow Fe(OH)_2 + 2\ HCl$ *Eq 1.8*

Although the role of chloride-induced corrosion is not yet fully understood, it is considered that process of corrosion in reinforced concrete structures can be schematically represented by **Figure 1.3** (Silva. 2013).
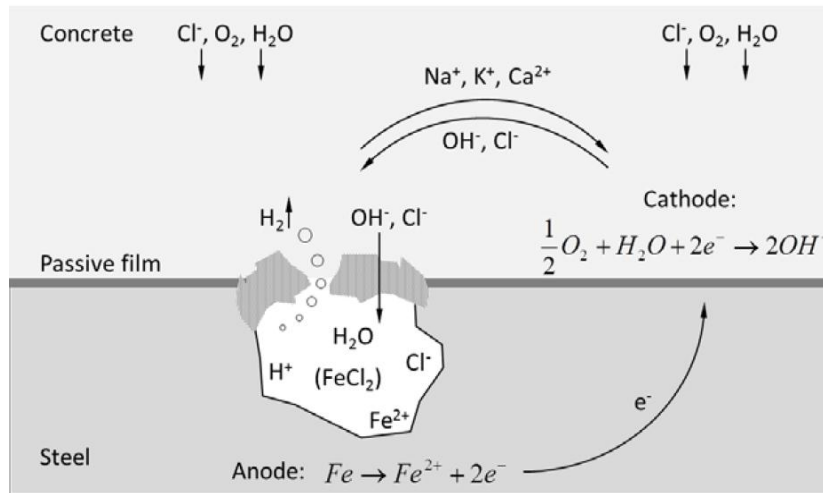
Figure 1.3 Schematic representation of chloride-induced corrosion *(Silva. 2013)*

1.3.3 Factors influencing chloride attack

In general, some factors, such as chloride ions, oxygen, and moisture contents are directly related to the corrosion as mentioned above. Additionally, other factors such as quality and design of concrete, construction progress, and environmental conditions are related to the penetration of chloride, oxygen, and moisture in concrete. Therefore, corrosion of steel can occur and proceed.

1.3.3.1 Chloride ions

Problem of chloride-induced corrosion is usually serious when chloride content attack from outside. When chloride ions penetrate into the depth of reinforcing bars, the passive film can be broken down and it leads to steel corrosion. Sources of chloride ions are supplied from seawater that contacts with concrete, the airborne very fine droplets of seawater carried by wind, and de-icing salts spraying. Chloride attack also occurs if a large content of chloride ions exists in concrete materials such as sea-sand and cement at the time of concrete casting.

1.3.3.2 Oxygen

Following the reaction of corrosion mentioned above, oxygen is necessary for steel corrosion. Hence, it is necessary to construct concrete structures with good quality that restrict oxygen penetration from outside.

1.3.3.3 Moisture (hydrated state of concrete)

As well as oxygen, moisture is also necessary for the steel corrosion progress and moisture condition of concrete has a great influence on the occurrence and the

progress of corrosion. Moisture (pore solution) in concrete also plays a significant role as a connection path for ion transference. Thus, diffusion of chloride ions and oxygen is greatly affected by moisture content of concrete. Since the moisture content in concrete has a correlation with relative humidity, the influence of moisture in concrete can be examined from the viewpoint of relative humidity (Akita. 1994).

1.3.3.4 Design and quality of concrete

In general, concrete with a low water-cement ratio normally has dense microstructure and it is possible to suppress direct penetration of deteriorating factors such as chloride ions, oxygen from outside. Thus, the occurrence of steel corrosion can be restricted. In designing concrete members, it is also important to settle suitable concrete cover depth. The Japan standard specifications for concrete structures show the minimum thickness of concrete cover, according to environmental conditions (JSCE. 2010).

1.3.3.5 Construction of concrete

The quality of concrete changed greatly due to curing condition at the initial stage of construction. Without adequate curing, cracks due to drying shrinkage occur early, and deteriorating factors such as chloride, water, oxygen, etc., can permeate into the concrete through cracks. Hence, concrete is easier to deteriorate and steel corrosion can occur.

1.3.3.6 Environmental conditions

It is considered that influence of environmental conditions on corrosion of reinforcing bars is crucial. The penetrating possibility of degradation factors greatly depends on the degree of saturation. In addition, temperature of concrete also depends on the environmental temperature. The steel corrosion progress tends to promote when the temperature of concrete increases. In the experiment of corrosion promotion under the humid environment with varying temperature, it was reported that corrosion rate increased from two to four times when the concrete temperature reached from 20 ℃ to 60 ℃ (Masuda. 1992).

1.3.4 Countermeasures against chloride attack

The deterioration progress of concrete structures due to chloride attack is divided into four stages that include the initiation, propagation, acceleration and deterioration stages, respectively. **Figure 1.4** shows the performance degradation of

structure and the deterioration due to chloride attack regarding the difference of deterioration stages.
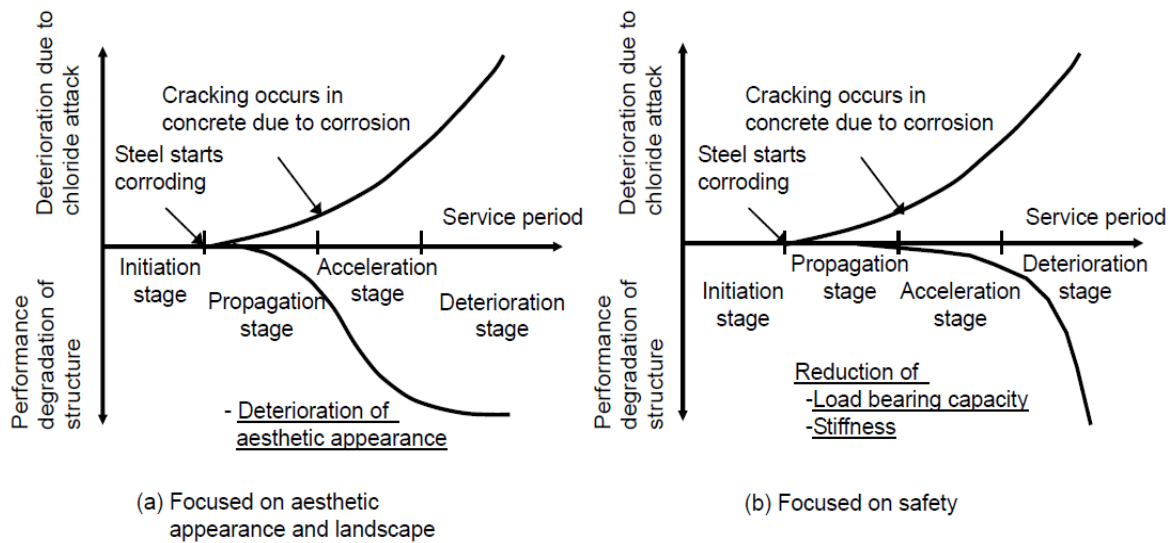
Figure 1.4 Deterioration progress due to chloride attack (JSCE.2010)

The countermeasures (methods and materials) should be selected to achieve required performances of structures, taking into account of performance deterioration due to chloride attack and life-cycle cost. In other words, methods of repair and strengthening depend on deterioration stages of concrete structures. Recently, many countermeasures have been applied and studied for actual concrete structures, even after the application of maintenance. The recommended countermeasures for concrete structures deteriorated due to chloride attack in each deterioration stage are listed in **Table 1.5** (JSCE.2010).

In the initiation stage, the deterioration of structures due to chloride attack has not occurred. At this stage, the remedial measures might be conducted as a preventive maintenance for structures. Countermeasures such as surface treatment should be applied to prevent chloride ions from penetrating into the concrete.

In the propagation stage, passive film of steel is broken down due to chloride ion, reinforcing bars in concrete has started to corrode and corrosion products have been accumulated. In addition, some cracks in concrete cover due to expansion pressure and the degradation of structures have also occurred. At this stage, surface treatment is commonly selected and the patching or the electrochemical desalination methods might be applied to remove chloride ions penetrated into concrete cover.

Table 1.5 Standard methods of countermeasure against chloride attack (JSCE.2010)

Stage of deterioration	Definition	Standard method
Initiation stage	Until the chloride ion concentration on the surface of steel reaches the marginal concentration for the occurrence of corrosion *	Surface treatment (Preventive method)
Propagation stage	From the initiation of steel corrosion until cracking due to corrosion	Surface treatment, patching, cathodic protection, and electrochemical desalination
Acceleration stage	Stage in which steel corrodes at a high rate due to cracking due to corrosion	Surface treatment, patching, cathodic protection, and electrochemical desalination
Deterioration stage	Stage in which load bearing capacity is reduced considerably due to the increase of corrosion amount	FRP bonding, patching, external cable, jacketing and thickness increasing

The standard value is 1.2 kg/m^3

In the acceleration stage, cracks occur in concrete cover due to steel corrosion, the deteriorating factors such as moisture and oxygen can easily penetrate from outside, corrosion of steel is promoted and it also influences the performance of concrete cover. Patching or electrochemical desalination methods to eliminate chloride ions in the concrete cover may be considered. As a part of the patching method, surface treatment might also be conducted after repairing. In particular, at the latter of this stage, concrete cover is delaminated or spalled due to deterioration of stiffness and expansion pressure. Thus, concrete cover is necessary to remove and patching material or even replacement of reinforcing bars should be considered.

In the deterioration stage, the load carrying capacity decrease and the cross-section of reinforcing bars reduces significantly. Therefore, the appropriate countermeasure should be applied such as FRP plates/sheets bonding, use of external cable, jacketing, increasing of thickness by patching materials, or even replacement of reinforcing bars. These methods should be conducted after removing the deteriorated concrete cover and surface treatment should be performed to prevent the re-deterioration.

Among these countermeasures, the surface treatment and patching material methods commonly applied to concrete structures such as road bridges deteriorated by chloride attack in Japan. Surface treatment method suppresses and restricts the penetration of degradation factors from the concrete surface, improves durability and the appearance of concrete surface. Patching method restores the cross-section portion of the existing concrete, which degraded due to chloride attack, suppresses the corrosion of reinforcing bars, etc. The deteriorated parts are needed to remove and then repaired, reinforced by patching materials to recover the initial shape of structures.

1.4 Deterioration due to ASR and chloride attack, and its countermeasures

1.4.1 Influence of combined deterioration due to ASR and de-icing salts

In several existing concrete structures, the combined deterioration caused by some degradation mechanisms can occur. Mechanism of combined deterioration in concrete structures is complicated due to the effect of integrating factors such as alkali-silica reaction, carbonation, freeze-thaw action, chemical attack, salt damage, etc. In particular, some studies showed that combined deterioration due to ASR and de-icing salts was considered more complicated and the extent of deterioration was more serious than single deterioration (Nomura. 2002, Tamura. 1997). The main reason for this is that water leakage included a high concentration of chloride causes a higher risk of corrosion, the increase of moisture in concrete promotes ASR progress. Therefore, the density and magnitude of cracking caused by ASR expansion are also increased. As a result, progression of cracks leads to more chloride and oxygen penetration into concrete and steel bars are easier to corrode. Finally, this combined deterioration accelerates the degree of degradation, decreases the durability and load carrying capacity, and lessens the aesthetics of concrete structures.

Currently, de-icing salts have been extensively used in Japan to clear the highways of snow/ice accumulation during the winter for safety of vehicles. The de-icing salts used in some areas such as the Hokuriku region are mainly of sodium chloride (NaCl) type (Katayama. 2004). In addition, many concrete structures located on highway such as roads, bridges and tunnels have been deteriorated by ASR. Some structures such as abutments, wing walls, wheel guards, etc., of concrete bridges that have been deteriorated by ASR are directly affected by chloride penetration through

the influence of water leakage included de-icing salts. The main scope of this study was primarily focused on the combined deterioration of concrete structures affected by ASR and de-icing salts.

1.4.2 Countermeasures against combined deterioration of ASR and de-icing salts

Adequate assessment of combined deterioration mechanism caused by ASR and chloride attack has not been fully elucidated. Thus, the proper repair and maintenance methods for reinforced concrete structures affected by this combined deterioration have not yet been fully established. Current countermeasures mainly based on the repair and strengthening methods applied to deteriorated-structures affected by only ASR or chloride attack such as patching, crack injection, surface treatment, and others. Many studies have shown that the performance of repair materials is significantly affected by this combined deterioration. Therefore, it is necessary to conduct further studies to clarify the mechanism and recommend proper countermeasures to deal with the combined deterioration of concrete structures.

1.5 Objective and scope of this study

In some regions of Japan, there are many concrete bridges have been deteriorating due to alkali-silica reaction. These bridges were mainly primarily built during the high economic growth period. At that time, coarse aggregates used in concrete were diversified and some of them were the reactive rocks such as Andesite, Rhyolite, Chert, etc. In addition, the high alkali cement was produced to supply for the construction works in this period. The use of reactive aggregates, high alkali cement combined with high moisture content of concrete causes ASR deterioration in concrete structures.

In the winter, a large amount of de-icing salts has been sprayed on the highway to ensure safety of vehicles. The mainly used of de-icing salts is sodium chloride (NaCl) type. Furthermore, concrete structures along coastline of Japan are also affected due to the airborne chlorides from the sea. Hence, these concrete structures are significantly influenced by a permanent saline environment.

This study focused on some specific structures of concrete bridge such as abutments, wing walls, wheel guards, etc., of several bridges located in the Hokuriku region. These structures have been deteriorating by ASR and influenced by water leakage that contained a high concentration of chloride due to de-icing salts spraying.

Figure 1.5 shows the areas in the Hokuriku region where concrete bridges have been deteriorating by ASR (Moriyama. 2011). In this expressway, ASR occurs in almost areas of Toyama prefecture and parts of Ishikawa and Fukui prefectures.
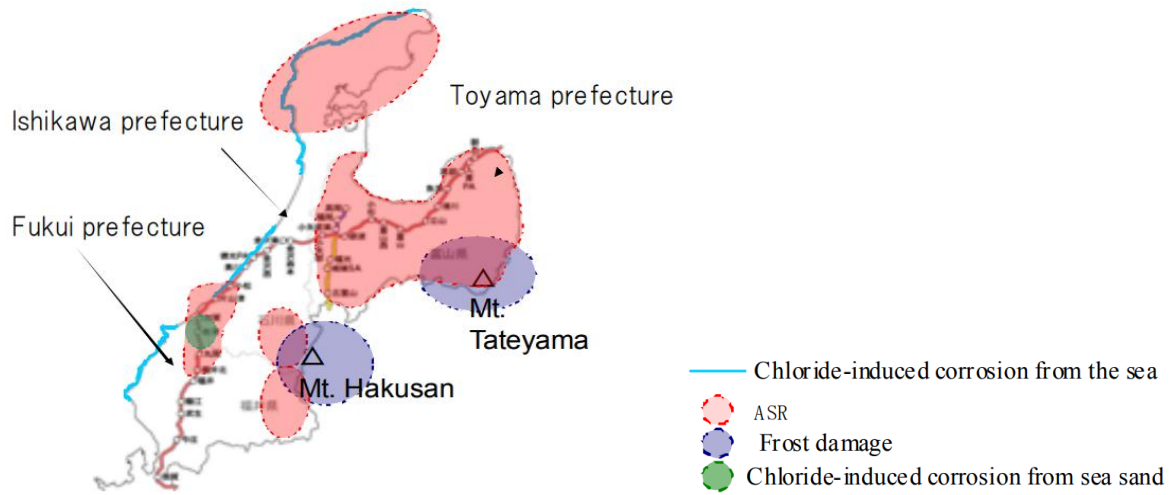
Figure 1.5 Map of deterioration in Hokuriku region (Moriyama. 2011)

From the practical point of view, this study was conducted to assess the actual states of concrete members and the effectiveness of countermeasures that had been performed for ASR-deteriorated concrete bridges affected by de-icing salts. This study was conducted based on in-situ surveys, sample analysis and concrete specimen in the laboratory.

The main objectives of this study are summarized as follows:

- To investigate the grade and the risk of steel corrosion, measure expansive strain, crack density and surface moisture of concrete of bridge abutments deteriorated by ASR and de-icing salts;

- To evaluate combined deterioration of concrete slab specimen in the laboratory;

- To investigate the effectiveness of patching method and the interface between ASR-deteriorated concrete and patching material due to ASR expansion;

- To investigate the performance of countermeasures such as patching materials and surface treatment for the wheel guard structures affected by combined deterioration;

- To evaluate the risk and the rate of steel corrosion in wheel guard structures based on in-situ measurements.

The results of this study have assessed the current stage of concrete members and the effectiveness of countermeasures for some structures of the road bridges located on the Hokuriku Expressway that have been deteriorated due to ASR and deicing salts.

1.6 Structure of this dissertation

This dissertation consists seven chapters and the flow of this study is shown in **Figure 1.6**. In chapter 1, the backgrounds of alkali-silica reaction, chloride attack and countermeasures, objectives of this study were introduced.

In chapter 2, the penetration of chloride ions and steel corrosion were investigated on ASR deteriorated concrete abutments affected by de-icing salts. The influence of de-icing salts and ASR was investigated by the in-situ survey and laboratory tests. Then, the influence of combined deterioration due to ASR and de-icing salts was clarified on these structures.

The deck slabs can be deteriorated considerably by fatigue deterioration combined with material deterioration caused by de-icing salts, frost damage, alkali-silica reaction, etc. In chapter 3, the experimental investigation was conducted to clarify the performance of bridge deck specimens that was degraded by a single or combined deterioration of alkali-silica reaction and chloride attack. The results attained in comparison with sound concrete specimens clarified the significant influence of combined deterioration on these specimens.

The patching method has been applied as one of proper methods for concrete structures deteriorated by ASR. The ASR residual expansion could be affected remarkably for patching material and the interface between ASR-deteriorated concrete and patching material. In chapter 4, the experiments were conducted to investigate the performances of patching material and the interface due to ASR residual expansion and chloride ion penetration.

Some proper countermeasures have been applied for concrete structures affected by combined deterioration of ASR and de-icing salts such as patching, crack injection, surface treatment, etc. In chapter 5, the in-situ survey was carried out to investigate the influence of ASR and de-icing salts on applied countermeasures for the wheel guard structures of a bridge.

In chapter 6, the influence of de-icing salts and alkali-silica reaction on the steel corrosion was investigated by the in-situ survey and laboratory test. From the results of this in-situ survey, it is considered that steel corrosion risk can be evaluated in the ASR-deteriorated concrete structures affected by de-icing salts.

Finally, the main results of the study are concluded and summarized in chapter 7.

General background and objectives

Chapter 1 Introduction

Investigations of combined deterioration in concrete structures

Chapter 2 Steel corrosion in ASR-deteriorated concrete affected by de-icing salts

Chapter 3 Evaluation of combined deterioration in concrete bridge decks using FWD method

Influence of combined deterioration on applied countermeasures

Chapter 4 Influence of ASR expansion on the interface between patching material and ASR-deteriorated concrete

Chapter 5 Effectiveness of countermeasures applied on ASR-deteriorated concrete bridge affected by de-icing salt

Evaluation of steel corrosion risk on concrete structures affected by ASR and de-icing salts

Chapter 6 Evaluation of steel corrosion on ASR-deteriorated concrete affected by de-icing salts

Conclusions of dissertation

Chapter 7 Conclusions

Figure 1.6 Structure of this dissertation

References

Akita, H., Fujiwara, T., and Ozaka, Y., *An analytical method of moisture transfer within concrete due to drying*. Concrete library of Japan Society of Civil Engineers (JSCE), No.25, pp. 77-92, June 1995.

Bauer, S., Cornell, B., Figurski, D., Ley, T., Miralles, J., and Folliard, K., *Alkali-Silica Reaction and Delayed Ettringite Formation in Concrete: A Literature Review*. Technical Report No. FHWA/TX-06/0-4085-1, Center for Transportation Research, Austin, TX, 73 pp, February 2006.

Federal Highway Administration (FHWA) – U.S. Department of Transportation, *Alkali-Aggregate Reactivity (AAR) Facts Book*, 224 pp, March 2013.

Dent Glasser, L.S., and Kataoka, N., 1981. *"The chemistry of alkali-aggregate reactions."* Proceedings of the 5th International Conference on Alkali-Aggregate Reaction, Cape Town, S252/23.

JSCE (Japan Society of Civil Engineers), 2005. Subcommittee report " *The countermeasures for Alkali Aggregates, reinforcement and new response"*, Japan Society of Civil Engineers, August 2005, 316 pp.

JSCE (Japan Society of Civil Engineers), *Standard specifications for concrete structure - 2007 "Maintenance"*, JSCE guidelines for concrete. No.17, 309 pp, December 2010.

Katayama, T., Tagami, M., Sarai, Y., Izumi, S. and Hira, T., *Alkali-aggregate reaction under the influence of deicing salts in the Hokuriku district, Japan*. Material Characterization 53, pp. 105- 122, June 2004.

Masuda, Y., Kakegawa, M., Hanae, H., *Experiment on the influence of various factors on the rate of corrosion loss of reinforcing bar in concrete*. Proceedings of the Japan Concrete Institute, Vol. 14, No.1, pp. 781-786, 1992. (in Japanese)

MLIT (Ministry of Land, Infrastructure, Transport, and Tourism-Japan), 2002: *Measures to suppress alkali-aggregate reaction*, August 2002. (in Japanese)

Moriyama, M., and Nomura, M., *Maintenance of ASR-affected structures in Hokuriku Expressway, Japan*. Proceeding of the 27th U.S. - Japan bridge engineering workshop, pp. 167-174, November. 2011.

Neville, A., *Chloride attack of reinforced concrete: an overview*, ACI Materials and Structures. 28, pp. 63-70, 1995.

Nomura, M., Aoyama, M., Hira, T. and Torii, K., *Case study on deterioration of concrete in road structures due to alkali-silica reaction (ASR) in Hokuriku region and its evaluation methods*. Concrete Research and Technology, Vol. 13, No. 3, pp. 105-114, September 2002. (in Japanese)

Silva, N., Thesis for the degree of doctor of philosophy, *Chloride-Induced Corrosion of Reinforcement Steel in Concrete*, Chalmers University of Technology, Sweden, 52 pp, 2013.

Tamura, T., Nomura, M., and Iida, K., 1997. *Road bridges undergoing AAR and the influence of de-icing agents.* Proceedings of the 22nd Road conference, Japan, 1997.

Wakizaka, Y., *Alkali-silica reactivity of Japanese rocks*, Engineering Geology, Vol. 56 (2000), pp. 211-221, March 1999.

Wald, D. M., *ASR expansion behavior in reinforced concrete – Experimentation and numerical modelling for practical application*, Dissertation of The University of Texas at Austin, 300 pp, August. 2017.

CHAPTER 2 STEEL CORROSION IN ASR-DETERIORATED CONCRETE AFFECTED BY DE-ICING SALTS

2.1 Introduction

In Japan, a large number of concrete structures had been constructed during the high economic growth period and has been stocked as the social infrastructure. These structures were considered durable and maintenance-free. However, a lot of early deterioration of concrete structures has been reported when these structures were affected by various severe conditions such as coastal areas and under spraying of de-icing salts. Thus, deterioration or degradation of concrete structures could occur due to alkali-silica reaction, chloride-induced corrosion and other deteriorations. Then, recognition of maintenance-free was revised and shifted to the concept of preventive maintenance.

Chloride-induced corrosion and alkali-silica reaction (ASR) are typical deteriorations of concrete structures. Preventive maintenances are needed to shift and to establish since early deterioration can occur under severe conditions. In mountainous areas and cold climate areas, some cases of significantly deteriorated concrete structures in the short time were reported due to combined deterioration of ASR and de-icing salts. Consequently, it is urgent to consider the countermeasure for them. In this chapter, in order to clarify the deteriorating situation of combined deterioration due to ASR and chloride-induced corrosion, in-situ survey was conducted. The effect of de-icing salts and alkali-silica reaction on steel corrosion was investigated. As a result, cracks caused by alkali-silica reaction promoted the penetration of chloride ions that also promoted chloride-induced corrosion.

When early deterioration occurs in concrete, it is important and essential to identify deterioration mechanism, causes, and degradation progress. For this reason,

many investigations have been performed to identify various deterioration mechanisms of these existing concrete structures and various countermeasures have been applied against them. In Japan, the standard of countermeasure is established for chloride-induced corrosion that is known as one of typical causes of concrete structure deterioration. However, effective countermeasures have not established for concrete structures affected by ASR since the deterioration mechanism of alkali-silica reaction is very complicated and it is not easy to remove or to reduce deterioration factors such as reactive aggregates, alkali, and moisture in concrete with current techniques. For this reason, the proper repair method has not been established, whereas the effectiveness of applied repair should continue for a long time.

Furthermore, in the past, it was pointed out that reactive aggregates such as andesite, rhyolite, chert, etc., were used in the concrete structures in Kansai and southwest regions in Japan (Wakizaka. 1999). However, from the viewpoint of geological aspect, it has been reported that the reactive aggregate was distributed widely all over Japan (Wakizaka. 1999 and Hirono. 2011). It is concerned about the possibility of the occurrence of ASR in other areas where deterioration of concrete structures due to ASR has not been reported until now.

Additionally, after the prohibition on the use of the studded tire, some concrete structures were deteriorated significantly in a short-term due to chloride-induced corrosion. This phenomenon occurred due to a large amount of de-icing salts was used during the winter for safety of traffic in cold regions (Yokoyama et al. 2008, Honjo et al. 2010). It is known that de-icing salts accelerate chloride-induced corrosion and promote alkali-silica reaction simultaneously by supplying of alkali (sodium) and moisture (JCI. 2008). Therefore, it is considered that combined deterioration of alkali-silica reaction and chloride-induced corrosion can occur easily in ASR deteriorated concrete affected by de-icing salts. It was reported that alkali-silica gel, which produced by the alkali-silica reaction, surrounded reinforcing bars and contributed to against steel corrosion since this gel suppressed the supply of oxygen and water. However, steel corrosion also occurred in ASR deteriorated concrete structures affected by de-icing salts (JCI. 2008). The real situation of steel corrosion due to de-icing salts in ASR deteriorated structures is not clarified precisely.

In this chapter, the penetration of chloride ions and steel corrosion were investigated on ASR deteriorated concrete abutments affected by de-icing salts. The influence of de-icing salts and alkali-silica reaction was investigated by in-situ survey

and laboratory test. In the in-situ survey, crack density and surface moisture content of concrete were measured and chipping investigation was conducted to take samples for chloride ion analysis. Then, the corrosion grade of steel bars was determined to clarify the influence of de-icing salts and alkali-silica reaction on steel corrosion.

2.2 Target bridge abutments

Hokuriku Highway Express is located in the central of Northern part in Japan. Target concrete bridge abutments, which were constructed between 1975 and 1983, are located between Toyama Nishi Interchange and Asahi Interchange. There are a lot of ASR deteriorated concrete bridges since reactive aggregates were used in this area and the alkali-silica reaction was identified by petrology observations.

Furthermore, during the winter, de-icing salts have sprayed on this highway to avoid the road surface freezing and to keep safety for transport vehicles. In this study, seven concrete bridge abutments were selected for the in-situ survey. On these abutments, ASR has progressed and they have been affected by de-icing salts through water leakage from the expansion joints of bridges. However, progress of ASR in these abutments was not significant since crack width and crack density (total crack length per unit area (m/m^2)) caused by ASR expansion were relatively small. Therefore, the countermeasures such as surface coating and/or patching methods have not been implemented to repair these target abutments.

The in-situ survey was conducted on the front wall of target abutments. The occurrence of cracks due to ASR was relatively small and the crack width was almost smaller than 0.5 mm. In addition, the exudation of rust due to steel corrosion on the surface of abutments could not observe by visual inspection. The front walls of these abutments were distinguished into two parts (the up line and the down line) and ten detailed investigation points were selected to observe corrosion grade of reinforcing bars by chipping concrete cover and to analyse chloride ion penetration (chloride ion content profile). **Figure 2.1** shows the current state of abutment A as an example of ASR deteriorated concrete abutment.

Figure 2.1 Abutment A deteriorated by ASR

2.3 Contents of the in-situ survey

2.3.1 Outline of in-situ survey

In this in-situ survey, seven target abutments have already affected by ASR and de-icing salts. This survey was conducted to assess the crack propagation on surface of front walls and to calculate crack density as an evaluation index of ASR progress. The surface water content of concrete was measured and used as an evaluation index of the content of de-icing salts supplied through water leakage. Ten detailed investigation points were selected based on the measurement results of surface moisture content of concrete and crack density on the surface of abutments. The overview of target abutments and the number of detailed investigations are shown in **Table 2.1**.

Table 2.1 Abutments of in-situ survey

Bridges	Name	Up line or Down line	A number of detailed investigations
A	AU	Up line	1
	AD	Down line	1
B	BU	Up line	1
	BD	Down line	1
C	CD	Down line	1
D	DU	Up line	4
E	EU	Up line	1

2.3.2 Crack density measurement

The crack density of an area on the surface of abutments was measured at the height of 0.8m to 1.8m from the ground. The measured area of each abutment was divided horizontally into many sections (1m × 1m) (shown in **Figure 2.2**).
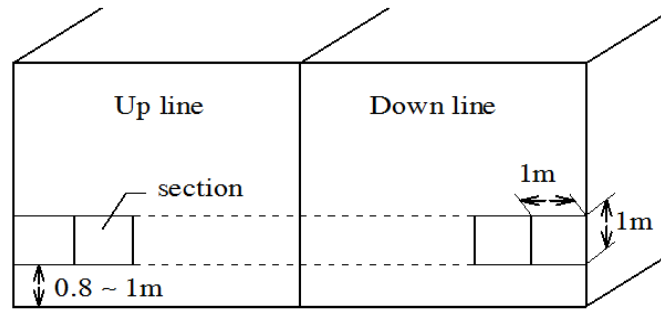
Figure 2.2 Outline of survey sections on each abutment

: Crack width > 0.4mm   *: Crack width from 0.2 to 0.4mm*
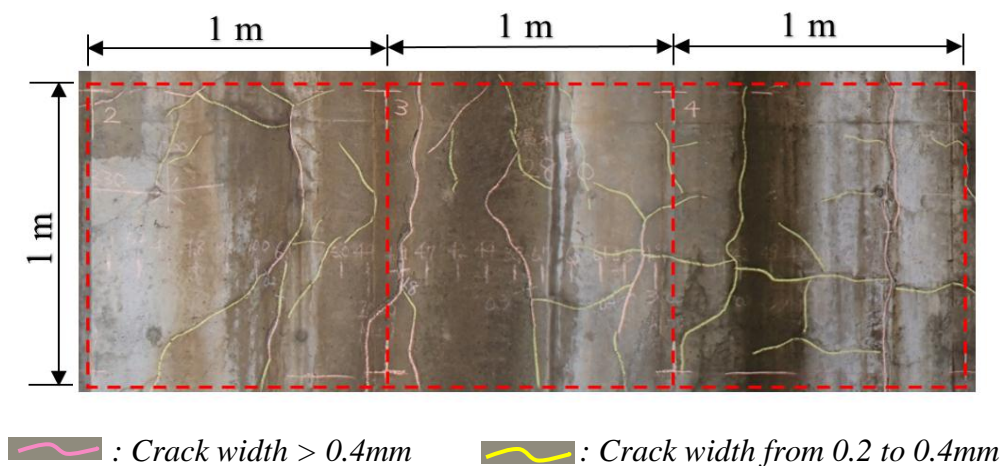
Figure 2.3 Example of crack density measurement

The degree of crack width was classified into two grades. The smaller grade of crack width ranges from 0.2mm to 0.4mm and the larger grade of crack width is larger than 0.4mm. The crack density of each grade was calculated by the total length of cracks per each section area (m/m^2) and this value was defined as a crack index. **Figure 2.3** shows cracks distribution on the surface of abutment as an example of crack density measurement.

2.3.3 Surface moisture content measurement

It is inferred that the larger influence of de-icing salts for concrete structures occurred since the amount of water leakage of concrete increases. In areas with larger amount of water leakage, the surface moisture content of concrete tends to be higher.

Thus, the surface moisture content of concrete can be used as an index to evaluate the influence degree of de-icing salts to concrete structures.

Surface moisture content of concrete was measured by using a high-frequency surface moisture meter and these values were measured horizontally at intervals of 0.1m on the surface concrete of abutments. In each section (1m × 1m), the average value of surface moisture content was calculated from ten measured points of each section. The positions of surface moisture content measurement are shown in **Figure 2.4**. Each average value of surface moisture content compared with crack density of each section on abutment surface and the relation between them are discussed later to clarify the influence of water leakage or de-icing salts on the result of crack density.
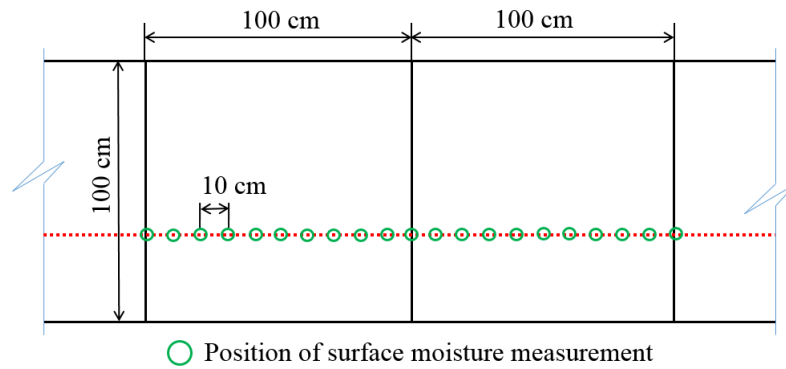
Figure 2.4 Measured positions of the surface moisture content

The previous study (Ibata et al. 2014) indicated that the degree of surface moisture content of concrete could not correspond to the amount of water leakage when the leakage paths were changed. Then, surface moisture content of concrete was used as an evaluation index with some variables in this study.

2.3.4 Steel corrosion investigation

In order to determine the steel corrosion grade, ten points were selected and the surface condition of steel bars was observed by visual inspection after chipping concrete cover. These investigation points were selected based on the measurement results of surface moisture content of concrete and crack density on the surface of abutments. The crack density values of these points ranged from small to large and values of surface moisture content of concrete ranged from low to high.

At each point to chipping concrete cover, the intersections of axial steel bars and lateral steel bars were detected by using the electromagnetic radar device. Then,

concrete cover was removed in a peripheral part (0.3m × 0.3m) at the intersection of each investigated point. The concrete cover depth of each point was measured and the surface of steel bars was observed to judge steel corrosion grade.

The steel corrosion grade was evaluated based on the guideline in "Survey of cracks in concrete, repair and reinforcement guidelines 2003: Japan Concrete Institute". The criteria to judge corrosion grade of steel bars are shown in **Table 2.2**. The steel corrosion grades, which were observed by visual inspection after chipping concrete cover, are shown in **Figure 2.5**.

Table 2.2 Steel corrosion grade

Grade	State of steel corrosion
I	Surface with mill scale and/or no corroding surface are observed.
II	Partially floating of rust in the small spot was observed.
III	Sectional defects do not observe by visual observation, but floating rust occurs around the steel bars or over the full length.
IV	Cross-section defects of steel bar occurred.

Grade I   *Grade II*   *Grade III*

Figure 2.5 Examples of steel corrosion grade

2.3.5 Chloride ion permeation and profile

The samples of concrete powder to obtain chloride ion content profiles were collected by drill method at each investigated point (within the distance 0.15 m from intersection of steel bars). The maximum depth of collecting samples was up to 120 mm and each sample was taken every 20 mm of depth. Concrete powder samples

were sealed in plastic bags and chloride content was measured in the laboratory by the potentiometric titration method (JCI-SC5).

2.4 Results and discussion

2.4.1 Relationship between crack density and surface moisture content

Surface moisture content of concrete for each abutment (discriminated between up line part and down line part) is shown in **Figure 2.6**. The value of surface moisture content of concrete was the average value of all measured points on each abutment.
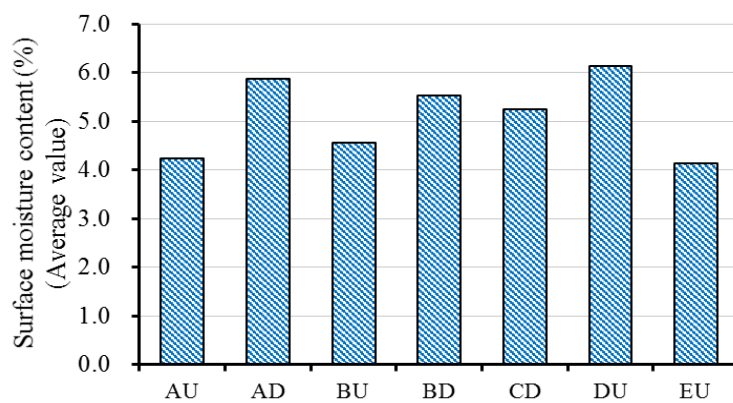
Figure 2.6 Surface moisture content of all abutments

These values of all bridge abutments ranged from 4% to 6%. A previous study (Ibata et al. 2014) showed that the influence of de-icing salts was insignificantly when the surface moisture content of concrete was about 4% or lower. In addition, the averaged values of these abutments concluded values of sections that could not affect by water leakage. Therefore, it is considered that the effect of water leakage or de-icing salts on concrete abutments is significant when the surface moisture content is larger than 4%.

The crack density (m/m^2) of each abutment (discriminated between up line part and down line part) is shown in **Figure 2.7**. The value of crack density was the average value of all measured sections of each bridge abutment. The crack density of small grade of crack width (from 0.2mm to 0.4mm) occurs on most bridge abutments. Almost values of this grade are larger than $2m/m^2$ while those values of large grade of crack width (more than 0.4mm) on all abutments are smaller than $2 \ m/m^2$. Although many small cracks occurred, result showed that the ASR progress of these abutments was not significant since the crack density of large grade was small.
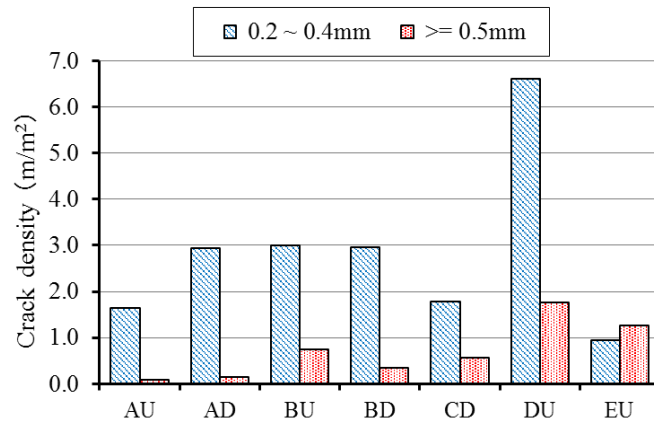
Figure 2.7 Crack density of abutments

The relationship between crack density of the small grade of crack width (0.2 ~ 0.4mm) and surface moisture content of concrete of each section is shown in **Figure 2.8**. The surface moisture content of concrete in each section (1m × 1m) was averaged of all measured points of that section. In this figure, the square symbol means the value measured at ten points of chipping investigation.
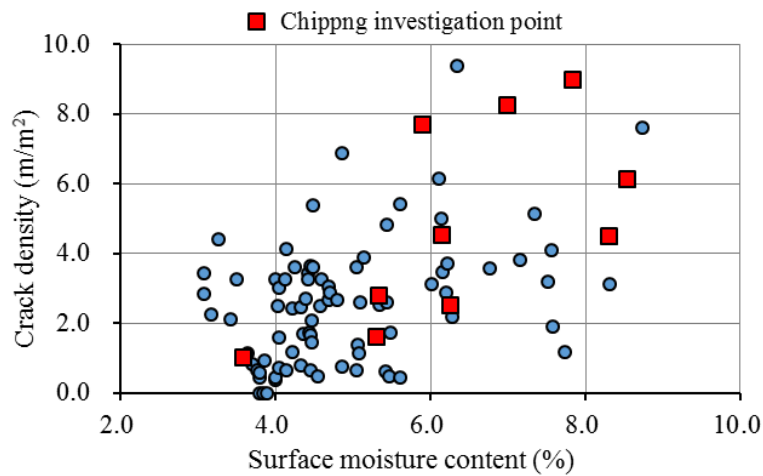
Figure 2.8 Crack density and surface moisture relationship

The crack density tends to increase with the increase of surface moisture content of concrete. However, the variation of data was somewhat large and the relationship between crack density and surface moisture content had a weak correlation. As the reason for this, it is inferred that the amount and the paths of water leakage could be changed for a long term. For example, the large values of crack density may be obtained with small values of surface moisture content of concrete in the same section of same abutment. This could explain by a change of the amount and/or paths

of water leakage while large crack density had already occurred due to a large amount of water leakage in the other period. The degree of water leakage on the front wall of abutment can be changed easily since the extent of water leakage on this wall is generally vast. The larger value of crack density tends to obtain due to larger content of surface moisture of concrete in the same section. Thus, it is considered that ASR is promoted by water and de-icing salts supplied through water leakage.

2.4.2 Chloride ion penetration

The chloride ion contents of concrete at the depth from 80 mm to 100 mm corresponding to the designed cover depth of these abutments are shown in **Figure 2.9**. The samples of concrete powder for obtaining chloride ion content were collected at each detailed investigation point.

The maximum value of chloride ion content of concrete at the designed cover depth was about $4kg/m^3$ and it was obtained in bridge abutment CU. However, the values of chloride ion content of most bridge abutments were lower than $2kg/m^3$. As mentioned above, the front walls of these target abutments were not repaired and crack density on concrete surface was relatively small except for bridge abutment DU. This corresponded to the visual aspect of crack propagation of these concrete abutments. Additionally, concrete cover depth of these abutments is sufficient to maintain the low chloride content at 80 mm of depth. The chloride ion penetration at concrete cover depth is relatively small although ASR deteriorated concrete abutments are affected by de-icing salts.
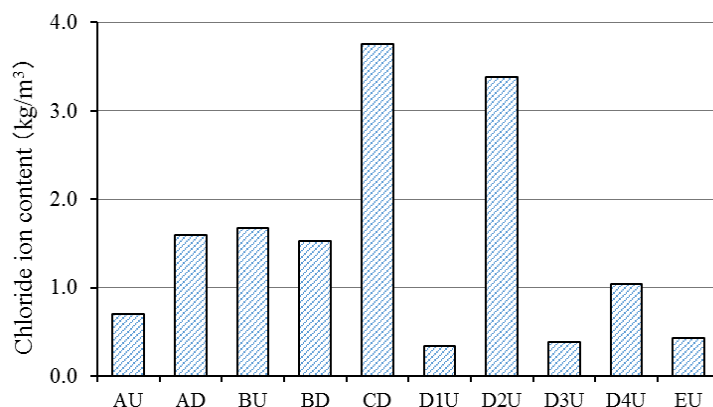
Figure 2.9 Chloride ion content at concrete cover depth

The chloride ion content profile of bridge abutment DU is shown in **Figure 2.10**. On this abutment, chloride ion content of concrete at concrete cover depth (80 ~

100mm) are smaller than 2.0kg/m^3 except for DU2. On the other hand, chloride ion content of concrete at 50mm of depth on bridge abutment DU2 and DU4 are larger than 4kg/m^3. The profiles of chloride ion content in abutment DU1 and DU3 show smaller values of chloride ion penetration due to the larger of concrete depth and all values are smaller than 2.0 kg/m^3. However, these values in abutment DU2 and DU4 are large and it shows larger content of chloride ion in depth from 20mm to 40mm in comparison with values near the surface (0 ~ 20mm). For this reason, water leakage does not contain chloride ions except for winter season. It is considered that water leakage without chloride ion washes the permeated chloride ion out of concrete surface during spring and fall seasons when de-icing salts were not sprayed (Hirano et al. 2010). Thus, chloride ion content near the surface could fluctuate seasonally. In this study, samples of concrete powder for the obtaining chloride ion content profile were carried out during September and October when de-icing salts were not sprayed in this season. Therefore, it is inferred that chloride ion content near the surface is strongly affected and is reduced by the washout action of water leakage without chloride ions for chloride ion content profiles obtained in abutments DU2 and DU4.
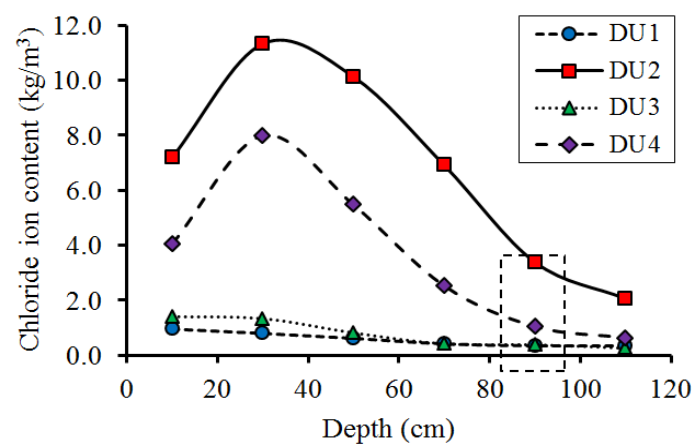
Figure 2.10 Chloride ion distributions in abutment D

2.4.3 Steel corrosion grade

The steel corrosion grades of axial and lateral steel bars in all abutments are shown in **Figure 2.11**. Steel corrosion grade of each axial steel bar corresponds to that of each lateral steel bar on most abutments. These steel corrosion grades of axial and lateral steel bars are grade I and II except for the abutment BU (grade III). None of abutment shows steel corrosion grade IV and it results higher rate of steel corrosion in loss of the steel bar section.

As mentioned above, almost chloride ion contents of concrete cover depth were less than 2.0kg/m^3. It was confirmed after chipping concrete that most concrete cover depths were larger than designing cover depth. Consequently, it is considered that chloride ion content of concrete at in-situ concrete cover depth is suppressed under the relatively small content of chloride ion penetration and it results in low steel corrosion grade on most abutments.
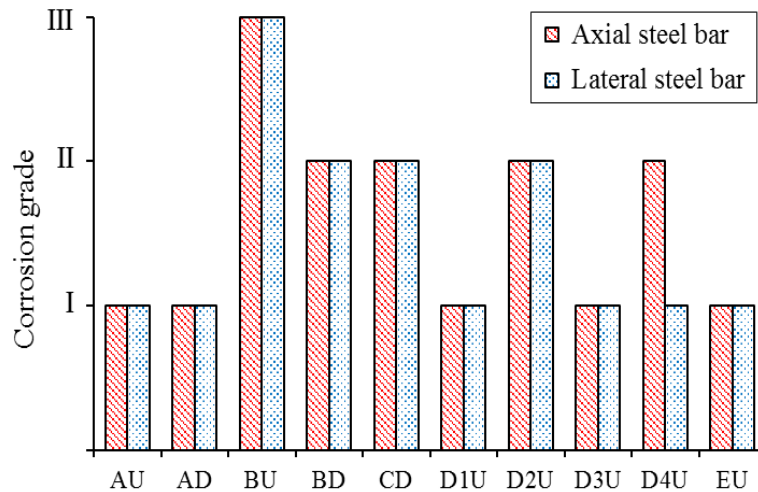
Figure 2.11 Corrosion grades of steel bars in all abutments

It is concluded that the occurrence and the progress of steel corrosion are not significant on these abutments at present since concrete cover depth is effective and sufficient to prevent chloride ion penetration and to suppress steel corrosion. However, the influence of de-icing salts is not small since the chloride ion penetration near concrete surface is relatively high on most half of abutments.

If the steel corrosion would occur and progress in these abutments in the future, a large scale of countermeasures such as patching, surface coating and a large cost might be needed. Therefore, the surface impregnation and surface coating and/or an intensified inspection as the preventive countermeasures should be planned in order to prevent the influence factor such as water and chloride that can be permeated into concrete beforehand.

2.4.4 Influence of ASR and de-icing salts

2.4.4.1 Influence of cracks caused by ASR expansion on chloride ion penetration

The relationship between crack density of detailed investigation points and chloride ion content at the designed concrete cover depth of all abutments is shown in

Figure 2.12. Although the variation of data was somewhat large and the relationships between them had a weak correlation, a few values showed the tendency of chloride ion content at concrete cover depth increased with the increase of the crack density of detailed investigation points. Cracks due to ASR influenced locally on chloride ion penetration near the generated crack while crack density was measured for one section (1m × 1m). Thus, it is noted that the crack density obtained in each section did not necessarily correspond to the content of chloride ion penetration of the detailed investigation point. For example, in the same section, crack density was not the same as the point of detailed investigation and crack density ranged widely. Although the relationship between the crack density and the chloride ion content shows a weak correlation, it is considered that the more penetration of chloride ion can be obtained at the position of large crack propagation.
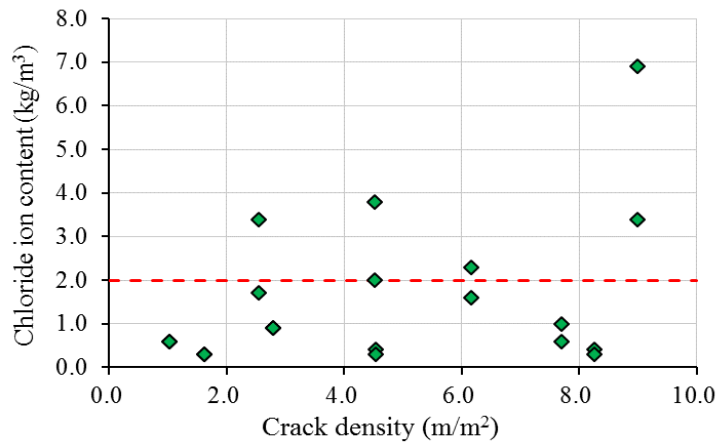
Figure 2.12 Relationship between crack density and chloride ion content

The deterioration caused by ASR in target abutments of this study has already progressed for a long time. In addition, many cracks due to ASR expansion were propagated before the amount of de-icing salts increased rapidly when the studded tires were banned in 1990 in Japan. It is considered that the occurrence of cracks on these abutments was caused by the ASR expansion except for a few cracks caused by the initial defect of cracks such as thermal stress and drying shrinkage of concrete, since the rust leakage on concrete surface was not observed by visual inspection. Therefore, it is concluded that the increase of crack density in these target abutments is related closely to the progress of ASR.

The relationship between chloride ion content of concrete at in-situ cover depth and steel corrosion grade of detailed investigation points on bridge abutments is

shown in **Figure 2.13**. In the case of more than 2kg/m^3 of chloride ion content of concrete, most steel corrosion grades were grade II or III. These grades indicated steel corrosion was progressed. The previous study (Higashida et al. 2010) investigated the relationship between chloride ion content of concrete at concrete cover depth and steel corrosion grade of steel bar. That study showed that steel corrosion grade III or IV occurred since chloride ion content of concrete at cover depth exceeded 2.4kg/m^3.
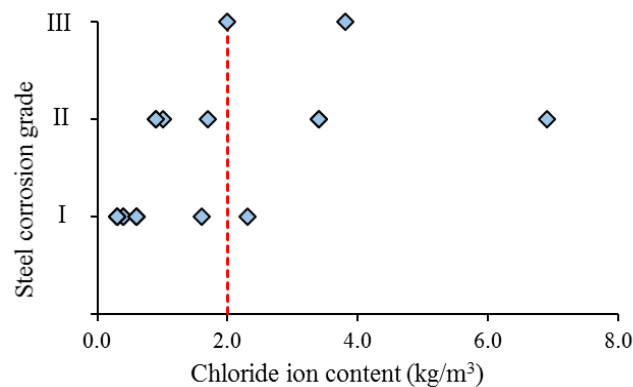
Figure 2.13 Relationship between chloride ion content and steel corrosion grade

In this study, three of detailed investigation points showed steel corrosion grade II even chloride content of concrete was smaller than 2kg/m^3. It inferred that the cracks caused by ASR could promote water and oxygen to permeate into concrete and steel corrosion proceeded. However, there are a few data obtained in this study and further investigation is necessary to clarify the influence of de-icing salts on ASR deteriorated concrete structures. Furthermore, it is necessary to clarify the threshold value of chloride ion content at the onset of steel corrosion in concrete structures affected by ASR.

2.4.4.2 Crack density and steel corrosion grade

The relationship between crack density and steel corrosion grade of detailed investigation points of all abutments is shown in **Figure 2.14**. When crack density was more than 2.0m/m^2, half values of steel corrosion grade were grade II or III. On the other hand, even in the case of more than 2.0m/m^2 of crack density, some values of steel corrosion grade were grade I. For this reason, although all abutments were influenced by de-icing salts, chloride ion content at concrete cover depth was not too large to onset the steel corrosion in this survey or the position of crack propagation did not correspond to detailed investigation points.
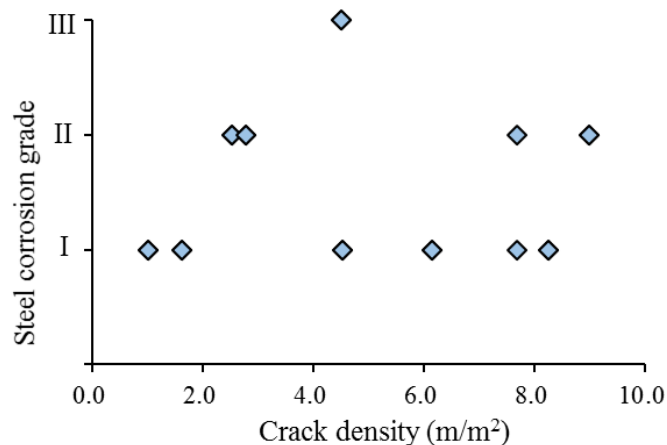
Figure 2.14 Relationship between crack density and steel corrosion grade

Although there are a few data obtained in this study, as results of the relationship between crack density and steel corrosion, there seems to be a tendency that higher grade of steel corrosion can be obtained with larger values of crack density of detailed investigation points. Therefore, it is considered that the increase of crack density due to ASR progress may promote water, oxygen and chloride ion penetration. Thus, steel bars are easier to corrode in ASR deteriorated concrete structures affected by de-icing salts.

In the previous study (Fujimura et al. 2009), it is reported that 5.7kg/m^3 of sodium chloride (3.48 kg/m^3 of chloride ions) was used in concrete to promote chloride-induced corrosion in concrete structures affected by ASR. The result of that study showed that steel corrosion in concrete was suppressed even ASR occurred in the concrete. NaCl supplied from seawater and de-icing salts during the service life may react with cement and hydrated cement in the different way of NaCl added initially in concrete mixing. This difference between them may have a different effect on the fixation of chloride ions as Friedel's salt and/or pH of pore solution in concrete. Finally, it is considered that these phenomena influence on steel corrosion in ASR deteriorated concrete due to chloride ion penetration and water from leakage on the in-situ concrete structures. Therefore, further detailed investigations and a data collection for ASR deteriorated concrete affected by de-icing salts are needed to clarify the combined deterioration mechanism.

On the other hand, in the result of this in-situ survey, it is noted that the suppression of steel corrosion due to Alkali-silica gel cannot attain sufficiently under severe conditions in ASR deteriorated concrete structures affected by de-icing salts.

2.5 Conclusion

The main results obtained in this chapter are shown as follows:

(1) Despite the variation of data are somewhat large, there seems to be a tendency that crack density increases with the increase of surface moisture content of concrete.

(2) There seems to be a tendency that chloride ion content at designing concrete cover depth increases with the increase of crack density.

(3) There seems to be a tendency that higher level of steel corrosion grade can be obtained with the larger of crack density.

(4) The values of chloride ion content of most bridge abutments were lower than 2 kg/m^3 at the designed cover depth. However, the influence of de-icing salts was not small since chloride ion content was high and chloride ion penetration was large near concrete surface.

(5) It is considered that the increase of crack density caused by ASR progress may promote water, oxygen and chloride ion penetration Thus, steel bars are easier to corrode in ASR deteriorated concrete structures affected by de-icing salts.

(6) It is noted that the effectiveness of suppression of steel corrosion due to Alkali-silica gel cannot attain sufficiently under severe conditions in ASR deteriorated concrete structure affected by de-icing salts.

(7) Even if the concrete cover depth of abutment is enough for the durability of structures, steel corrosion can occur under severe conditions. Repairing them and applying large-scale countermeasure such as patching are needed.

References

Fujimura, T., Habuchi, T., and Torii, K., *Corrosion properties of steel bars in concrete subjected to combined deterioration in ASR and seawater*, Proceedings of Annual Conference, Japan Concrete Institute, Vol. 31, pp 1285-1290, 2009. (in Japanese)

Higashida, N., Hosoya, J., and Kawaguchi, K., *The relationship between the corrosion grade of steel bar and chloride ion concentration caused by chloride attack*. The 65th Annual Scientific Proceedings, Japan Society of Civil Engineers, pp 127-128, 2010. (in Japanese)

Hirano, S., Ishikawa, Y., Aoyama, T. and Miyasato, M., *Seasonal variation of*

chloride ions by spraying of de-icing salts, Proceedings of Annual Conference, Japan Concrete Institute, Vol. 32, pp. 815-820, 2010. (in Japanese)

Hirono, S., *Domestic alkali-silica reactive aggregate from a petrology point of view.* Concrete Technology, Vol. 30, 11, pp 9-15, 2011. (in Japanese)

Hirono, S., *A basic study on geological distribution of reactive rocks in Japan and the assessment of Alkali-silica reaction for aggregates by petrographic examinations.* Ph.D. thesis of Kanazawa University, 2015. (in Japanese)

Honjo, K., Nakano, M., Fujiwara, N., Kazume, K. and Maki, H., *Investigation of deteriorated RC slabs by chloride attack of de-icing salts*, Repair of the concrete structure, reinforcement, upgrade paper report, Vol.10, pp. 51-56, 2010. (in Japanese)

Ibata, S., Yano, T., Kubo, Y. and Hashizume, Y., 2014. *Estimate the degree of influence of de-icing salts based on monitoring results on structures affected by de-icing salts spraying*, Proceedings of Annual Conference, Japan Concrete Institute, Vol. 36, 1, pp. 934-939, 2014. (in Japanese)

Japan Concrete Institute (JCI), *Survey of cracks in concrete, repair and reinforcement guidelines*, 2003. (in Japanese)

Japan Concrete Institute (JCI), *Report of Research on the suppressive measures and diagnosis of Alkali-aggregate reaction considering to action mechanism*, Proceedings of Japan Concrete Institute, 2008. (in Japanese)

Japan Society of Civil Engineers (JSCE), *Alkali-Aggregate Reaction Subcommittee Report*, Concrete Library 124, 2005. (in Japanese)

Yokoyama, K., Honjo, S., Katsuhime, K., and Fujiwara, N., *Study on clarification of the degradation mechanism accompanied on corrosion of steel bars of road bridge RC slab.* Proceedings of Annual Conference, Japan Concrete Institute, Vol. 30, 3, pp. 1687-1692, 2008. (in Japanese)

Wakizaka, Y., *Alkali-silica reactivity of Japanese rocks*, Engineering Geology, Vol. 56 (2000), pp. 211-221, March 1999.

CHAPTER 3 EVALUATION OF COMBINED DETERIORATION IN CONCRETE BRIDGE DECKS USING FWD METHOD

3.1 Introduction

Currently, the early deterioration of reinforced concrete structures requires the application of appropriate countermeasures to extend serving life of structures. In Japan, a large number of structures require to be maintained and repaired because an enormous number of works was constructed in the period of high economic growth in the past. Many concrete bridges, which were constructed in this period, have been deteriorating due to single deterioration or combined deterioration of chloride-induced corrosion, alkali-silica reaction (ASR), carbonation, frost damage, etc. In particular, the degradation or damage of deck slabs has been closely related to fatigue deterioration caused by loading and increasing of traffic vehicles. The mechanism of fatigue deterioration is studied based on accumulated research that included the wheel load running tests to determine appropriate countermeasures for deck slabs deteriorated by fatigue.

Beside of fatigue deterioration, some studies reported that concrete structures or even repair material have been deteriorated remarkably in a short period of time (Kazuaki et al. 2008 and Hosono et al. 2010). In the winter, many concrete bridges were affected by de-icing salts sprayed on the road to ensure the safety of traffic vehicles since the studded tires were banned in Japan. Additionally, many concrete structures, which used reactive aggregates, have been deteriorated by alkali-silica reaction (Ishikawa et al. 2012). Furthermore, these researchers also concluded that combined deterioration caused by de-icing salts and ASR affected seriously to the durability of deck slabs in the early stage of these structures. When this combined

deterioration occurred in concrete material, cracks was proceeded, developed and increased the supplying of water and oxygen from outside. Thereafter, fatigue deterioration could occur easier in concrete due to the reduction of the soundness of concrete.

When concrete structures were deteriorated by alkali-silica reaction, the ASR expansion was appropriately suppressed by the restraint of reinforcing bars in structures such as beams, piers, abutments, etc. Hence, the deterioration due to ASR influenced insignificantly to the load carrying capacity of these structures (JSCE. 2005). However, when ASR occurred in the deck slabs of bridges, it was reported that many horizontal cracks appeared due to ASR expansion because reinforcing bars did not restrain ASR expansion through the vertical direction in comparison with beams and piers (Kubo et al. 2009). Regarding the mechanical performance of deck slabs that were deteriorated by the alkali-silica reaction, the result of load test showed the strength of concrete decreased significantly. In particular, it was reported that the elastic modulus of concrete obtained from the compressive strength test reduced remarkably (Kubo et al. 2014).

Deterioration of material in the deck slabs affects considerably on the fatigue resistance of structures. Therefore, it is necessary to investigate the current state of fatigue deterioration in the early stage and to perform appropriate assessments to the fatigue resistance of structures. One of proper methods to evaluate the soundness of concrete deck slabs is the Falling Weight Deflection (FWD) method. Some researchers used this method to assess the soundness of deck slabs based on the evaluation of appropriate countermeasures for existing reinforced concrete deck slabs (Mikio et al. 2004, Kyohei et al. 2015). As the main features of FWD method, the information such as degradation levels of deck slabs or the presence/absence of local damage can be obtained by measuring the deflection of target deck slabs. On the other hand, it was reported that the deck slabs could be deteriorated considerably by fatigue deterioration combined with material deterioration caused by de-icing salts, frost damage, alkali-silica reaction, etc. (Tanaka et al. 2014, Kobayashi et al. 2014).

In this chapter, the experimental investigation was conducted to clarify the performance of concrete deck slabs by using the small FWD tester. All the investigated slabs were degraded by an individual or combined deterioration of alkali-silica reaction and chloride attack.

3.2 Outline of the experiment

3.2.1 Specimen

In this experiment, two types of aggregate were used in concrete slabs, one type was mixed with reactive aggregates and the other was mixed with nonreactive aggregates. The mixing amount of reactive fine aggregate was 30% (by volume) of total fine aggregate volume. In addition, sodium chloride (NaCl) was added into concrete mix proportions to attain the chloride ion content obtained from de-icing salts. The additional content of sodium chloride was adjusted in $5.8kg/m^3$ of equivalent alkali content (Na_2O_{eq}). In the case of combined deterioration of alkali-silica reaction (ASR) and de-icing salts, a larger content of NaCl was added in $8kg/m^3$ of equivalent alkali content. The mix proportions of concrete of all specimens are shown in **Table 3.1.**

Table 3.1 The mix proportions of concrete specimens

Concrete classification	W/C (%)	Unit (kg/m^3)							
		W	C	G	Sn	Sr	W$_{ra}$	AE agent	NaCl
Ordinary concrete	63	170	270	945	881	0	1.76	0.041	0
Ordinary concrete + Chloride attack	63	170	270	945	881	0	1.62	0.035	8.24
Reactive concrete + Chloride attack	63	170	270	945	613	268	1.62	0.035	12.39

Sn*: non-reactive fine aggregate,* Sr*: reactive fine aggregate,* Wra*: water reducing agent*

The dimensions of all specimens were 1150mm in length, 1150mm in width and 100mm in thickness. Steel bars D10 were used as reinforcing bars in these slabs and the ratio between steel and concrete was 1.07% (compressive side: 0.36% and tensile side: 0.71%). The number of main and distribution reinforcing bars in slabs was set equal and these bars were placed at 20mm, 80mm, and 30mm, 70mm from the top of concrete slabs, respectively. The positions and the number of steel bars in experimental concrete slabs were described in **Figure 3.1**.
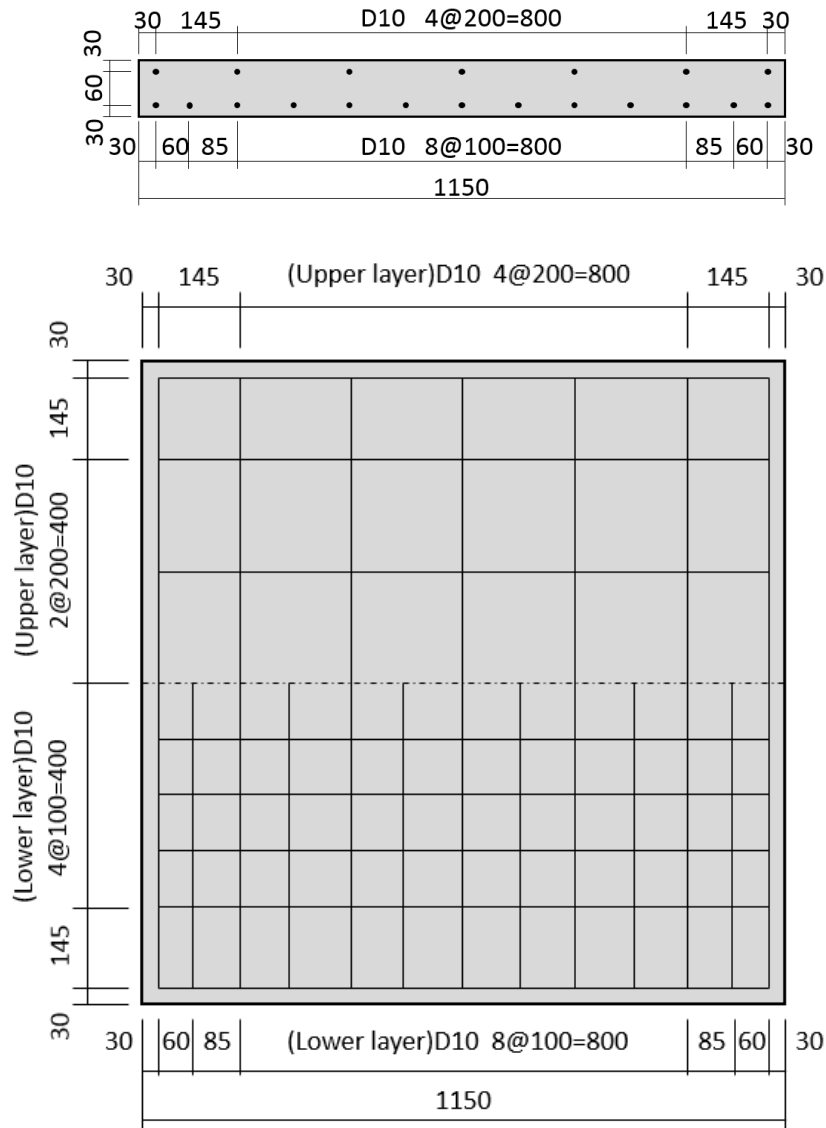
Figure 3.1 The position of steel bars in the specimens

When concrete slab specimen was affected by only ASR, the epoxy resin was coated to all steel bars (main and distribution reinforcing bars) before concrete casting, thus, steel corrosion was prevented due to the sodium chloride addition. In specimens were affected by combined deterioration of ASR and chloride attack, three types of steel bars were used in these concrete slabs. Epoxy resin was coated on the upper, lower or both layers of the main and distribution steel bars, respectively. Lastly, in specimens were deteriorated by only chloride attack, epoxy resin was coated to the upper or the lower layer of steel bars in these concrete slabs. In comparison with the ordinary concrete slab specimen, all steel bars were coated with the epoxy resin for both upper and lower layers of steel bars. **Table 3.2** shows the list of concrete slab specimens in this study.

Table 3.2 Name of specimens and deterioration factors

Explanation of deterioration causes	Slab name	Deterioration factor	Aggregates	Epoxy coating
Affected by ASR 1	AS-1	ASR	Reactivity	Coated both layers
Affected by ASR 2	AS-2	ASR	Reactivity	Coated both layers
Combined deterioration (deteriorated lower layer)	AC-L	ASR + chloride attack	Reactivity	Coated upper layer
Combined deterioration (deteriorated upper layer)	AC-U	ASR + chloride attack	Reactivity	Coated lower layer
Combined deterioration (deteriorated both layers)	AC-B	ASR + chloride attack	Reactivity	Uncoated both layers
Affected by chloride attack (deteriorated lower layer)	CH-L	Chloride attack	Normal	Coated upper layer
Affected by chloride attack (deteriorated upper layer)	CH-U	Chloride attack	Normal	Coated lower layer
Sound concrete	SC	None	Normal	Coated both layers

After casting all concrete slab specimens, steam curing (steam temperature was kept at 50°C) was carried out in the specimen molding room. Next step, the concrete molds were released and then outside specimens were covered with the vinyl sheets for about 2 to 3 weeks to suppress the drying. After the completion of curing by the vinyl sheet covering, all specimens except ordinary concrete slab were steamed at 50°C from 10 to 12 hours per day. Hence, the ASR expansion was promoted in the concrete slabs. These specimens were moved to the outdoor environment approximately one-year later.

3.2.2 Measurement and test methods

3.2.2.1 Observation of cracks

The appearance of cracks on the surface of specimens was observed by visual images, then, the diagram of cracks was drawn. The crack width was measured with a crack gauge ruler.

3.2.2.2 Expansive strain measurement

In order to ascertain the expansion behavior inside specimen, an embedded mold gauge (PMFL-50, manufactured by Tokyo Instruments Co., Ltd., base length:

50 mm) was buried via the vertical direction (thickness direction) at the center of a specimen and the vertical expansive strain was measured. Contact gauge chips were attached to the concrete surface at four sides of each specimen and the expansive strain via horizontal direction was measured (base length: 250 mm). The measurement positions of mold gauge and contact gauge chips of each specimen are shown in **Figure 3.2**.
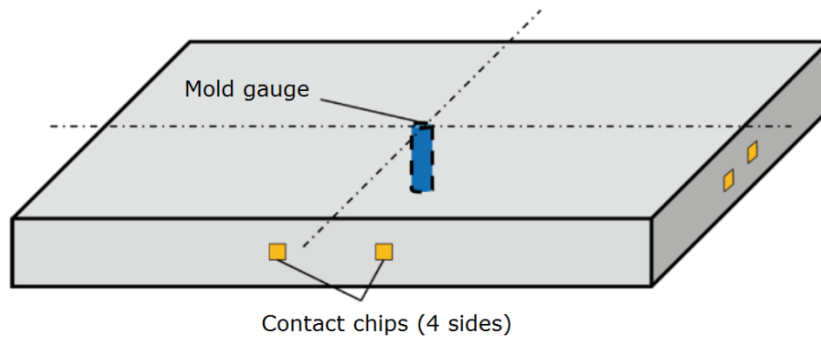
Figure 3.2 Positions of contact gauge chips and mold gauge

3.2.2.3 Corrosion measurement of reinforcing bars

In the cases of combined deterioration and only degradation caused by chloride-induced corrosion, measured copper wires were attached to reinforcing bars that were not coated with epoxy resin, and the half-cell potential and polarization resistance were measured by using a portable corrosion rate instrument. The electrodes were installed at the intersection of main and distribution steel bars for both upper and lower layers when concrete slabs were cast. The corrosion measurement was performed at three points near the center part of each specimen. The criteria of ASTM C-876 and CEB recommendation were used to evaluate steel corrosion by half-cell potential and polarization resistance, respectively.

3.2.2.4 Ultrasonic propagation speed

In order to clarify the influence of cracks generated inside slabs due to deterioration of only ASR, combined deterioration and only chloride attack, the ultrasonic propagation speed was measured by using the ultrasonic pulse velocity tester (Proceq). In order to avoid the influence of steel bars, the positions of the measured points were selected on the center lineof concrete slab sides. For each specimen, five to six positions on the side surface were chosen to measure ultrasonic propagation speed. This measurement was performed three to five times at each

measured point to assure the accuracy of data, then, the average value was calculated for each concrete slab specimen.

3.2.2.5 Deflection measurement by FWD method

Using the compact FWD equipment (see in **Figure 3.3**), the center displacement (maximum value) and the impact load were measured with a height of 50cm and a weight of 5kg. These concrete slabs were fixed at four sides on the firm steel frame (see in **Figure 3.4**) and the weight was loaded at the center of each slab. The deflection of each slab was measured from three to five times to ensure the accuracy of the data.
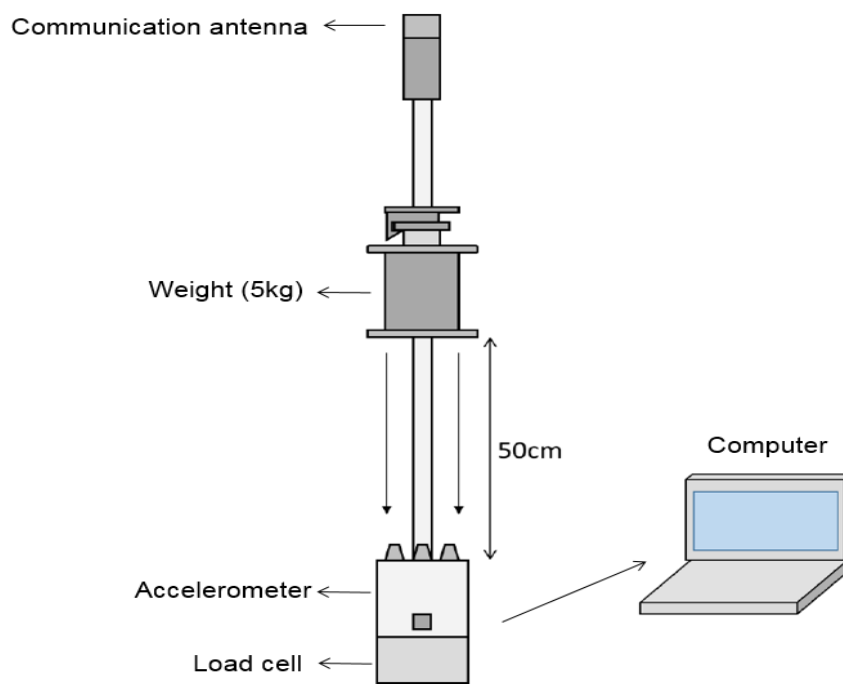
Figure 3.3 FWD equipment

Figure 3.4 The steel frame for FWD experiment

3.3 Results and Discussion

3.3.1 Observation of cracks on concrete surfaces

Table 3.3 shows the characteristics of the cracking properties based on the appearance observation result. Observation of cracks on the surface of some specimens is shown in **Figure 3.5**.

Table 3.3 Cracks description of each specimen

Slabs name	Top view	Bottom view
AS-1, AS-2	Small cracks occurred along the steel bars direction, crack width $\leq$ 0.2mm	Small cracks occurred along the steel bars direction, crack width $\leq$ 0.2mm
AC-L	Almost without cracks	Cracks shaped lattice along steel bars, crack width $\leq$ 0.2mm
AC-U	Many large cracks appeared along the steel bars (lattice shape) with crack width $\geq$ 0.2mm	Almost without cracks
AC-B	Cracks shaped lattice along the steel bars, crack width $\leq$ 0.2mm	Cracks shaped lattice along steel bars, crack width $\leq$ 0.2mm
CH-L	Almost without cracks	Almost without cracks
CH-U	Almost without cracks	Almost without cracks

In the specimen affected by only ASR, a few cracks along the position of reinforcing bars occurred on both upper and lower surfaces. Many small cracks that did not appear at steel bar positions could be observed on the surface of this slab. However, most small cracks (crack width is smaller than 0.2mm) appeared except some cracks near the side of this specimen were larger than 0.2mm.

Conversely, in specimens deteriorated by combined deterioration, many large cracks (crack width was from 0.2mm to 0.4mm) occurred along steel bar positions on the upper surface of slab AC-U. In this specimen, the upper layer of steel bars was not coated with epoxy resin and these bars could be corroded easier. It could become a significant reason for the appearance of many large cracks on the upper surface of this slab. However, on the lower surface slab AC-L where the epoxy was not coated for the lower layer of steel bars, few cracks could be observed and most of them had crack width was smaller than 0.2mm. In this case, the more steel bars of lower layer

could contribute significantly to reduce the number and the width of cracks in comparison with specimen AC-U. In particular, the more steel bars of lower layer had a better effect for the tensile strength of concrete and it could result in the smaller number and width of cracks caused by ASR expansion. In the specimen AC-B that both layers of steel bars were not coated with epoxy, many cracks on upper surface occurred along steel bar positions and these cracks did not become noticeable (almost crack width of 0.2mm or less). It is considered that ASR expansion in this slab was dispersed to both upper and lower surfaces, although both steel bar layers were corroded due to chloride attack.
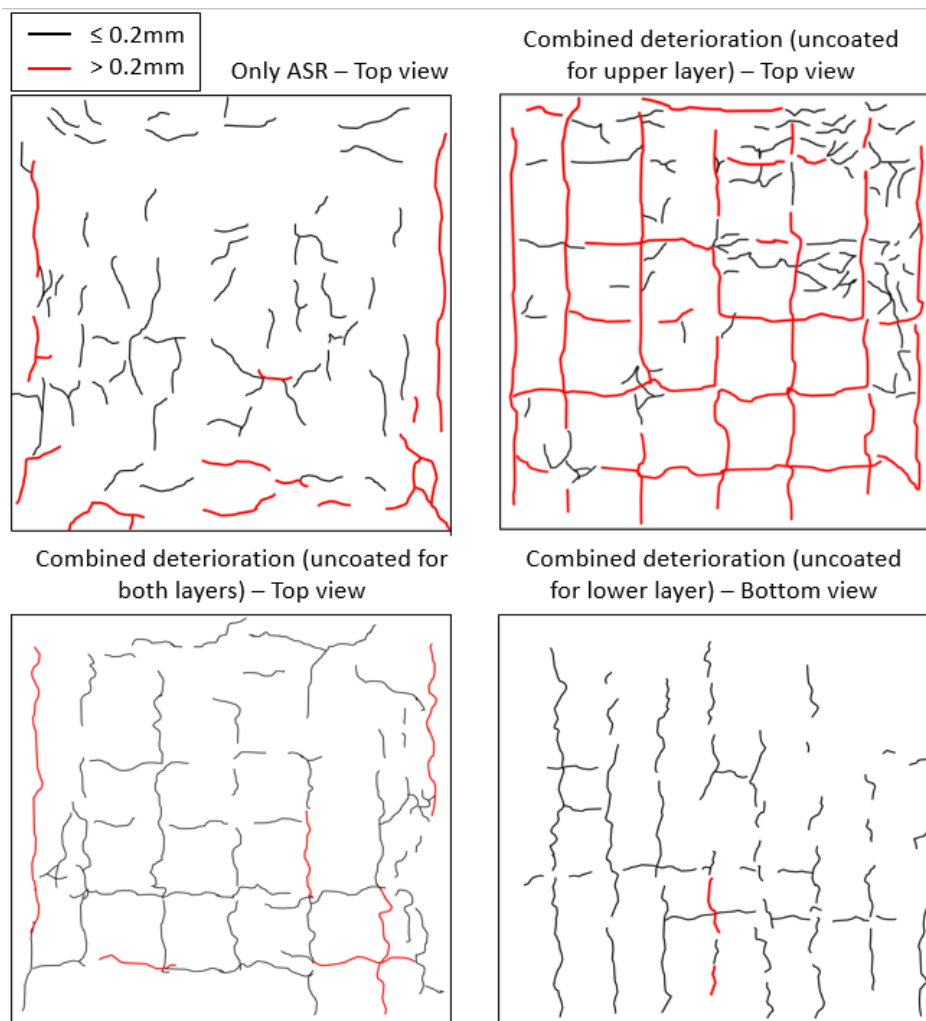
Figure 3.5 Sketching of cracks on the surface of some specimens

Lastly, on the surface of specimens deteriorated by only chloride attack, cracks were hardly observed on the surface of these slabs. At this stage, it is considered that the corrosion grade of the reinforcing bars may not reach the point for the occurrence of cracks due to chloride attack.

From this observation results, the influence deterioration factors such as ASR, chloride attack and a combination of ASR and chloride attack showed some significant results. In specimens affected by combined deterioration, it was confirmed that the occurrence of cracks was more noticeable than the case of only ASR deteriorated to concrete slab. Many cracks occurred along steel bar positions and it showed the sufficiency of chloride ion content in steel corrosion. In addition, all specimens were cured and stored in the condition to promote ASR. Few small cracks on the surface of slabs CH-L and CH-U suggested that the occurrence of cracks due to ASR expansion could occur earlier than the case of chloride attack.

3.3.2 Expansive strain

The horizontal expansive strain measured on the side surfaces of slab specimens is shown in **Figure 3.6**. Since the ratio of the main and the distribution steel bars was the same, the average value was calculated from the expansive strain at four sides and it was taken as the expansive strain of each specimen.
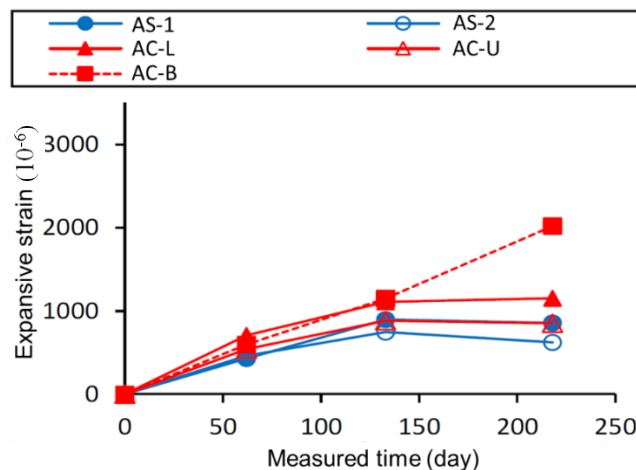
Figure 3.6 Expansive strains along the horizontal direction

Most values of expansive strain along the horizontal direction are from 800 to 1500 x 10^{-6}. It is considered that the horizontal expansion of concrete slabs caused by ASR and combined deterioration is restrained due to the large ratio of steel bars and concrete (1.07%). In the previous study in the relationship between reinforcement restraint and ASR expansion, when the reinforcement restraint reached 0.8% or more, the expansion was suppressed greatly in comparison with the unrestrained specimen (JSCE. 2005). In specimens affected by combined deterioration (AC-B), steel bars of both upper and lower layers were deteriorated by chloride attack, and the expansion

tended to increase during the last measured period. In this specimen, steel bars of both layers were corroded and the adhesion between steel and concrete decreased significantly. In addition, the ASR expansion had continued to occur. Therefore, the horizontal expansion of this case could be increased for the last period of measurement.

In a real environment, when the concrete cover depth is small, the chloride ion is easier to penetrate into concrete material and corrodes steel bars through water leakage included de-icing salts. It seems that corrosion of steel bars and ASR progress at the same period leads to the larger expansion and cracking in concrete. As the cracking observation mentioned above, many cracks also occurred in specimens affected by ASR alone. However, the shape of cracks was not the same as the specimen affected by combined deterioration (AC-U). Although the expansion behavior of concrete of all specimens is quite similar, the expansion caused by both ASR expansion and chloride attack tends to be larger than other specimens affected by only ASR.

The expansive strain along the thickness direction of concrete slabs is shown in **Figure 3.7** and these values were from 2500 to 3500 x 10^{-6} at the end of measurement. This measurement was carried out by the mold gauge buried at the center of slabs. The values of expansion along the thickness direction of all specimens affected by ASR or combined deterioration were similar or it seems that there is no significant difference between these cases. The large expansive strain could be explained due to steel bars did not restrain the expansion along the thickness direction in both cases of specimens affected by only ASR and combined deterioration.
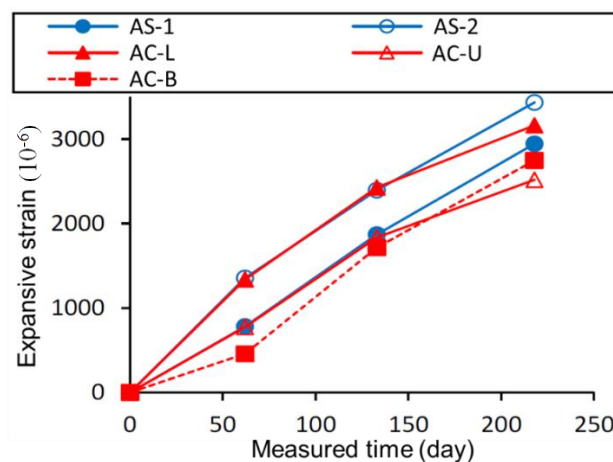
Figure 3.7 Expansive strains along the thickness direction

The horizontal cracks are shown in **Figure 3.8** as an example of cracking occurred on the side of specimens that were affected by ASR alone or combined deterioration. If a large expansion occurs through the unconstrained thickness direction, it is considered that the horizontal cracks and cracking damage corresponding to ASR expansion will occur inside the slabs.
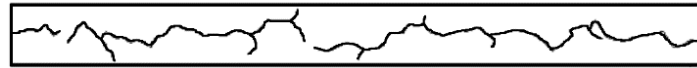
Figure 3.8 An example of cracks occurred on the side of a specimen

3.3.3 Measurement of reinforcing bar corrosion

The measurement results of half-cell potential and polarization resistance of specimens affected by only ASR and combined deterioration are shown in **Figure 3.9** and **Figure 3.10**, respectively. Most of the values of half-cell potential shown in the corrosion zone indicate steel bars in all specimens could be corroded. The content of chloride ion mixed in specimens affected by combined deterioration and only chloride attack was 7.6 kg/m^3 and 5.0 kg/m^3, respectively. The suitable content of NaCl or chloride ion added in these specimens revealed the corrosion risk of steel by half-cell potential measurement. Additionally, all specimens were kept in the environmental conditions to promote the ASR (steamed at 50°C from 10 to 12 hours per day), thus, steel corrosion could be developed faster in this environment. Before the measurement by electrochemical method (half-cell potential and polarization resistance), the steam curing was stopped and all specimens were stored in room temperature, then the measurement was carried out.
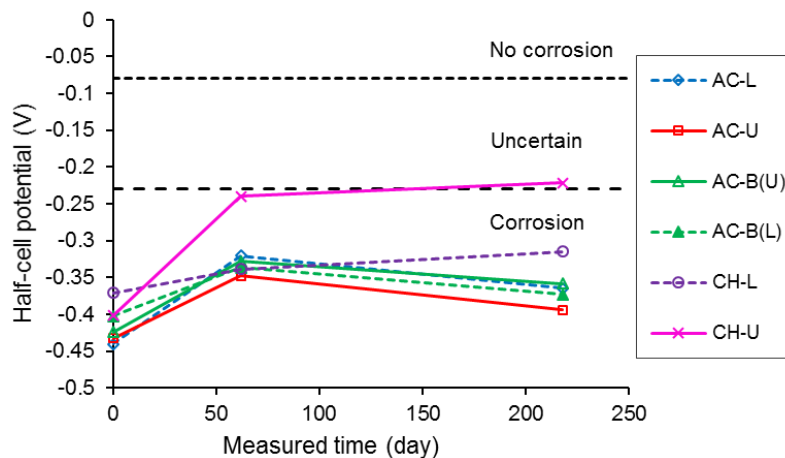
Figure 3.9 Half-cell potential of specimens affected by chloride attack

Regarding the polarization resistance values, although the result showed a tendency that these values had been increasing (decrease in corrosion rate) with the increase of promotional period, most value was shown in the high and the moderate to high corrosion zones. In the calculation of polarization resistance value, the polarization range was assumed of 10 cm. The polarization range decreased when corrosion occurred and there was a possibility that it was shifted to a smaller polarization range than the presumption. Therefore, it is necessary to conduct concrete chipping and to investigate the actual situation of steel corrosion.
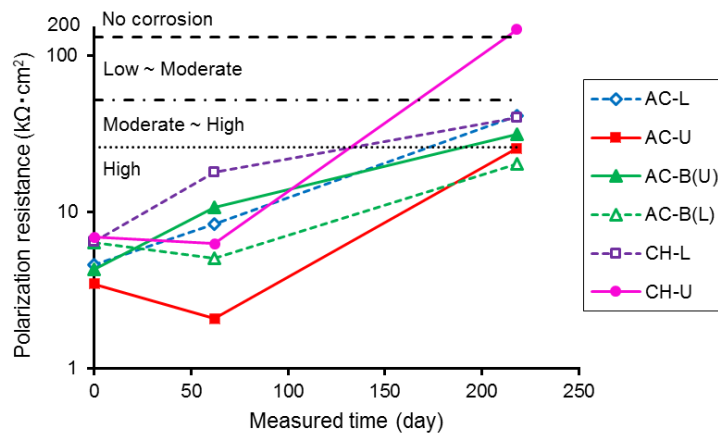
Figure 3.10 Polarization resistance of specimen affected by chloride attack

As stated in the cracking observation results above, cracking behavior was different between combined deterioration and chloride attack alone, and the occurrence of cracks along the reinforcing bars was most conspicuous in the case of combined deterioration. However, the polarization resistance results showed an insignificant difference, in other words, cracking behavior of concrete slabs did not affect significantly. The reason for this can be presumed that the water content near vicinity of steel bars is nearly the same in the promoting environment (steaming condition), regardless of the presence or absence of cracking properties. Regarding the corrosion measured by the electrochemical method, since the difference between chloride attack alone and combined deterioration did not appear clearly in the promoting environment, it is necessary to investigate and to clarify the influence of environmental conditions in the future.

3.3.4 Ultrasonic wave propagation speed

Figure 3.11 shows the ultrasonic wave propagation speed of each specimen which was measured through the thickness direction of slabs. These average values

were calculated from all measured points on each specimen, the maximum and minimum values are shown in this figure. As for the average value, the ultrasonic propagation speed of sound concrete slab was about 4700 m/s while these values of slabs affected by ASR alone and combined deterioration were lower than 4300 m/s or even below 4000 m/s in the case of combined deterioration. However, in the case of specimens affected by chloride attack alone, the ultrasonic wave propagation speed is same as the case of sound concrete. The horizontal cracks and/or cracks inside specimens, which was the result of ASR expansion along the thickness direction, became a significant reason for the decrease of ultrasonic propagation speed of specimens affected by ASR alone and combined deterioration.
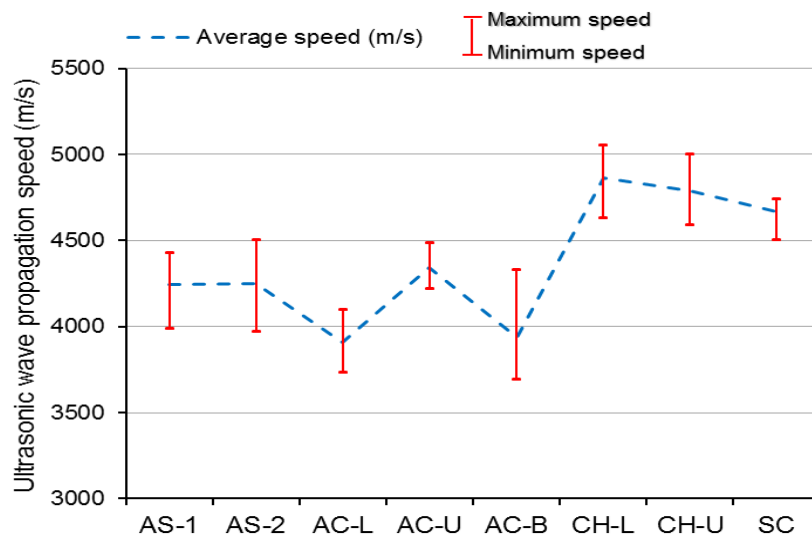
Figure 3.11 The ultrasonic propagation speed of all specimens

3.3.5 Deflection measurement by FWD method

The maximum impacted load of each specimen measured by FWD method is shown in **Figure 3.12**. The maximum load of ASR alone and combined deterioration were slightly smaller than sound concrete and only chloride attack. However, all maximum loads were about 5000 N for all specimens. There was no notable difference in the maximum load due to the presence or absence of ASR deterioration, chloride attack and combined deterioration in this experiment.

The displacement attained at the center of each slab is measured by FWD method and this result is shown in **Figure 3.13**. The average displacement of sound concrete slab and slabs affected by only chloride attack were about 0.12 mm, whereas

these values of ASR specimens and combined deterioration specimens were about 0.15 mm and about 0.15 to 0.17 mm, respectively.
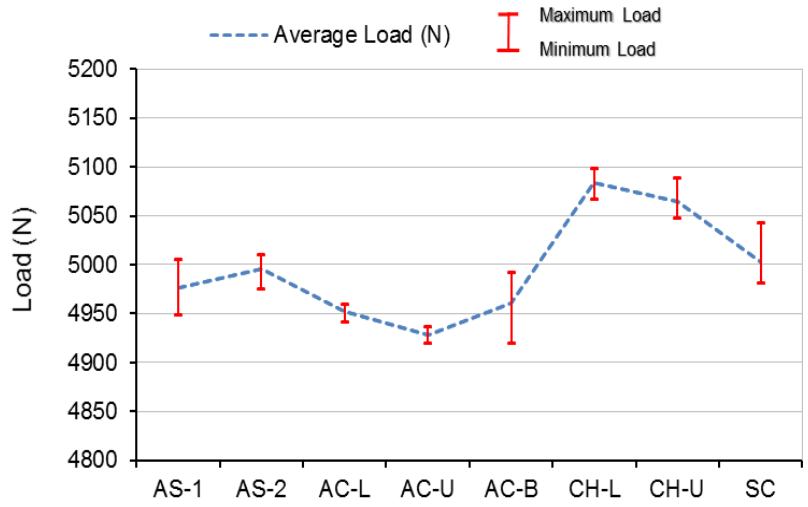
Figure 3.12 The impacted load of all specimens by FWD measurement
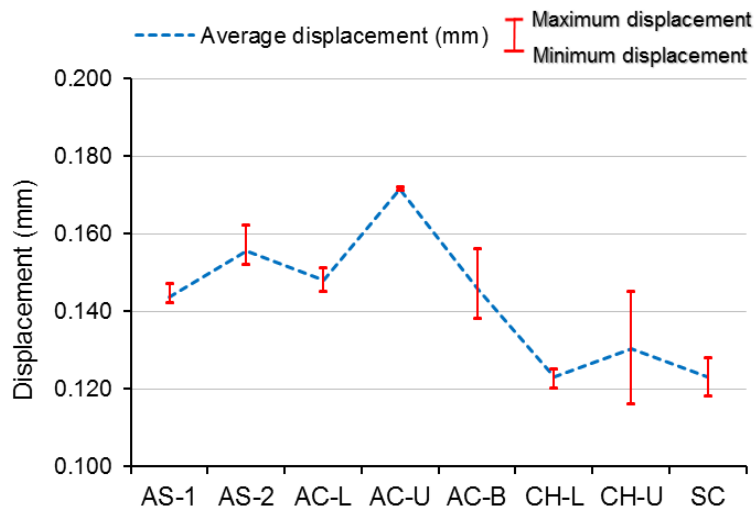
Figure 3.13 The center displacement of all specimens by FWD measurement

Since the soundness of the slabs decreased due to the ASR expansion, the displacement of specimens affected by ASR alone or combined deterioration was larger than that value of sound concrete. On the other hand, in the comparison between chloride attack and sound concrete specimens, the displacement results showed no difference. It seems that the current corrosion progressing did not affect significantly the displacement of these slabs.

3.4 Conclusion

The main results obtained in this chapter are shown as below:

(1) From the results of cracking observation, cracks occurred along steel bars direction were more conspicuous in combined deterioration specimens than specimen affected by only ASR.

(2) When ASR and chloride attack are combined, the possibility of expansion and crack development is large. Furthermore, there is a high possibility that the cracks caused by ASR occur earlier than that due to the corrosion caused by chloride attack alone.

(3) From corrosion measurement results, the corrosion progression of reinforcing bars was confirmed in both cases of chloride attack alone and combined deterioration. However, the notable difference between them at this stage could not be confirmed in this study.

(4) From the result of ultrasonic wave propagation speed through the thickness direction of slabs, it could be confirmed that the horizontal cracks or cracking damage occurred due to ASR expansion in specimens affected by ASR and a combination of ASR and chloride attack.

(5) By FWD method, the center displacement of ASR-affected and combined deterioration concrete slabs are larger than that value of sound concrete, and it can be recognized whether or not degradation has occurred. In the specimen influenced by chloride attack alone, it cannot confirm the significant difference with sound concrete in the early stage of concrete.

(6) It is necessary to conduct further investigations to clarify the influence of promotion environment (curing, stored condition, etc.) between specimens affected by ASR and combined deterioration, and the corrosion progression due to varied states of deterioration in concrete.

References

Yokoyama Kazuaki, Honjo Sushiji, Katsuhime Kazuhiro, Fujiwara Norio, *Study on the elucidation of deterioration mechanism accompanied by rebar corrosion of road bridge RC deck*, Concrete engineering annual paper, Vol. 30, No. 3, pp. 1687-1692, July. 2008.

Hokkaido Hosono, Masahiro Nakano, Masao Fujiwara, Kazuhiro Kuzuma, *Detailed survey of Steel Bridge RC slab with salt damage deterioration due to de-icing salts spraying*, Repair of concrete structure, Reinforcement, upgrade paper report collection, Vol. 10, pp. 51 - 56, 2010.

Hiroyuki Ishikawa, Yoshimori Kubo, Hiroyuki Yokoyama, Kazuya Yuya, *Survey on the influence of de-icing salts on concrete structures*, Annual Concrete Engineering Work, Vol. 34, No.1, pp. 766- 771, July. 2012.

Japan Society of Civil Engineers (JSCE): *Report on Subcommittee on Alkali-Aggregate Response Countermeasure*, Concrete Library 124, August. 2005.

Yoshimori Kubo, Takashi Sako, Fumiaki Kawasaki, Hiroshi Yokoyama, *ASR expansion behavior of floor panel members and expansion suppression by FRP sheet affixation*, Annual Concrete Engineering Proceedings, Vol. 31, No. 1, 2009.

Yoshimori Kubo, Kohani Ichihara, Hiroyuki Yokoyama, Hiroshi Masuya, *Basic Study on Elastic Behavior of ASR-Deteriorated Slab*, Report of the 8th Symposium on Road Bridge Deck Reports, pp. 45-48, October. 2014.

Mikio Sekiguchi, Katsuro Kunifu, *Investigation of the soundness assessment of deck slabs by FWD method*, Papers of science and engineering, Vol.50A, pp. 697-706, March. 2004.

Yamaguchi Kyohei, Hayasaka Yohei, Soda Nobuo, Ohnishi Hiroshi, *A consideration on soundness assessment method of existing RC deck using FWD*, Papers of science and engineering, Vol. 61, pp. 1062 - 1072, March. 2015.

Yoshiki Tanaka, Junichi Murakoshi, *Diversification of Degradation Morphology and Waterproofing Measures of Reinforced Concrete Slabs of Road Bridge*, Report of 8th Road Bridge Deck Symposium Papers Report, pp. 281-284, October. 2014.

Koichi Kobayashi, Yu Shikano, Ebisu Rokugo, *Case of combined deterioration due to frost damage and ASR of RC deck slab in the mountain and cold regions, and the verification of experiments*, papers of JSCE, Vol.70, No. 3, pp. 320-335, 2014.

CHAPTER 4 INFLUENCE OF ASR EXPANSION ON THE INTERFACE BETWEEN PATCHING MATERIAL AND ASR-DETERIORATED CONCRETE

4.1 Introduction

Recently, patching method (cross-sectional restoration) has been applied as one of proper methods for concrete structures deteriorated by ASR. However, the current techniques are not established to predict the high precision of expansion after the applying of patching material. This method is applied for ASR-affected concrete after removing the deteriorated parts or concrete containing chloride ions. Then, patching material and the interface between substrate concrete and patching material is expected to expand and deform. Nevertheless, the adhesion properties of the interface could be deteriorated or cracks could occur at the interface when the expansion of ASR-affected concrete was too large. Hence, this phenomenon could be affected in the performance of patching method. In particular, some researchers reported that when repair materials such as surface coating and/or patching material were implemented, the residual expansion could continue to occur (Kubo and Miyano. 2009, Kubo and Torri. 2002) and crack had still occurred (Nomura et al. 2013).

In this chapter, the experiments were carried out to investigate the influence of ASR residual expansion on patching material and the interface between "substrate concrete" and patching material. The substrate concrete was made to simulate the condition of concrete affected by ASR expansion. Additionally, adhesion tests were conducted to evaluate the performance of the interface properties and patching material. The images of cracks were observed with a fluorescence microscope to determine the influence of ASR expansion upon cracking behavior. Furthermore, when cracks occurred, there was a possibility that chloride could attack substrate concrete or even patching material. The Electron Probe Micro-Analyzer (EPMA) test was carried out to recognize the chloride ion penetration.

4.2 Outline of the experiment

In order to clarify the influence of ASR expansion on the interface and patching material, two series of this experiment were performed. In the experimental series 1, reactive aggregates and sodium hydroxide (NaOH) were mixed in substrate concrete to create the ASR expansion. Three specifications of patching materials were conducted to compare the effectiveness of different types of patching materials. The expansive strain and the adhesive strength were measured by contact gauge chips and pull-off test, respectively.

When the large expansion occurred in substrate concrete, some cracks appeared on the surface and inside this substrate concrete specimen. In the experimental series 1, all failures occurred in substrate concrete when adhesion tests were carried out. However, in specimens used natural reactive aggregates and NaOH, it was difficult to attain the target expansion levels in the simulation of ASR expansion. Therefore, the experimental series 2 were conducted to expect the integrity of substrate concrete was maintained and the failure could occur at the interface or patching material. In this series, the expansive concrete was cast into the hollow part of the substrate concrete specimen. The suitable amount of expansive admixture was added to ensure the attaining expansion and remain the integrity of substrate concrete. After that, the expansive strain and adhesive strength of specimens were measured similarly as the methods in the experimental series 1.

4.2.1 The experimental series 1

4.2.1.1 Specimens

Substrate concrete specimens were prepared to simulate concrete structures affected by ASR. In this experiment, the Kimitsu river sands and the Tedori river gravels were used. The andesite aggregates were used as reactive fine aggregates. The mixing amount of reactive fine aggregates was 30% by mass of fine aggregates. Additional alkali content was added to promote ASR and its expansion. The equivalent alkali content (Na_2O_{eq}) was set to 5 kg/m^3 by sodium hydroxide.

The water-cement ratio of substrate concrete was 55% and ordinary Portland cement was used. The coarse aggregate was gravel (density: 2.60g/cm^3, water absorption: 1.97%, fineness modulus: 7.00) and the fine aggregate was river sand

(density: 2.59g/cm^3, water absorption: 1.81%, fineness modulus: 2.80). The mix proportion of substrate concrete is shown in **Table 4.1**.

Table 4.1 Mix proportion of substrate concrete in series 1 (kg/m^3)

W/C (%)	W	C	G	S	Sr	AE agent	NaOH
55	168	305	980	550	236	0.16	5.23

W/C: Water Cement ratio; W: Water; C: Cement; S: Fine Aggregate; Sr: Reactive Fine
Aggregate; G: Coarse Aggregate; AE: Air Entraining Admixture

In this experiment, substrate concrete specimens were cast by using reactive aggregates, and the dimension of a substrate concrete specimen is shown in **Figure 4.1**. After this step, patching material was patched on the upper side of the substrate concrete specimen. Regarding the specifications of patching material, three specifications were prepared by the same high strength mortars together with acrylic primer (specification A1), epoxy resin primer (specification B1) and without primer (specification C1). The specifications of patching materials and a list of specimens are shown in **Table 4.2**. After patching, these specimens were exposed again under accelerating conditions. The expansive strain of the upper part of substrate concrete reached the average values at three levels: 0 (no expansion), from 500 to 800 x 10^{-6} (low-level) and from 1200 to 1500 x 10^{-6} (high-level). The amount of expansive strain of substrate concrete before and after patching in three specifications of patching material is depicted in **Figure 4.2**.

Table 4.2 Specifications of patching material in series 1

Patching Specifications	Name	Specimens name		
		0	**Low-level expansion**	**High-level expansion**
High strength mortar + acrylic primer	A1	A1-N	A1-L	A1-H
High strength mortar + epoxy primer	B1	B1-N	B1-L	B1-H
High strength mortar	C1	C1-N	C1-L	C1-H
Objective expansion (substrate concrete)		No	500 ~ 800 x 10^{-6}	1200 ~ 1500 x 10^{-6}
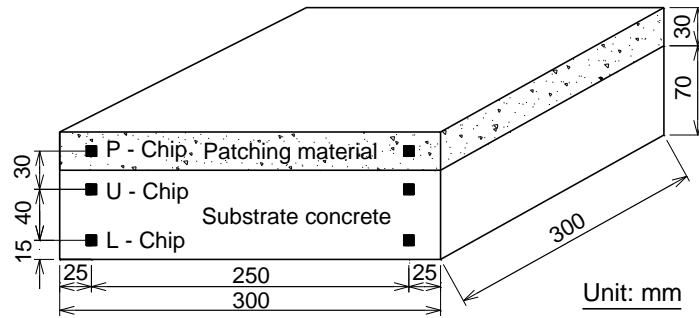
Figure 4.1 Dimension and contact chips position of specimens in series 1
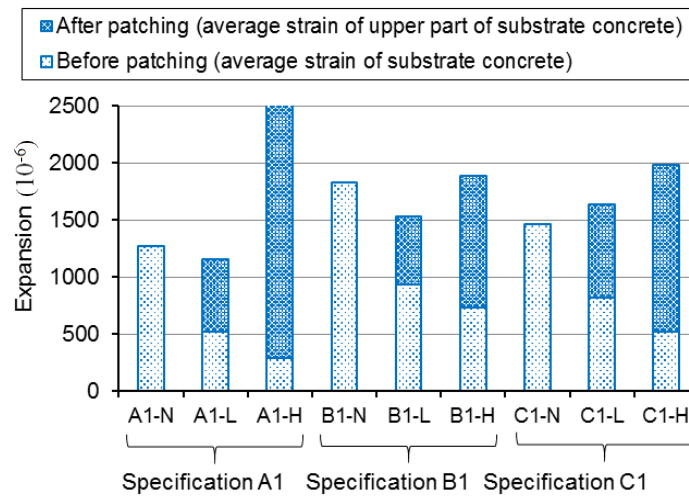
Figure 4.2 Expansive strains of substrate concrete specimen in experimental series 1

4.2.1.2 Expansive strain measurement

The expansive strain of a specimen was measured by contact gauges (base length: 250mm). The contact gauge chips were attached at four sides of the specimens. On each side of a specimen, the chips were glued at three positions: the upper part (U-Chip), the lower part (L-Chip) of substrate concrete and at the middle of patching material (P-Chip) as shown in **Figure 4.1**.

4.2.1.3 Adhesive strength test

In order to investigate the influence of expansion on the interface between patching material and substrate concrete, the adhesive strength was measured by the pull-off test. On the surface of specimens, notches were formed along a square of 50mm × 50mm, and the depth of notches was 40mm. Adhesion tests were carried out in three stages of attaining expansion of low-level, high-level and no expansion. The cutting notch position and the concrete blocks obtained after adhesion test are shown in **Figure 4.3**.
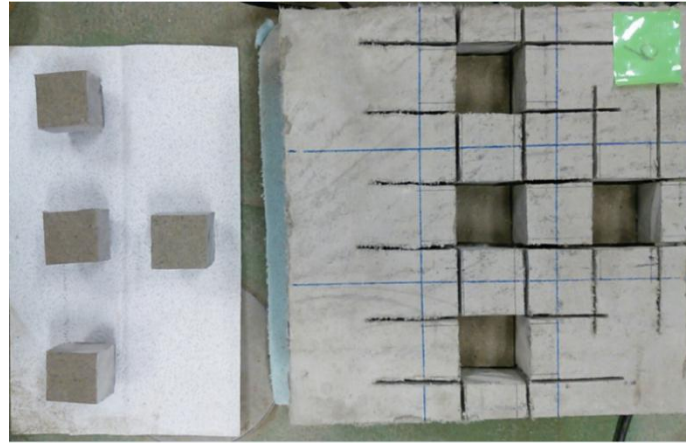
Figure 4.3 The positions of adhesion test on the upper surface

4.2.2 Experimental series 2

4.2.2.1 Specimens

The substrate concrete specimens were constructed with a hollow part (250mm × 250mm × 50mm) in each specimen. These specimens were cast and cured for 14 days. Afterward, they were restored in the room condition (20°C) and three types of patching materials were patched, then, specimens were cured for 4 weeks. An outline of the specimen in this series is described in **Figure 4.4**.
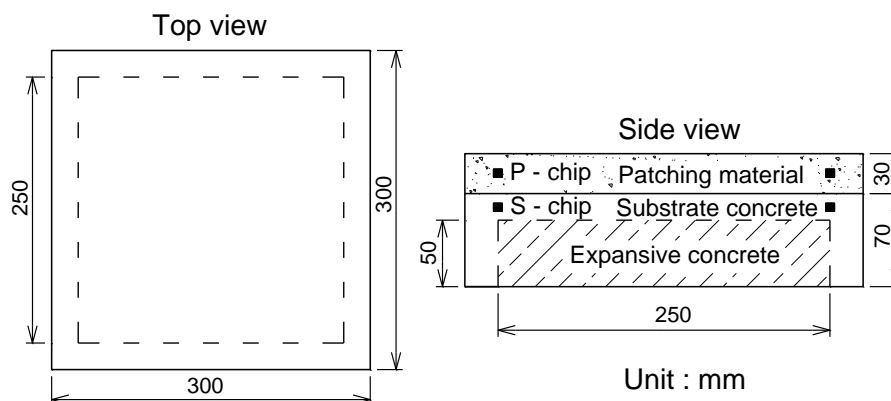
Figure 4.4 Dimension and contact chips position of specimens in series 2

Next step, expansive concrete was cast into the hollow part of substrate concrete, and the measurement of the expansion was started. Many levels of expansive admixture were tested to determine the suitable amount of admixture to ensure the large expansion and the integrity of substrate concrete. Finally, the amount of expansive admixture was mixed in expansive concrete at two levels: 120kg/m^3 (low-level of expansion) and 140kg/m^3 (high-level of expansion). **Table 4.3** shows the

mix proportions of substrate concrete and expansive concrete in this experiment. The ordinary Portland cement was used for all concretes. The water-cement ratio of substrate concrete was 55% and expansive concrete was 40%, respectively. The coarse aggregates were gravel (density: 2.60g/cm^3, water absorption: 1.97%, fineness modulus: 7.00) and the fine aggregates were river sand (density: 2.59 g/cm^3, water absorption: 1.81%, fineness modulus: 2.80).

Table 4.3 Mix proportions of substrate and expansive concretes in series 2 (kg/m^3)

Type of concrete	W/C (%)	W	C	G	S	AE agent	Expansive admixture
Substrate concrete	55	168	305	980	550	0.16	0
Expansive concrete	40	200	380	833	713	0	0,120,140

W/C: Water Cement ratio; W: Water; S: Fine Aggregate;
C: Cement; G: Coarse Aggregate; AE: Air Entraining Admixture

4.2.2.2 Expansive strain measurement

The expansive strain of specimens was measured in the same manner as the experimental series 1. On each side of a specimen, contact gauge chips were glued at two positions: one on patching material (P-Chip) and the other on substrate concrete (S-Chip). The positions of contact gauge chips are shown in **Figure 4.4** above. After patching, the expansive strain of substrate concrete specimen was measured as shown in **Figure 4.5** to simulate the expansion of ASR deteriorated concrete, then, the expansion of patching material and substrate concrete was measured.
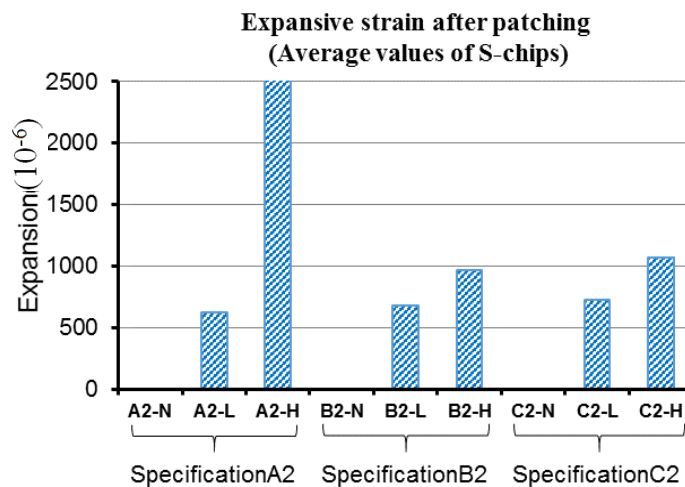
Figure 4.5 Expansive strains of substrate concrete in experimental series 2

4.2.2.3 Adhesive strength test

The adhesive strength test was conducted in the same manner as the experimental series 1. In comparison, one case of this experiment did not cast expansive concrete and the adhesion test was performed in the state of none expansion. The specifications of patching materials and a list of specimens are shown in **Table 4.4**.

Table 4.4 Specifications of patching material in series 2

Patching specifications	Name	Specimens name		
		0	**Low-level Expansion**	**High-level Expansion**
High strength + acrylic primer	A2	A2-N	A2-L	A2-H
High strength + epoxy primer	B2	B2-N	B2-L	B2-H
High strength mortar	C2	C2-N	C2-L	C2-H
The amount of expansive admixture		Not cast	120 kg/m^3	140 kg/m^3

4.2.3 Interface properties of specimens

The interface properties of specimen were carried out on the experimental series 1 in the case of high-level of expansion by microscopic observation and EPMA test.

4.2.3.1 Fluorescence microscope observation

The existence or absence of cracks due to the expansion of patching material and the properties of the interface was observed. Samples for microscope observation were made after the adhesion test. The fluorescence epoxy resin was injected into the concrete under low vacuum condition for 24 hours. The outline of the making of an observation sample is shown in **Figure 4.6**.
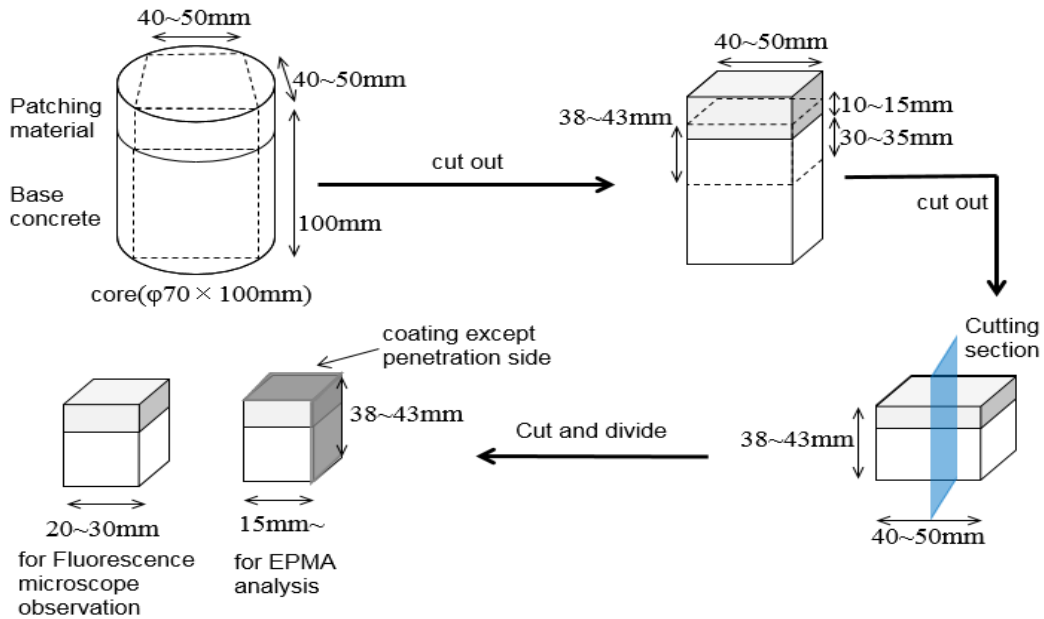
Figure 4.6 Observation sample for EPMA test and fluorescence microscope analysis

4.2.3.2 EPMA analysis

The interface between the substrate concrete and the patching material could be affected by the ASR expansion. When cracks occurred, the vicinity near the interface could become chloride attack routes. In order to confirm the state of chloride attack, samples in the cases of B1-H and C1-H were cut and the chloride attack tests were carried out. The outline of a sample preparation is shown in **Figure 4.6**. All samples were coated with epoxy resin to prevent the permeation of moisture and chloride except for one side for penetrating purpose. This uncoated surface was immersed in sodium chloride (NaCl) solution with 10mm of depth in 6 hours. After immersion in saline, each sample was cut into some slides. The cutting surface was ground smooth for EPMA analysis and then the penetration of chloride ions was observed.

4.3 Results and Discussion

4.3.1 Expansion behavior after patching

4.3.1.1 Expansion behavior in experimental series 1

The results of the expansive strain of substrate concrete and patching material are shown in **Figure 4.7**. These expansive strains were the average values of the strain of P-chip, U-chip, and L-chip on four sides of each specimen. The expansive strain was measured in 18 days in the case of low-level of expansion and in 36 days in the

case of high-level of expansion. In both levels, the deformation of patching material was nearly the same with the expansion of substrate concrete when the strain was not too large and was lower than approximately 500 x 10^{-6}. Hence, the integrity of the interface between substrate concrete and patching material could be maintained when expansion was small.
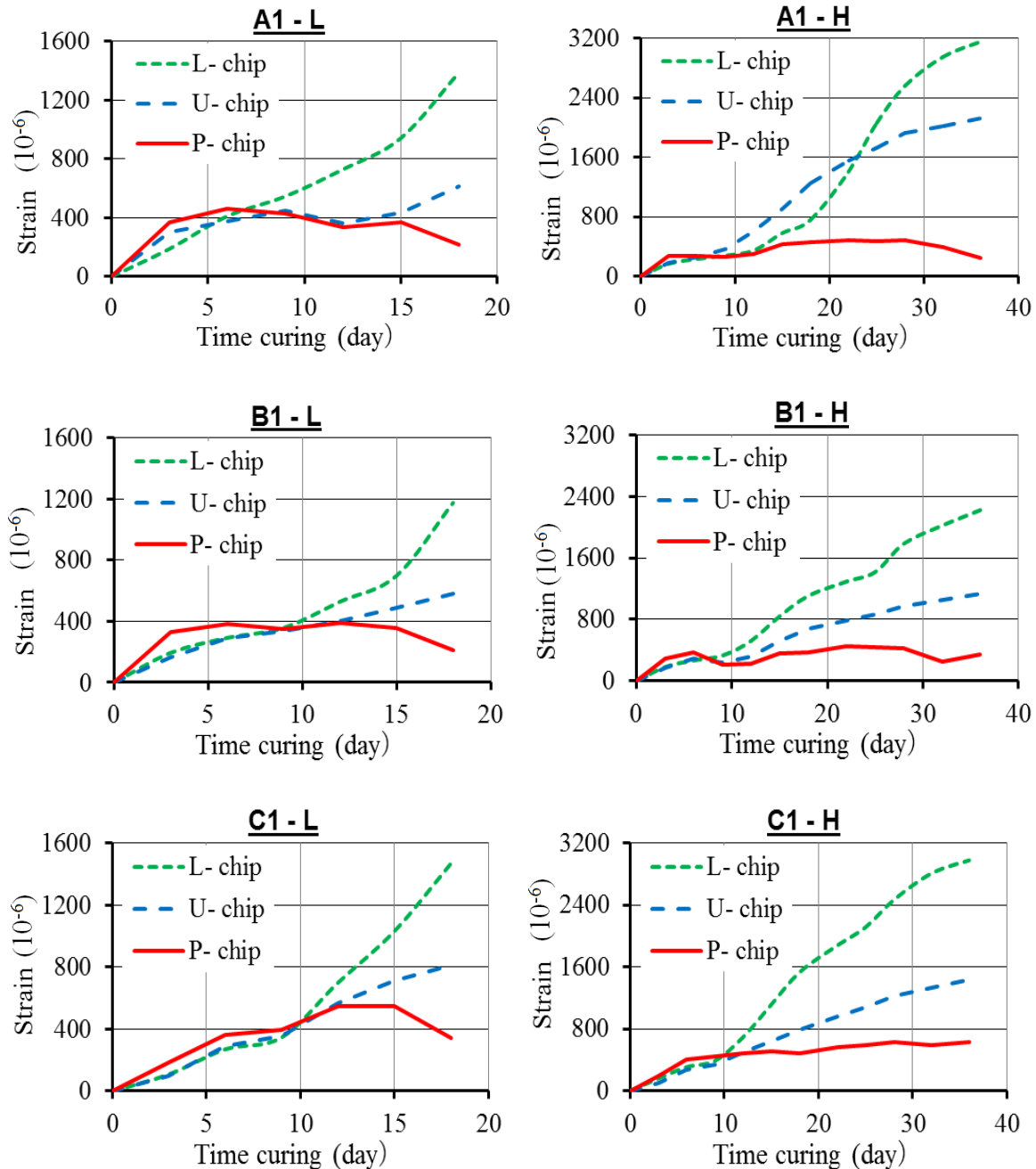
Figure 4.7 Expansion behavior of specimens in series 1

However, when expansive strain was larger than 500 x 10^{-6}, the expansive strain of substrate concrete of the lower part was larger than that value of the upper part. On

the other hand, those values of patching material were changed slightly. Although the patching material restrained expansion of the upper part of substrate concrete, the integrity of inner side of substrate concrete could be reduced.

Regarding specification A1-H (high strength mortar + acrylic primer), substrate concrete and patching material of this specimen were peeled off after 18 days. Visual observation showed a gap about 5 mm occurred on the final day of measurement. For this reason, the expansive strain on upper side of substrate concrete was larger than those values of other specimens that were not peeled off in this experiment.

4.3.1.2 Expansion behavior in experimental series 2

In this series, the expansive material was cast in the hollow part of substrate concrete and expansive strain was calculated by the average values of strain of the P-chip, B-chip at four sides of the specimens. The expansive strain had been measured for 13 days, in both cases of low-level and high-level of expansion. The results of expansive strain of substrate concrete and patching material are shown in **Figure 4.8**.

In relation to the low-level of expansion, all specifications showed the similarity of expansion behavior of substrate concrete and patching material. However, there were some differences between expansive strains of substrate concrete and patching material. The expansive strain of substrate concrete attained around 600×10^{-6} while that value of patching material achieved approximately 200×10^{-6} in all patching specifications.

With the high-level of expansion, the results of specifications B2-H and C2-H showed expansion behavior nearly the same with the case of low-level. However, the strain of high-level was larger than low-level because of using a higher volume of expansive admixture. The expansive strain of specification C2-H was larger than that value of B2-H in both substrate concrete and patching material. It is considered that the epoxy primer, which was used in specification B2-H, had a better effect on adhesion between substrate concrete and patching material even specimens were affected by large expansion.

As shown in the above results, it is concluded that patching materials have a small effect on the confinement of expansion of substrate concrete since the expansive strain of patching material was small and the expansion of substrate concrete was large. Alternatively, the mechanical properties of patching material may be less affected by the expansion than substrate concrete.
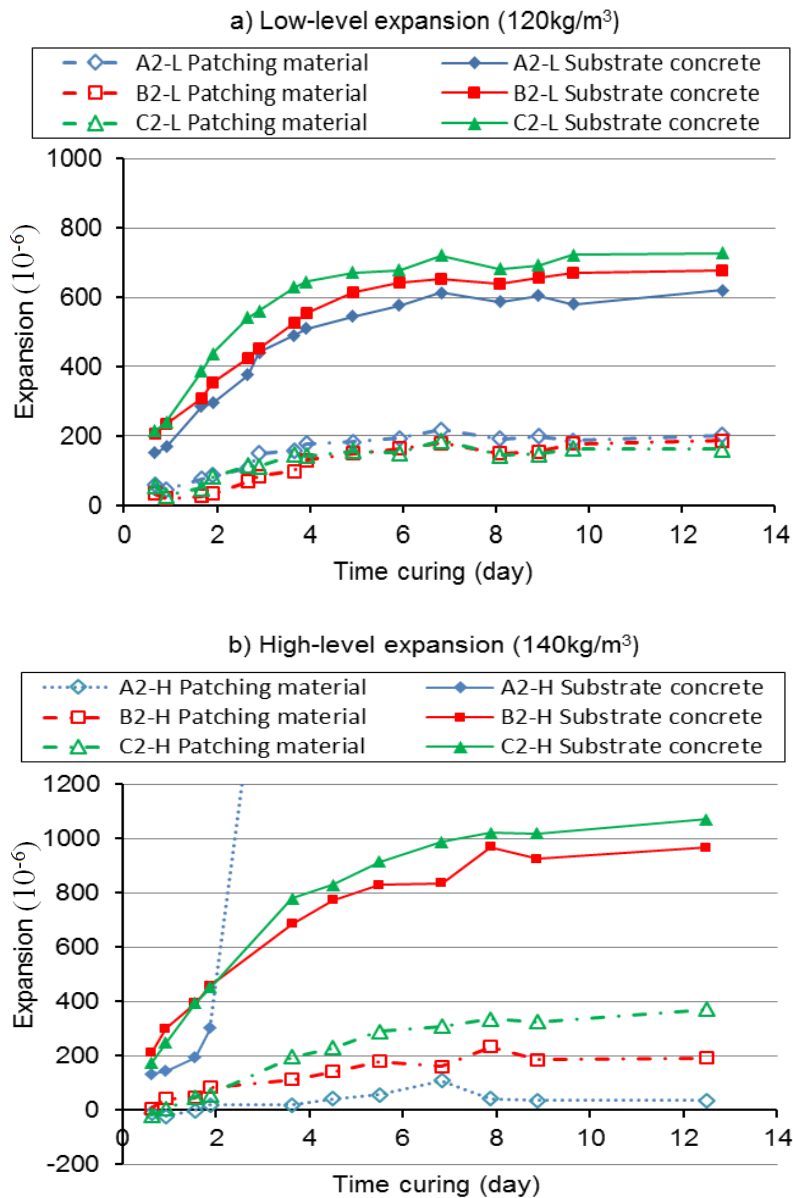
Figure 4.8 Expansion behavior of specimens in series 2

Regarding specification A2-H, large cracks near the interface appeared and the expansive strain of substrate concrete after 48 hours was remarkable while these values of patching material were nearly 0. In addition, the cracks expanded in parallel with the interface and the partial separation between patching material and substrate concrete are shown in **Figure 4.9**. It seemed that patching material was separated from substrate concrete because the property of the acrylic primer did not have an adhesive performance like the epoxy primer. The stress and the expansion of the interface had large differences with these values of substrate concrete and patching material. Therefore, the expansion of patching material (A2-H) was small and the expansion of substrate concrete increased dramatically.
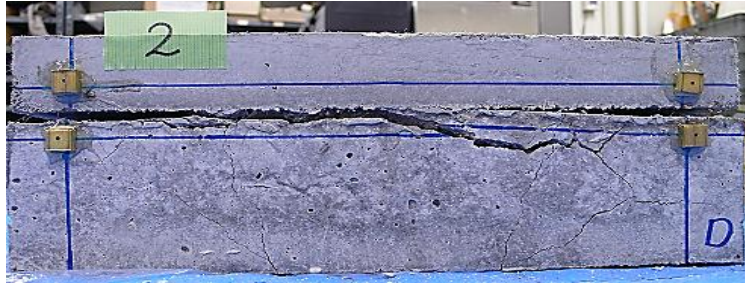
Figure 4.9 Appearance of cracks in the specimen A2-H

4.3.2 Adhesion test after expansion

4.3.2.1 Adhesive strength in experimental series 1

The adhesive strength results of the experimental series 1 at the attained expansive strain of 0, 800 x 10^{-6} and 1500 x 10^{-6} are shown in **Figure 4.10**. In the case of specification A1-H, when the expansive strain was larger than 800 x 10^{-6}, patching material was peeled off and a gap of about 5mm occurred finally. Consequently, the adhesion test could not perform in this case of high-level of expansion.
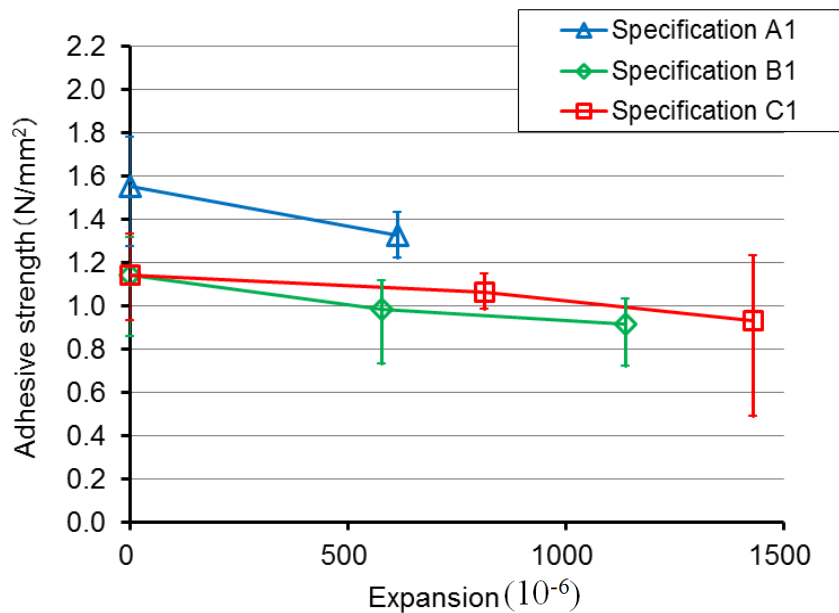
Figure 4.10 Adhesive strengths of experimental series 1

The adhesion tests showed all failure surfaces occurred only in substrate concrete and most values of adhesive strength were lower than the required value of patching material (1.5 N/mm^2). Even in the cases of B1 and C1 of no expansion, these adhesive strengths were lower than 1.5 N/mm^2. Furthermore, the adhesive strength value was slightly reduced with the increase of expansion. The decrease of

adhesive strength occurred due to larger expansion of substrate concrete. The ASR expansion could be resulted in the reduction of mechanical properties of substrate concrete such as compressive and tensile strengths. In other words, it is considered that the mechanical properties of substrate concrete were reduced by the excessive ASR expansion. For this reason, in this experiment, the adhesion tests could not clarify the "adhesive strength" of the interface between substrate concrete and patching material.

4.3.2.2 Adhesion strength in experimental series 2

Similarity as series 1, adhesion tests of experimental series 2 were carried out in three stages of expansion: no expansion, low-level and high-level of expansion. The results of adhesive strength in this series are shown in **Figure 4.11**. In the case of specification A2-H, the patching material was peeled off when the expansive strain was larger than 600×10^{-6}. Hence, the adhesion test could not perform in this case.
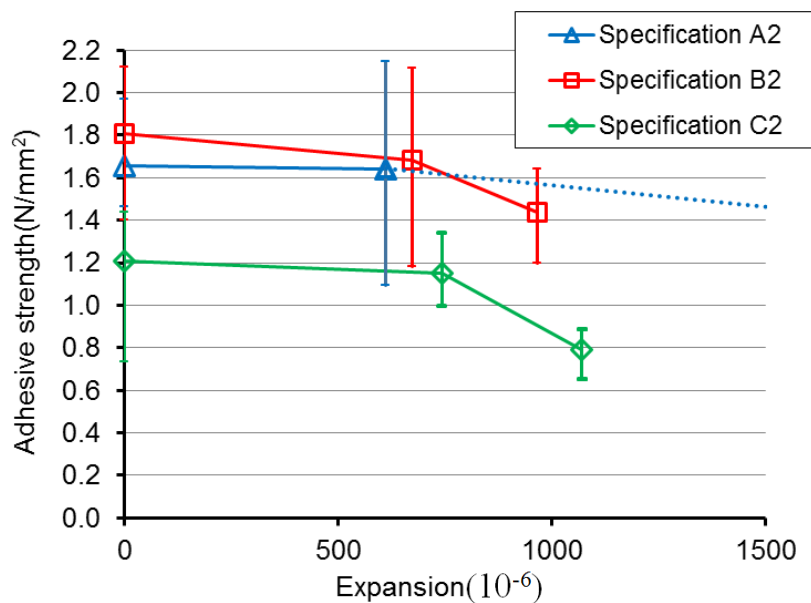
Figure 4.11 Adhesive strengths of experimental series 2

The average of adhesive strength results for all cases showed that when the expansion was larger, the adhesion strength was smaller. All failures surfaces occurred in substrate concrete in the pull-off test. The reason is considered as the same as experimental series 1.

In general, in both experimental series, the results indicated that the adhesive strength decreased when the expansive strain of substrate concrete increased. It is

concluded that the adhesive strength depends on the strength of substrate concrete since the failure surface occurred in substrate concrete for all specimens. On the other hand, if the strength of substrate concrete would be maintained, the adhesive strength of concrete might be larger than these values obtained in this experiment. In this pull-off test, the adhesive strength of the interface could not sufficiently clarify. Thus, further investigation is needed to clarify this problem.

4.3.3 Fluorescence impregnation test

The fluorescence impregnation test was carried out in the case of high-level of expansion in the experimental series 1. The images of cracks of specimens B1-H and C1-H are shown in **Figure 4.12**. In the case of specification A1-H, the peeling of patching material and substrate concrete occurred. Hence, the core extraction could not perform and the fluorescence impregnation test was omitted.

The images showed that all cracks occurred only in substrate concrete. None of cracks appeared in the interface and patching material. Thus, the integrity of patching material and the interface between patching material and substrate concrete is preserved in both specifications B1 and C1.

As the result this test, the influence of ASR expansion on the interface property is not significant even in the case of high-level of expansion. On the other hand, further study is necessary to investigate the mechanical properties of the interface, since the adhesive strength of the interface could not be confirmed in this study.

Specification B1   *Specification C1*
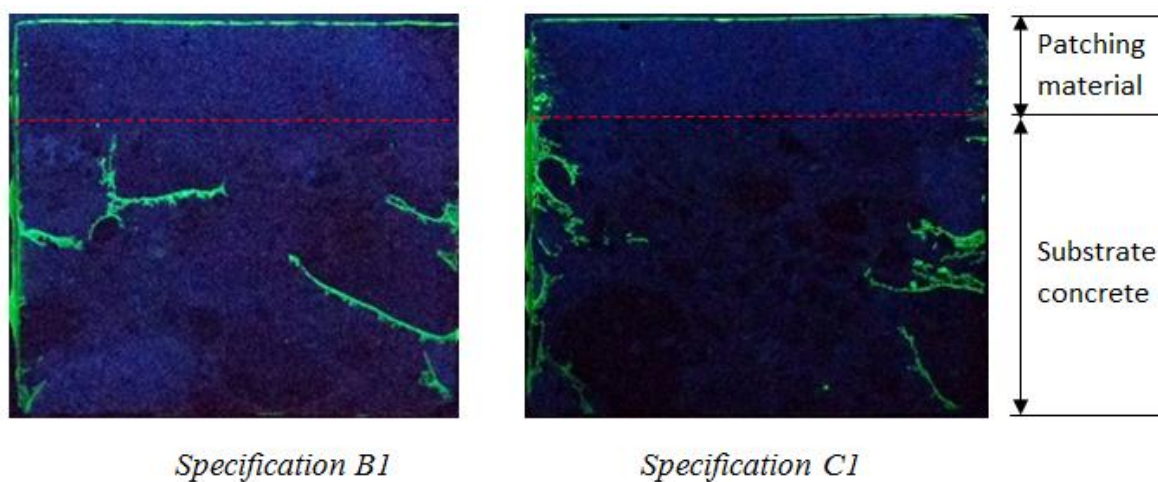
Figure 4.12 Fluorescence impregnation images in series 1

4.3.4 EPMA analysis

In specification A1, the EPMA analysis could not conduct as the same reason as the fluorescent impregnation test. The EPMA images of specifications B1 and C1 in the case of high-level of expansion are shown in **Figure 4.13**.

The color of EPMA image is close to red color providing that more chloride ions are contained and penetrated. In comparison with specification C1, the interface of specification B1 showed warmer color because little chloride ions were contained originally in the epoxy resin primer while the specification C1 did not use primer. Thus, both images of specifications B1 and C1 showed no chloride ion penetration into concrete through the interface between substrate concrete and patching material. As a result, no chloride ions penetrated into patching material. Therefore, even in the case of high-level of expansion, the integrity of the interface between substrate concrete and patching material was maintained and it contributed to prevent the penetration of chloride ions.

(a) Specification B1

(b) Specification C1
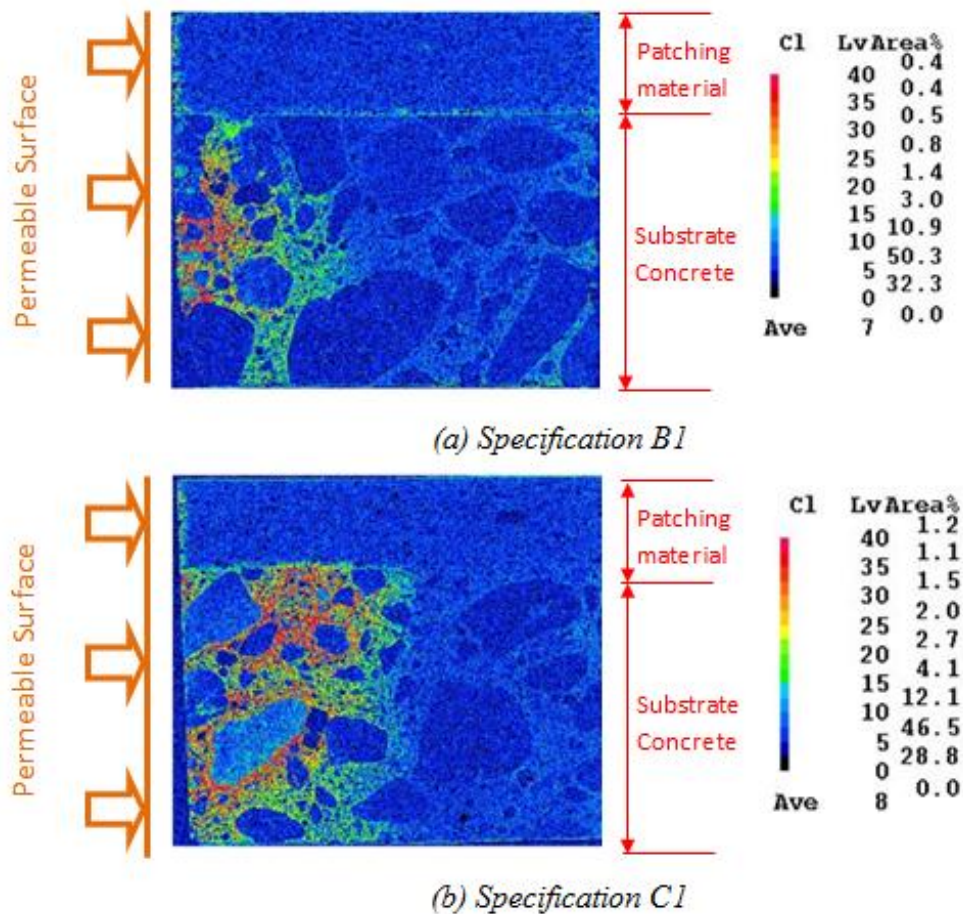
Figure 4.13 EPMA images of specimens in series 1

4.4 Conclusion

The main results obtained in this chapter are shown as follows:

(1) **P**atching material had contributed to restrain the expansion in the upper part of substrate concrete when the expansive strain was smaller than $200 \sim 500 \times 10^{-6}$. However, patching material had a little effect on the expansion confinement of substrate concrete in the case of large expansion.

(2) The mechanical properties of the patching material may be less affected by the expansion than that of substrate concrete.

(3) When no expansion occurred after patching, the adhesive strength values were lower than 1.5N/mm^2 and these values were reduced slightly with the increase of expansion.

(4) The adhesive strength depends on the strength of substrate concrete and the decrease of adhesive strength might be caused by the expansion of substrate concrete.

(5) From the fluorescent observation and EPMA images, the influence of ASR expansion on the interface property is not significant even in the case of high-level of expansion. The integrity of the interface between substrate concrete and patching material is maintained and it contributes to prevent the penetration of chloride ions.

References

Kubo, Y., and Miyano, N., *Study on repair method with fiber modified mortar for Spalling of a Concrete due to ASR*, Proceeding of 12th Euro-seminar on microscopy applied to build materials, pp. 301-308, Sep. 2009.

Kubo, Y., and Torii, K., *Case Study on Deterioration of Concrete Structures due to Alkali-Silica Reaction (ASR) and its Recent Rehabilitation Techniques*, Concrete Journal, Vol.40, No.6, pp. 3-8, Jul. 2002.

Nomura, M., Komastubara, A., Fujimoto, K., and Torii, K., *Evaluation of maintenance methods for ASR-damaged structures in Hokuriku district, Japan,* Third International Conference on Sustainable Construction Materials and Technologies, Session W1-4, Kyoto-Japan, August. 2013.

CHAPTER 5 EFFECTIVENESS OF COUNTERMEASURES APPLIED ON ASR-DETERIORATED CONCRETE BRIDGE AFFECTED BY DE-ICING SALTS

5.1 Introduction

In the winter, the de-icing salts are sprayed widely on the highway in the Hokoriku region in Japan. There is a possibility that more chloride ions could penetrate into the concrete through water leakage that contained a high concentration of de-icing salts. Many structures of concrete bridges can be affected significantly by de-icing salts or chloride attack such as abutments, girders, deck slabs, wheel guards and other concrete structures below. It was reported that the risk of steel bars could be corroded seriously in a short period in the ASR-deteriorated concrete structures that were affected by de-icing salts (Kubo *et al*. 2015). In the case of structures affected by ASR, the appropriate countermeasure should be applied after a certain period of observation. However, the alkali could be derived from de-icing salts and it could promote the ASR in concrete (Ishikawa *et al*. 2012). Furthermore, more moisture and chloride ions can permeate into the concrete through cracks caused by ASR and it increases the risk of steel induced corrosion. One of effective countermeasures against the penetration of chloride ions is the surface coating. However, cracks are still generated on the surface due to the residual ASR expansion after repairing (Nomura *et al*. 2016) and it may cause complicated deterioration after repair. The press-fit method of lithium nitrite and the surface impregnation method can be considered as countermeasures against combined deterioration of ASR and de-icing salts (Matsumoto *et al*. 2010; Kubo *et al*. 2016). It is expected that the inhibition of ASR and the steel corrosion risk can be reduced because nitrite ions have the anti-rust effect and lithium ions have the non-expansion effect with ASR gel. In other cases, when surface impregnation method has been applied, it is expected to restrain ASR

and corrosion risk by suppressing the permeation of water leakage into concrete and reducing the moisture content of concrete. In comparison with patching method and others, these methods mentioned above are possible to reduce the cost and time required for repair because it is applied only on the surface of concrete and since the change of appearance is quite small, the followed observation after repairing is easier.

In this chapter, the crack injection and surface impregnation were carried out after examining the degradation state of wheel guard structures of a bridge that were deteriorated by ASR and chloride attack including de-icing salts. The moisture content of concrete and the half-cell potential were measured periodically, and the effect of countermeasures on ASR-deteriorated concrete was examined.

5.2 Summary of the research

5.2.1 The target bridge

Figure 5.1 shows the outline of the bridge that is the subject of this in-situ survey. This bridge is located on the local road, in the middle part of Noto district, Ishikawa prefecture in Japan. The sides of wheel guard structures were selected as the specific positions of this study (4 surface sides of wheel guard structures are shown in **Figure 5.1**). This bridge is located on the road where many vehicles pass in the winter. Thus, a large amount of de-icing salts was sprayed on this road to ensure the safety of vehicles.
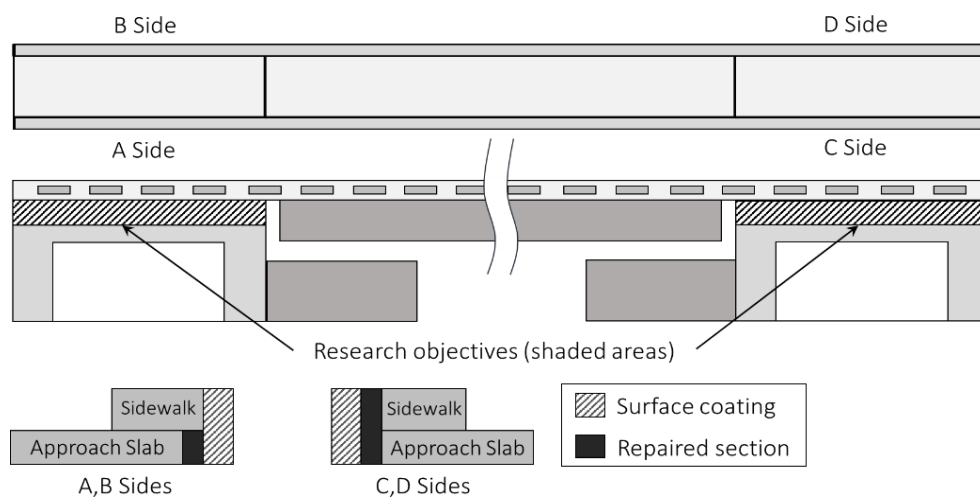
Figure 5.1 Outline of the target bridge

In 1997, the crack injection and the surface coating methods were applied as countermeasures against alkali-silica reaction. Furthermore, patching material with the thickness from 50 mm to 70 mm was conducted on the side surfaces C and D of wheel guard structures. By the time, cracks occurred in the entire repair material due to ASR and cracks appeared on the backside of this structure. The appearance of cracks is shown in **Figure 5.2** as the examples of cracking in concrete.

a) Side view   *b) Upper view*

Figure 5.2 Cracks appearance on patching material

5.2.2 Outline of applied countermeasures

In November 2016, these following countermeasures were conducted to the sides of wheel guard structures of the target bridge.

5.2.2.1 Crack injection

The repair material was injected into the concrete through the cracks on the surface sides of the concrete. In this repair, the ultra-fine particle cement was injected on A and B sides while the lithium nitrite ($LiNO_2$) was injected on C and D sides. Additionally, in the repair method injected by lithium nitrite, the ordinary pressure for injection was adopted from the result of chloride ion measurement in this study.

5.2.2.2 Surface impregnation

Each side of wheel guard structure was divided into four parts as shown in **Figure 5.3** and the film coating was removed on three parts excluding the film coating part. Thereafter, the commercial availability of silane/siloxane agents was applied to the impregnation parts. The properties of impregnating agents are shown in **Table 5.1** and the surface impregnation methods are summarized in **Table 5.2**.
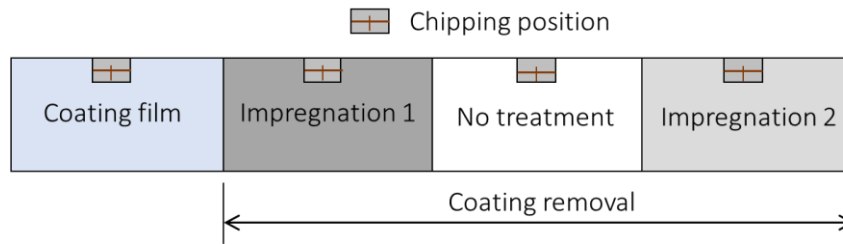
Figure 5.3 Position of surface impregnation parts

Table 5.1 Specifications of surface impregnated materials

Impregnated material	Object recognition	Principal component	Active ratio (%)	Applied amount (g/m²)
a	White gel	Octyltrietthoxysilane	95 ~ 99	200
b	Colorless liquid	Alkoxysilane	94	150
c	Light grey gel	Silane / Siloxane	90	350
d	Colorless liquid	Alkylsilane	98	265

Table 5.2 Outline of surface treatment

Side	Crack injection	Surface treatment section			
		Coating film	Impregnation 1	Untreated	Impregnation 2
A	Ultra-fine particle cement		a		b
B	Ultra-fine particle cement		c		d
C	LiNO2 + Ultra-fine particle cement	Coating film	c	No treatment	d
D	LiNO2 + Ultra-fine particle cement		a		b

5.2.3 Measurement contents

5.2.3.1 Observation of cracks

Cracks appearance was observed by visual images and the crack width was measured by a crack ruler on the concrete surface after removing of film coating. The degree of crack width was classified into three grades. These grades include crack width is smaller than 0.2mm, from 0.2 mm to 0.4 mm and larger than 0.4mm, respectively. Then, the sketching of cracks was drawn for cracks observation.

5.2.3.2 Steel corrosion grade

In order to determine steel corrosion grade on each side of wheel guard structure, four positions on each repaired or no treatment parts of side A, B, C, and D were chosen for chipping investigation. The concrete cover at the intersection of axial steel bars and lateral steel bars was removed in small areas (about 0.15m x 0.15m) by concrete hammer and drill, then, corrosion grade of steel bars was observed visually. Steel corrosion grade of steel bars was evaluated based on criterion 8 in "Concrete cracks analysis, repairing and reinforcement guidelines 2003: Japan Concrete Engineering Association" and was shown in **Table 2.2** – Chapter 2.

5.2.3.3 Concrete neutralization depth

After chipping concrete to observe steel corrosion grade, 1% phenolphthalein solution was sprayed on the chipping positions and the neutralization depth was determined based on the coloration on the concrete surface.

5.2.3.4 Chloride ion penetration

Silver nitrate solution ($AgNO_3$) was sprayed on the concrete surface of treated or untreated parts of each side and the penetration depth of chloride ions was analyzed. In addition, in order to determine chloride ion content penetrated into the concrete, six positions along each side of wheel guard structure (D1 to D6) were chosen to collect the internal concrete samples by using drill method. These samples were taken every 20mm of depth. Then, the chloride ion analysis was performed in the laboratory based on the potentiometric titration method (JCI-SC5) to obtain profiles of chloride ion penetration at the depth of 20, 40, 60 and 80mm, respectively.

5.2.3.5 Surface moisture content of concrete

The surface moisture content of concrete (%) was measured by using a high-frequency concrete moisture tester at 3 different times: before repair, after repair and 9 months after repair. The measurements were conducted at intervals of 0.3m along the axial steel bars of wheel guard structure.

5.2.3.6 Half-cell potential

In order to evaluate the corrosion of the steel bar, the copper wire was connected to the portable corrosion meter (reference electrode: silver/saturated silver chloride electrode) and to the steel bars. The half-cell potential was measured at the

times same as the surface moisture content measurement. The criteria of ASTM C-876 were used to evaluate steel corrosion by half-cell potential. **Table 5.3** shows the criteria to evaluate steel corrosion based on half-cell potential measurement.

Table 5.3 Corrosion evaluation of half-cell potential

Half-cell potential (mV vs. SSE)	Corrosion evaluation
E > -80	No corrosion (more than 90%)
-80 ≥ E ≥ -230	Uncertain
E < -230	Corrosion (more than 90%)

5.2.3.7 Internal moisture content

The internal moisture content of concrete was measured by commercial moisture meter at the depths of 20, 40 and 70 mm, respectively. This measurement was conducted after 9 months of repairing, and the internal moisture content distribution was determined in this study.

5.2.3.8 Half-cell potential monitoring

In order to measure the temporal change of half-cell potential at each chipping position, a titanium rod was embedded to the axial steel bar and the potential difference between titanium rod and steel bar was recorded with a frequency of every 60 minutes using an automatic potential logger. The measurement was started from the 2nd of December in 2016 and stopped at the 9th of November in 2017. At the same time, a temperature and humidity logger was installed at the bottom of target structure, and temperature and relative humidity in this area were recorded.

The measurement contents from (5.2.3.1) to (5.2.3.4) were performed before repair, the items (5.2.3.5) and (5.2.3.6) were conducted before and after repair, and the items (5.2.3.7) and (5.2.3.8) were measured after repair.

5.3. Results and discussion

5.3.1 Observation of cracks

Figure 5.4 shows the distribution of cracks on the side surface of wheel guard structure before repairing. On the A and B sides, cracks have the width of 0.4 mm or more occurred along axial steel bars in the upper part and the longitudinal cracks along lateral steel bars also existed. Generally, cracks mostly appeared in the upper

part and not occurred on the lower part. In the film coating part, cracks also occurred inside film coating before removing and the transformation of film coating did not follow the ASR expansion. Although the cracks reached the surface of concrete, the film coating was not affected significantly by cracks caused by ASR expansion.
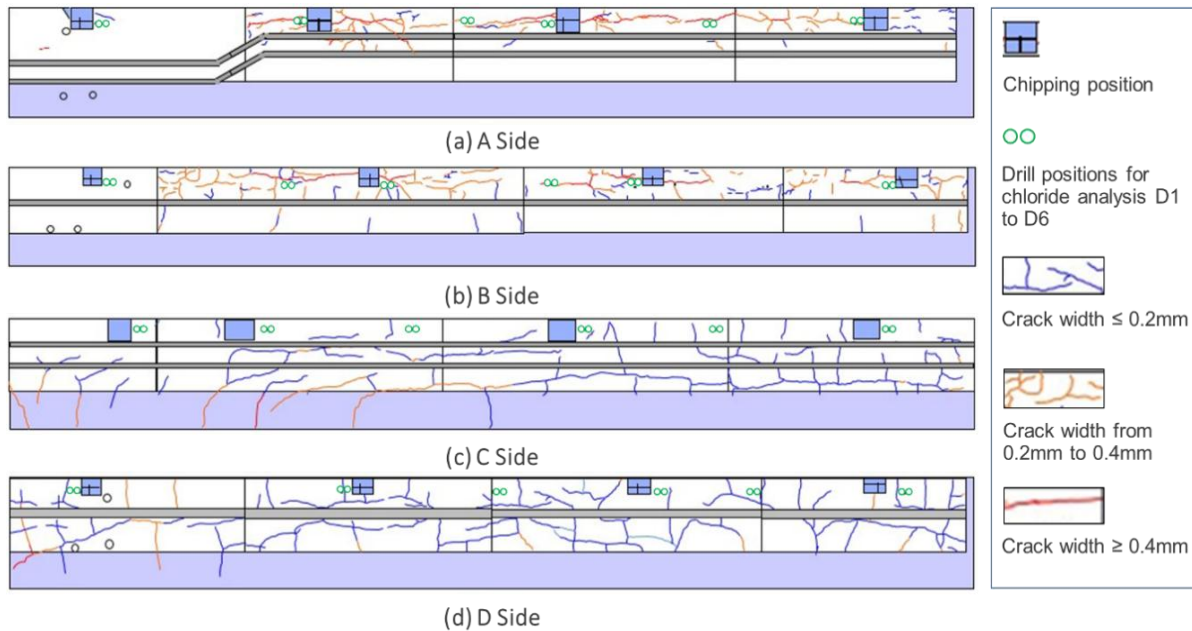
Figure 5.4 Cracks sketching on four sides of wheel guard structure

On the other hand, on the C and D sides, cracks had the width of 0.2 mm or less were observed in the entire areas and some cracks that were continue occurred in the deck part below were also observed. In C and D sides, the cracks continued to occur in both patching material on wheel guard and deck part below. The crack widths of C and D sides tended to be smaller than A and B sides. In C and D sides, the patching material of polymer cement mortar was used and since it suppressed partially crack expansion caused by ASR, the crack width decreased in comparison with A and B sides that only applied coating treatment.

5.3.2 Steel corrosion grade

The corrosion grades of axial steel bars and lateral steel bars in the upper part of structure are shown in **Figure 5.5** and **Figure 5.6**, respectively.

Regarding the axial steel bars, there are two positions showing the corrosion grade III on each of A and B sides, and it occurred on the impregnation 1 and no treatment parts. On the other hand, on C and D sides, corrosion grade II or less were

shown in all chipping positions, which is considered that the corrosion condition was less corrosive than A and B sides. In case of lateral steel bars, most position of A and B sides showed the corrosion grade III, and only one position reached the corrosion grade IV that showed the cross-section of steel bar had defected. On C and D sides, many positions showed the corrosion grade II and three positions showed the corrosion grade III. In comparison with axial steel bars, the concrete cover depth of lateral steel bars is smaller than that of axial steel bars. Therefore, the moisture and oxygen could penetrate easier and steel corrosion occurred faster.
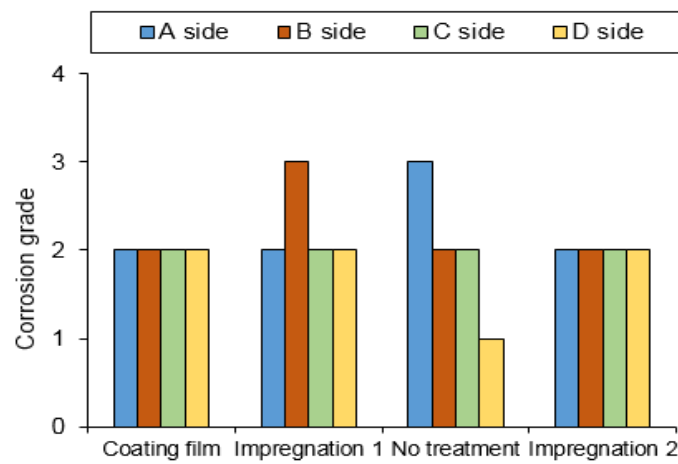
Figure 5.5 Corrosion grade of axial steel bars
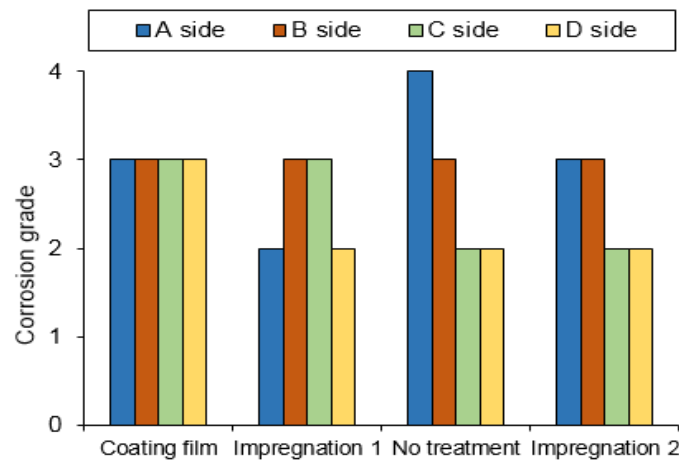
Figure 5.6 Corrosion grade of lateral steel bars

The result showed that the corrosion grade of C, D sides tended to be smaller than that of A and B sides. In the cases of C and D sides, the patching material contributed to suppress the expansion caused by ASR. Hence, the supply of moisture, oxygen, etc., from the concrete surface was considered smaller than the cases of A

and B sides that was only treated by a surface coating method. It is considered that the influence of patching material is significant to decrease the risk of steel corrosion.

In the upper part of this structure, a small part of the axial steel bar was broken and it could be seen by visual observation. This was not as same as the cause of the reduction of cross-section of steel bar due to the corrosion. It was considered that the high stress, which was occurred at the corners of the structure due to ASR expansion, could become the significant reason for that.

5.3.3 Concrete neutralization depth and chloride ion penetration

In this in-situ survey, the coloration of the phenolphthalein solution could be examined at 0 mm (on the surface side of the wheel guard) and no neutralization could be observed at all chipping positions. In addition, the coloration of silver nitrate solution could not observe and the penetration of chloride ions was not confirmed. The chloride ion penetration was analyzed in the laboratory and the results were shown in **Figure 5.7**.
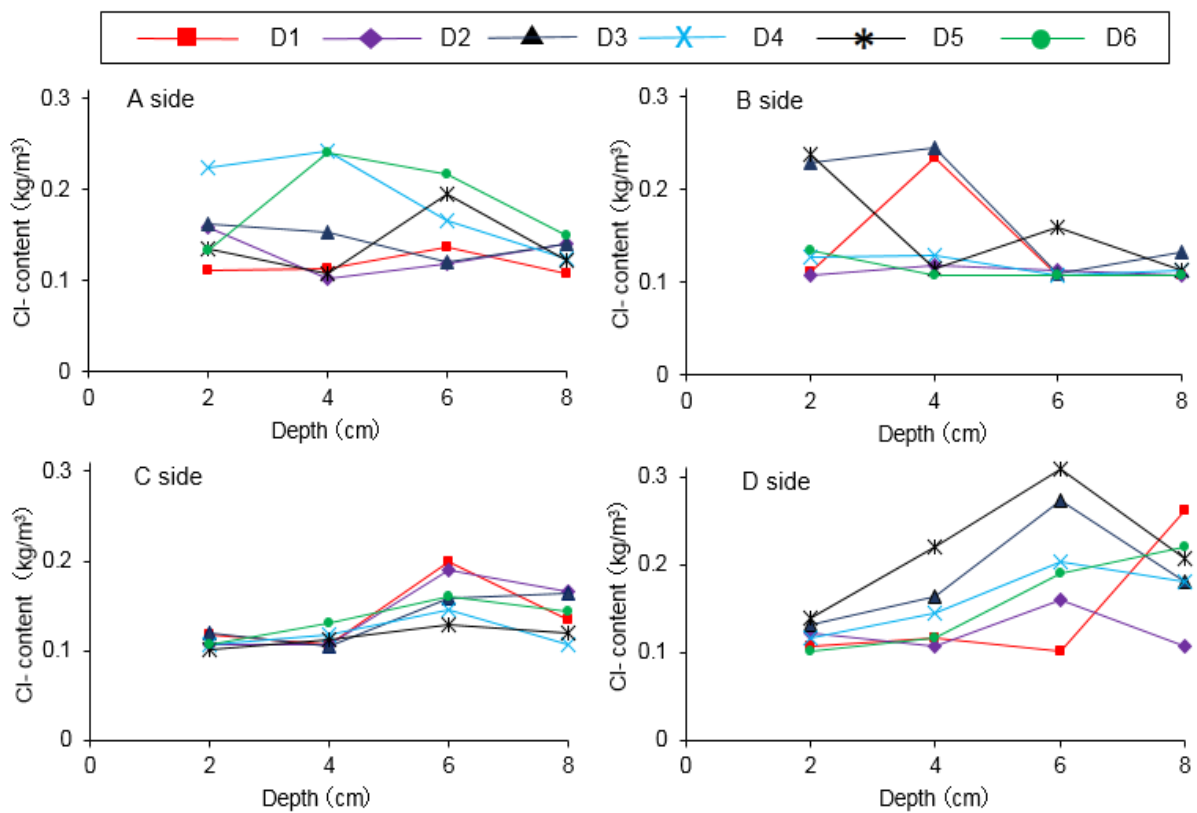
Figure 5.7 Chloride ions content distribution

The content of chloride ion remained from 0.1 to 0.3 kg/m^3 at most of measured points. Although there was a possibility that chloride ion permeated locally through cracks, however, the content of chloride ion penetration through the cracks seem to be small. The samples were collected and analyzed before the winter when the de-icing salts were not sprayed on the highway. The content of chloride ion in all measurement points was small because of chloride content near the surface was affected and reduced by the washout action of water leakage without chloride ion on the rainfall season. However, the result of the steel corrosion grade showed the corrosion of steel bars was not small. Therefore, it will be necessary to examine the chloride ion content in the concrete after the period time of de-icing are sprayed in the future.

5.3.4 Surface moisture content of concrete

Figure 5.8 shows the results of the surface moisture content of concrete on the sides of the wheel guard structure. The surface moisture content of concrete was measured along the position of axial steel bars before repair, after repair, and 9 months after repair.

Figure 5.8 Surface moisture content of concrete

The result showed that the surface moisture content on the A and B sides of the impregnated parts was lower than that of the untreated parts. It is considered that the significant effect of surface impregnation resulted in the lowing of surface moisture of concrete. The surface moisture on A, B sides fluctuated from 5 to 9 %, while these values on C, D sides changed from 2 to 4 %. As a result, the patching material had a small crack width contributed to reduce the surface moisture of concrete.
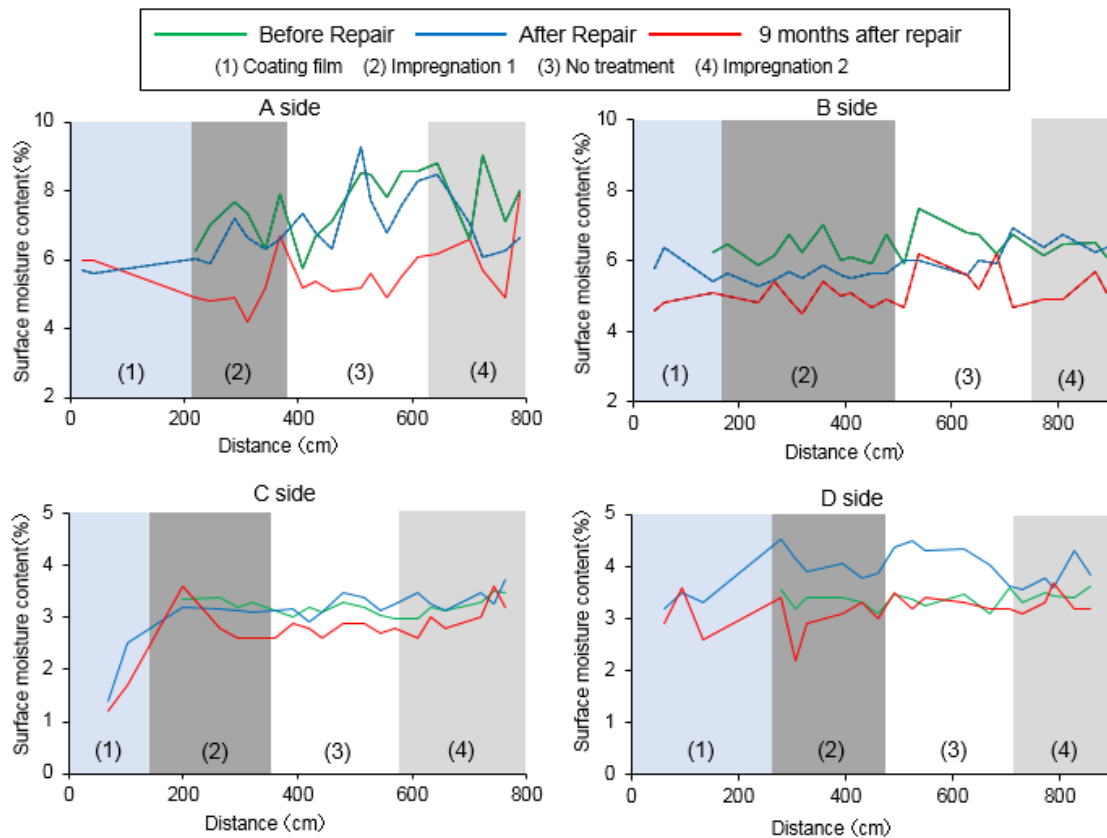
Regardless of whether or not surface coating treatment was carried out, the surface moisture content of concrete showed the decrease tendency over time. It is considered that the vicinity of the surface was dry partially by the removal of film coating. From this result, it is suggested that the film coating is deformed and the moisture can permeate easier into the film coating, then this film prevents the escape of moisture and keeps the moisture of concrete is higher.

5.3.5 Internal moisture content of concrete

Figure 5.9 shows the internal moisture content of concrete with different depths after 9 months of repair. The moisture percentage at the depth of 70 mm was highest and remained approximately from 6% to 8% in almost measured points. It was unknown exactly at the time of repair, the crack width from 1 mm or larger might also have occurred in the backside of structures and the water leakage could be supplied through the cracks on the backside. Thus, it could become a noticeable reason for the high value of moisture content of concrete at the depth of 70mm for all sides of this structure. At 70 mm of depth, the moisture content in C, D sides tended to be slightly higher than that in A, B sides. The moisture was hardly escaped due to the effect of patching material, thus it could become the reason of high moisture of concrete in this part.

On the other hand, the moisture content at the depth 20mm was small in all sides of wheel guard structure. The removing of film coating and impregnation treatment could make the surface drier and moisture near the surface was small. However, the moisture in C, D sides at this depth was under 2 %, while these values in A, B sides were from 4 to 6%. It is considered that the smaller of the crack width on patching material causes moisture near the concrete surface drier.
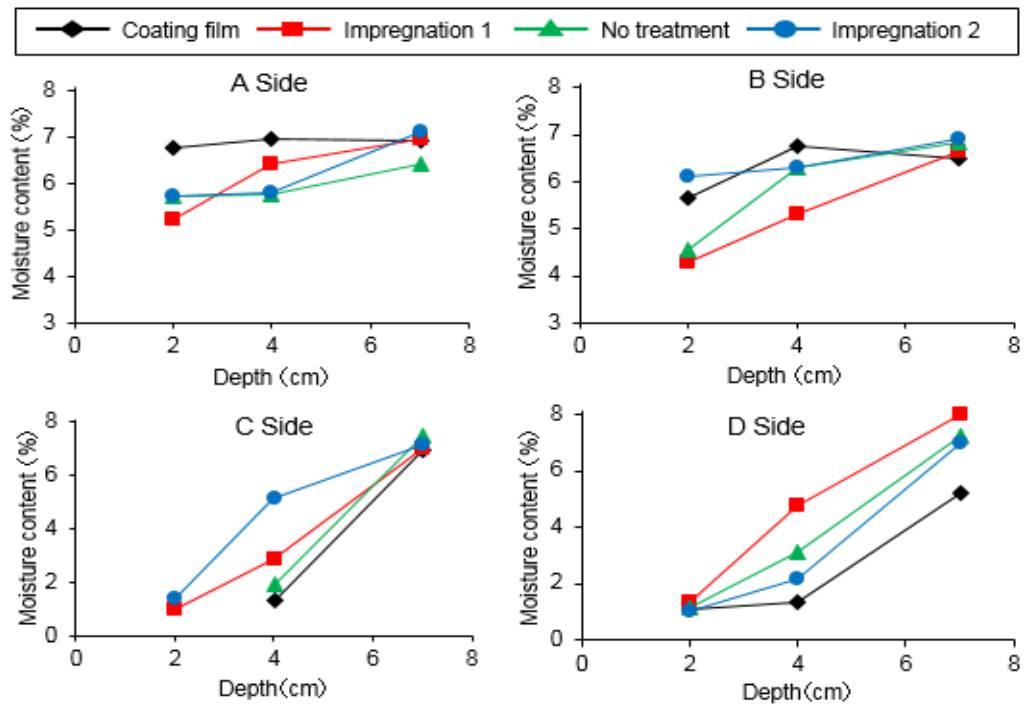
Figure 5.9 Internal moisture content of concrete

5.3.6 Half-cell potential

Figure 5.10 shows the half-cell potential values along the axial steel bars before repair, after repair, and 9 months after repair. During repairing, most values of half-cell potential in all sides of the wheel guard structure were shown in the uncertain corrosion zones. As the reason for the half-cell potential values did not show near the base side of the corrosion zone, it is considered that the content of chloride ions permeated into concrete was quite small. In both directions of the bridge, the half-cell potential measured on the sides of wheel guard structure tended to be smaller than these values at the center part. At the direction of the approach road, the water leakage amount tends to concentrate on the side of road due to the downward slope of the road. However, at the direction of the bridge, the water leakage amount was larger than the center part because this part was located near the joint of the bridge. It is considered that the content of moisture and chloride ions supplied with both directions is larger than the centre part, and it increases the risk of corrosion with steel on these parts.

In the case of half-cell potential after repair, there was no recovery in the no corrosion zone or even the corrosion continued to occur in the impregnated part on the A and B sides. The supply of moisture from the backside could be still large and

affected significantly in steel corrosion. On the other hand, on the C and D sides, the recovery of potential was observed in both treated and untreated parts. This could be explained due to the lithium nitrite injected into concrete had an inhibition effect for the rust, and it made steel was less susceptible to corrosion.
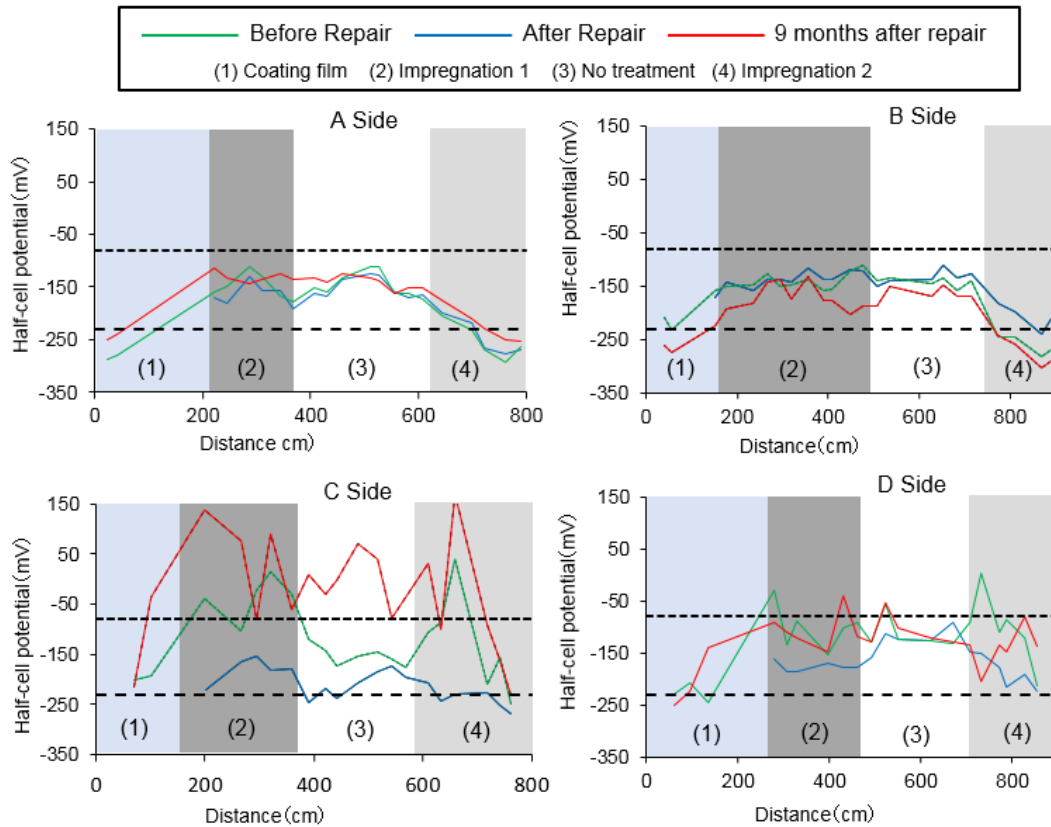
Figure 5.10 Measurement of half-cell potential

5.3.7 Half-cell potential monitoring

The monitoring result of half-cell potential is shown in **Figure 5.11.** Half-cell potential on the A and B sides reduced largely to the base side (corrosion zone) after 50 to 100 days from the started measuring. At that time, the temperature fell to $0^{o}C$ or lower, it is considered that the content of de-icing salts was larger at the time later. Therefore, water leakage contained a high content of chloride ion penetration and the potential tended to be lower. The water leakage including de-icing salts could permeate through cracks from the backside of structure. The water leakage could not permeate from the surface sides because the potential was also lower in the impregnated part. Particularly, the potential on the A side was reduced greatly. The reason for the large reduction of potential on the sides of slabs could be explained due to water leakage tended to concentrate to both sides of this structure.
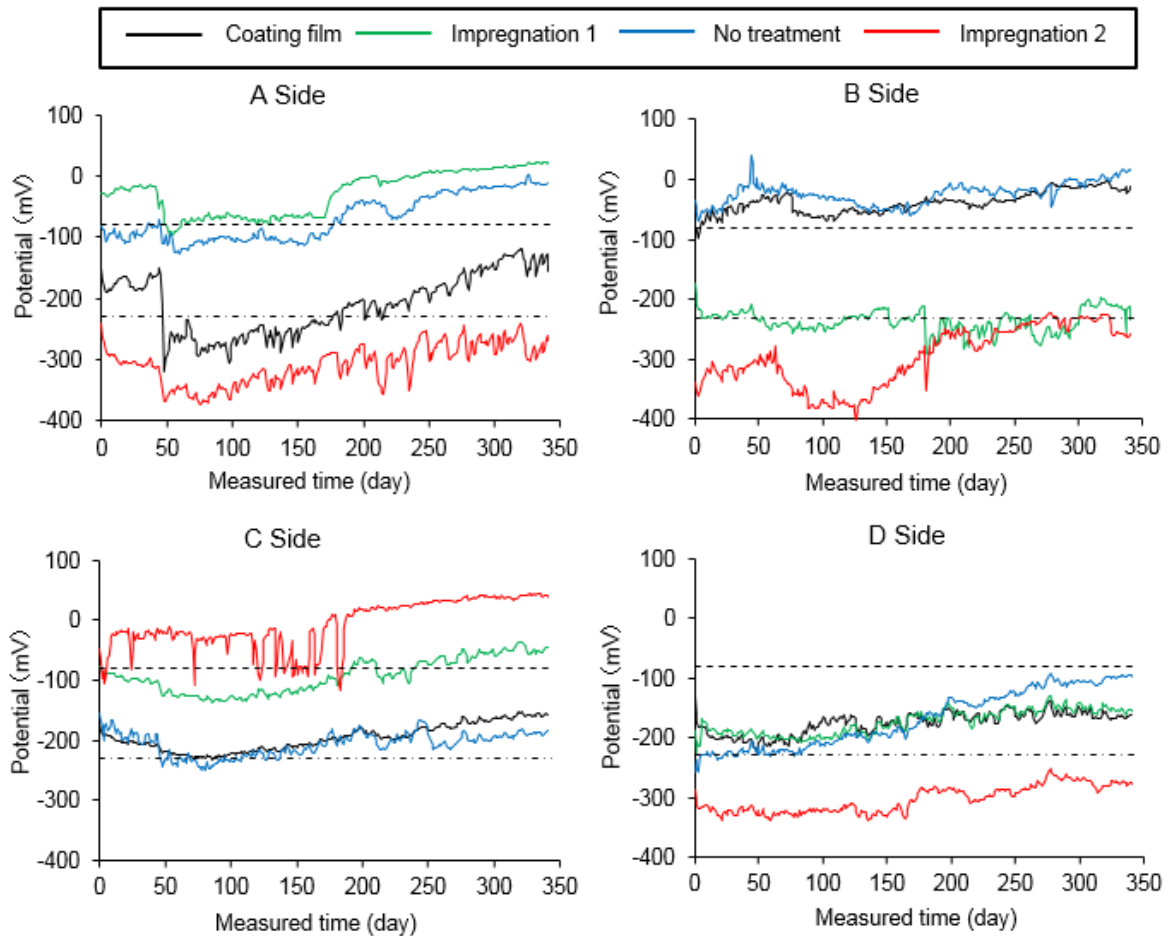
Figure 5.11 Half-cell potential monitoring

After 100 days of measuring, the potential tended to recover to the uncertain or no corrosion zones regardless of the impregnation treatment parts. This treatment restricted partly the influence of de-icing salts. In addition, the removal of film coating could contribute to suppress the steel corrosion due to the lower moisture of concrete near the surface.

On the D side, the potential recovery was small despite lithium nitrite was injected to prevent steel bar corrosion. The crack width and the crack depth caused by ASR were suppressed due to the effect of patching material. Thus, the penetration of moisture and chloride ions from outside could be reduced by patching material. Therefore, it has a possibility of small amount of the preventive agent (lithium nitrite) was injected into concrete or a significant change of environment in concrete did not change in the reducing of steel corrosion risk in this case.

The monitoring results of temperature and humidity are shown in **Figure 5.12**. The humidity near the position of the potential measurement fluctuated frequently

through the year and varied from about 70% to more than 90%. In general, the high humidity tends to increase the moisture content in concrete and the value of half-cell potential might reduce or the risk of steel corrosion might increase.
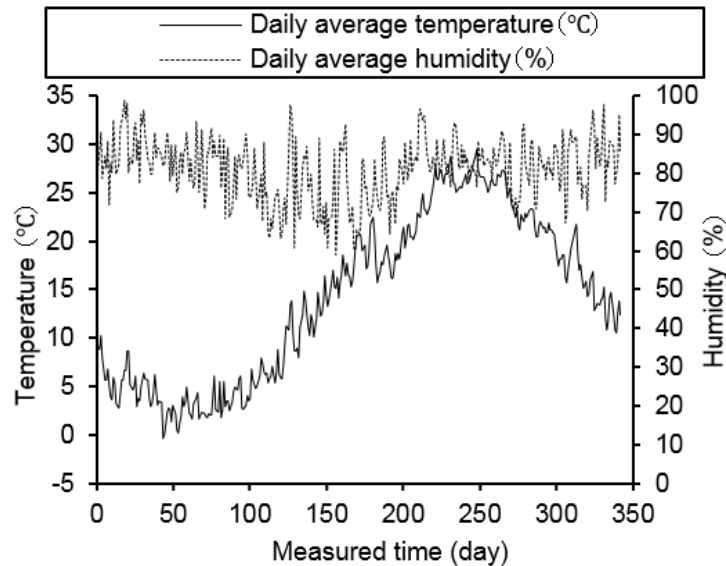
Figure 5.12 Temperature and humidity monitoring

5.4 Conclusion

The results obtained in this study are shown as follows.

(1) Cracks along the axial steel bars were observed on the concrete surface sides of the wheel guard structure although the countermeasures were applied. The crack appearance results showed that the crack width in concrete structures, which was applied patching material, were smaller than other parts that only applied the surface coating treatment.

(2) Although the content of chloride ions penetrated into concrete was small, the steel corrosion had been progressed in both cases of axial and lateral steel bars. Additionally, the corrosion was suppressed due to the application of patching material.

(3) The moisture content in the interior of the wheel guard structures was relatively high while the moisture content near the surface was lower due to the removal of coating film. The moisture content of concrete near vicinity of steel bars could be favorable for steel corrosion since the deformation of the coating film occurred.

(4) The moisture supply from the backside could affect greatly to the moisture content distribution. It is considered that the investigation of the route of water leakage was necessary at the time of inspection.

(5) From the half-cell potential monitoring, no remarkable recovery of potential was observed. When surface coating treatment was applied, further time was needed for the lower of moisture content of concrete near the vicinity of cover depth. Thus, this measurement should continue to conduct in the future.

References

ASTM C 876-91, *Standard test method for half-cell potential of uncoated steel in concrete*, 1999.

Ishikawa, H., Kubo, Y., Hiroyuki Y., Kazuya Y., *Survey on the influence of de-icing salts on concrete structures*, Annual Concrete Engineering Proceedings, September 2012, 34(1), pp. 766-771, 2012. (in Japanese)

Kubo, Y., Yano, T., Kikuchi, T., and Ishikawa, Y., *Steel corrosion in ASR deteriorated structures affected by de-icing salts*, Repairing, reinforcing, upgrading concrete structures report, Vol. 15, pp. 541-546, October. 2015. (in Japanese)

Kubo, Y., Atsuka, A., Kikuchi, S., *Study on the applicability of silane impregnated material in cracked part*, Repairing, reinforcing, upgrading concrete structure report, Vol. 16, pp. 545-560, October . 2016. (in Japanese)

Matsumoto, S., Tsutomu, S., Kazunori, E., Daisuke, M., and Toyoshi, M., *Basic study on the suppression of ASR expansion of Silane type surface impregnated materials and Lithium Nitrite,* Transactions of the Japan Society of Civil Engineers, 66(3), pp. 288-300, March. 2010. (in Japanese).

CHAPTER 6 EVALUATION OF STEEL CORROSION ON ASR-DETERIORATED CONCRETE AFFECTED BY DE-ICING SALTS

6.1 Introduction

Recently, many concrete bridges have been deteriorated by Alkali-silica reaction (ASR) in the Hokuriku region. Some countermeasures have been implemented, however, the reliable repair techniques for long-term have not established. On the other hand, the de-icing salts have sprayed to ensure the safety of transport vehicles during the winter in this region. On the highway, at the expansion joint position between the bridge decks and abutments, these concrete parts affected significantly by water leakage and the degradation of concrete structures may be promoted in a relatively short time (*Honjo et al. 2010, Yokoyama et al. 2008*). It has been reported that the steel corrosion in concrete affected by ASR was not significant than that of concrete not affected by ASR. The existence of ASR gel surrounds on steel bar is considered as a factor to reduce the risk of steel corrosion because of the assimilation of chloride ion and the reduction of water/oxygen supply due to the presence of this gel (*Yokoyama et al. 2008, Kawamura et al. 1997, Fujimura et al. 2009*). However, in recent years, it is reported that the steel corrosion in ASR-deteriorated concrete occurs similar to concrete not affected by ASR when the amount of chloride ion penetration reaches or exceeds certain limits. The previous study was carried out in abutments affected by ASR to investigate steel corrosion. The result showed that cracks caused by ASR promote chloride ion penetration and accelerate steel corrosion (*Kubo et al. 2015*).

In this chapter, the influence of de-icing salts and alkali-silica reaction on steel corrosion was investigated by the in-situ survey and laboratory test. The main content

of this investigation included the measurement of moisture content and chloride content on the concrete surface, analyzing of chloride ion content penetration into concrete and comprehension of steel corrosion rate based on the electrochemical method (half-cell potential and polarization resistance). From the results of this in-situ survey, steel corrosion risk can be evaluated in the ASR-deteriorated concrete structures affected by de-icing salts.

6.2 Contents of in-situ survey

6.2.1 Overview of abutments

In the winter, many bridges on the Hokuriku Expressway have affected by ASR deterioration and de-icing salts. Six bridge abutments were selected as the target of this in-situ survey. In these abutments, the un-repaired parts were selected as the target of the survey and the front wall of an abutment was divided into two sides: the up line side and the down line side. This in-situ survey was conducted on the front wall and wing wall of each abutment. The previous study (*Kubo et al. 2015*) reported that these abutments were affected and deteriorated by combination deterioration of ASR and de-icing salts. **Table 6.1** shows the overview of all survey abutments in this study. **Figure 6.1** shows the current state of an abutment affected by ASR expansion and water leakage, including de-icing salts as an example of combined deterioration.

Table 6.1 Survey abutments

Abutment	Investigated objects	Serving life (years)	Number of chipping
A (Up line)	Front wall	40	1
A (Down line)	Front wall	40	1
B (Down line)	Front wall	40	1
C (Down line)	Front wall	40	1
C (Up line)	Front wall	40	1
D (Up line)	Front wall	35	4
E (Down line-wing)	Down line-wing wall	32	1
F (Up line)	Front wall	32	1
F (Up line-wing)	Up line-wing wall	32	1
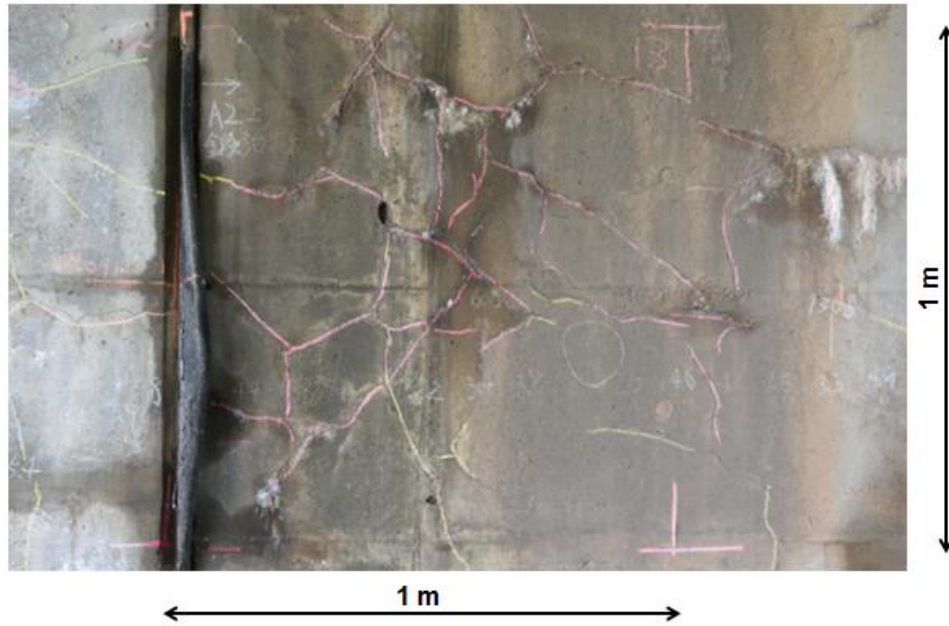
Figure 6.1 An example of abutment affected by combined deterioration

6.2.2 Outline of the in-situ survey

The in-situ survey was conducted to investigate the influence of ASR and de-icing salts on chloride penetration and the occurrence of steel corrosion. Regarding the effect of de-icing salts, the amount of water leakage from the joints was comprehended based on the moisture content of concrete surface. On the ASR progression, the crack density on the surface was used as an evaluation index. From the results of surface moisture content and crack density measurements, twelve positions were selected for detailed investigation (chipping investigation and chloride ion analysis). Additionally, a connection wire was attached to a steel bar to measure steel corrosion by electrochemical method. **Table 6.2** shows all contents of this investigation. Based on the measured data, the relationship between water leakage (de-icing salts) and corrosion occurrences of steel bars was investigated. The method used to determine the influence of de-icing salts based on the chloride ion content of concrete surface was referred in the previous study (*Kikuchi et al. 2016*). This in-situ survey was executed in sunny or cloudy days.

Table 6.2 In-situ survey summary

Content	Outline understanding
Surface moisture content	Evaluate the amount of water leakage.
Chipping investigation	Determine the corrosion grade of steel bars, wire setting for corrosion measurement.
Electrochemical corrosion measurement	Measure the half-cell potential and polarization resistance of steel bars.
Chloride ion analysis	Collect samples by the drill method at chipping positions. Analyze the chloride ion content in different depths.

6.2.3 Measurement contents

6.2.3.1 Surface moisture measurement

The surface moisture content of concrete was measured at intervals of 0.1m along the horizontal straight line of each front wall by using a high-frequency concrete moisture tester. The average value of surface moisture content of concrete was calculated on each side of a front wall. Surface moisture content of concrete was used as an index to evaluate indirectly the influence of water leakage or the influence of de-icing salts.

6.2.3.2 Chipping investigation

In order to determine steel corrosion grade in abutments affected by ASR and de-icing salts, twelve positions were selected to conduct the chipping investigation. These positions were chosen based on the results of surface moisture content of concrete and crack density survey, and it covered a wide range (from small to large of crack density, from high to low of the moisture content of concrete). The concrete cover was removed in small areas (about 0.2m x 0.2m) by concrete hammer and drill to observe steel corrosion grade and analyze the chloride ion content penetration. The steel corrosion grade was evaluated based on the guideline in "Survey of cracks in concrete, repair and reinforcement guidelines 2003: Japan Concrete Institute". The criteria to judge the steel corrosion grade were shown in **Table 2.2** of chapter 2.

6.2.3.3 Chloride ion analysis

Samples for chloride ion analysis were collected at chipping positions by drill method. These samples were taken every 20 mm from the surface upon 120 mm and stored in the zip-plastic bags before the chloride ion analysis. These samples were

analyzed by the potentiometric titration method (JCI-SC5) to obtain the distribution of chloride ion penetration. The chloride ion content on concrete surface was measured by portable X-ray fluorescence meter.

6.2.3.4 Corrosion measurement by electrochemical method

Half-cell potential and polarization resistance were measured by a portable corrosion meter (reference electrode: silver/saturated silver chloride electrode) to investigate the steel corrosion rate in the abutments. Before measurement, the concrete surface at measured positions was wetted by water spraying. The criteria of ASTM C876 was used to evaluate steel corrosion by half-cell potential and shown in **Table 5.3** of chapter 5. The AC impedance method was selected to measure the polarization resistance. The AC voltage (ACV) was applied at 10 mV, the frequencies were 10 Hz and 20 Hz. **Table 6.3** shows the criteria used for judging corrosion rate based on polarization resistance measurement, according to the CEB recommendation.

Table 6.3 Corrosion rate evaluation based on polarization resistance

Polarization resistance ($k\Omega.cm^2$)	Corrosion rate
Rp > 130	No corrosion
$130 \geq Rp > 52$	Low ~ Moderate
$52 \geq Rp > 26$	Moderate ~ High
$Rp \leq 26$	High

6.3 Results and discussion

6.3.1 Effect of water leakage

Figure 6.2 shows the average values of the surface moisture content of all abutments (up line side and down line side of each wall) and these values range from 5% to 9%. In the previous studies (*Ibata et al. 2014, Kubo et al. 2015*), it was reported that the abutment of around 4% of the surface moisture content of concrete was not significantly influenced by water leakage and de-icing salts. In this study, the influence of de-icing salts is considered relatively small when the surface moisture content of concrete remains approximately 4%. On the other hand, the influence of de-icing salts is relatively larger in the case of exceeding 6% of the surface moisture content of concrete (*Kubo et al. 2015, Ibata et al. 2014*).
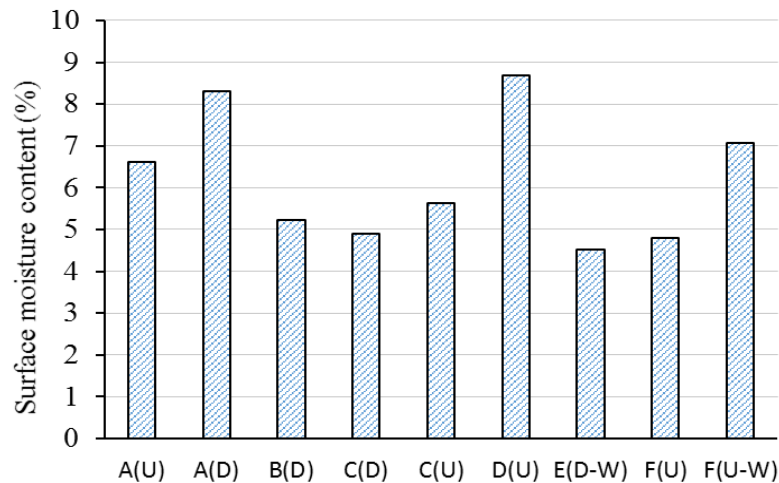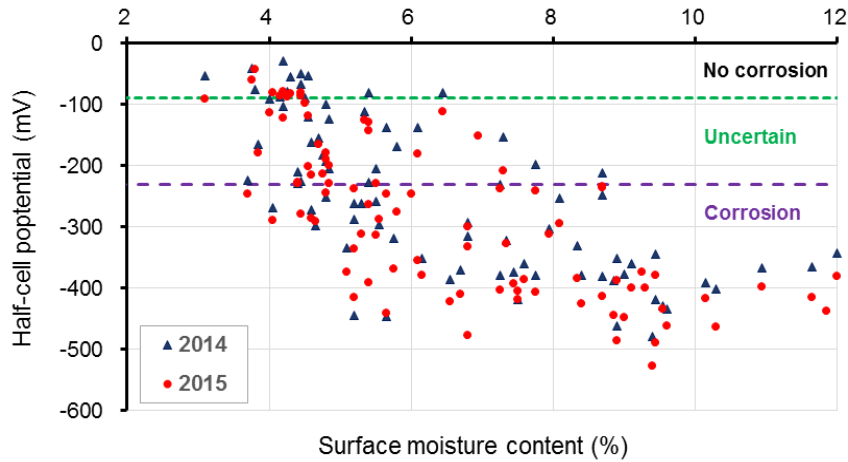
Figure 6.2 Surface moisture content of all abutments

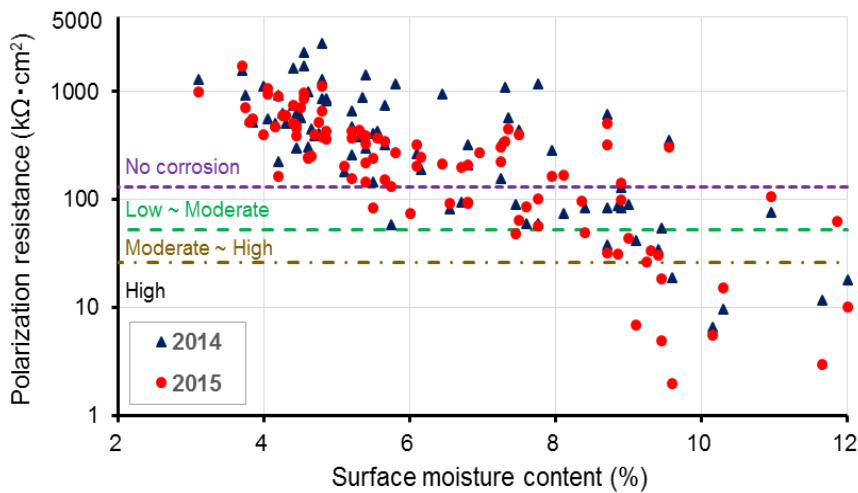## 6.3.2 Influence of moisture content on corrosion

Figure 6.3 shows the relationship between half-cell potential/ polarization resistance and surface moisture content of concrete. The surface moisture values were calculated by the average value of same measuring sections (1m x 1m) in 2014 and 2015, respectively.

Although the results showed some variations, the abutment of higher surface moisture content had the lower half-cell potential values or higher risk of steel corrosion. Additionally, when the surface moisture content of concrete exceeded 8%, most of the half-cell potential values were plotted in the corrosion zone. On the other hand, many values were plotted in the no corrosion zone when half-cell potential value was lower than 4%. The high value of surface moisture content indicated a significant effect of water leakage including de-icing salts. Thus, the steel corrosion risk may increase due to the high moisture content of concrete.

The similar tendency was also found in the relationship between surface moisture content and polarization resistance. When surface moisture content is higher, polarization resistance attained a lower value that showed the larger of steel corrosion rate. When the surface moisture content of concrete exceeded 6%, polarization resistance value was significantly decreased and most of polarization resistance values were plotted in the steel corrosion zone.

(a) Surface moisture content of concrete and half-cell potential relationship

(b) Surface moisture content of concrete and polarization resistance relationship

Figure 6.3 Surface moisture content and corrosion rate relationship

6.3.3 Influence of de-icing salts on corrosion (surface chloride ion content)

Figure 6.4 (a) and **(b)** show the relationship between half-cell potential or polarization resistance and surface chloride ion content, respectively. Although the values show some variations in the half-cell potential, values of half-cell potential tend to decrease in accordance with the increase of the surface chloride content. It is considered that the areas with high chloride ion content on the concrete surface have a large penetration of chloride ion into concrete and steel bars in the concrete becomes to be corroded easily.

In the polarization resistance measurement, although the value showed some variations, the polarization resistance tended to decrease with the increase of the

surface moisture content. Both polarization resistance and half-cell potential values were plotted in no corrosion zone in only a few areas where the surface chloride content exceeded 20 kg/m^3. These values were obtained in the abutment C where the moisture content of concrete was low. In this abutment, steel corrosion could be suppressed due to the low moisture content of concrete.
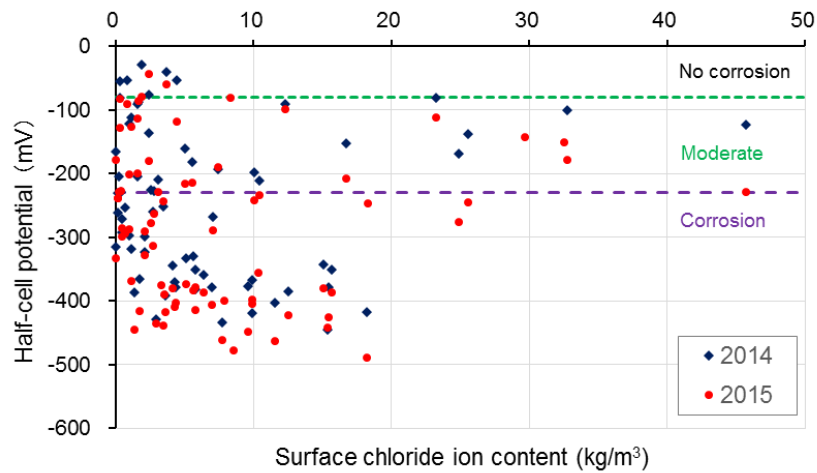
(a) Half-cell potential and surface chloride relationship
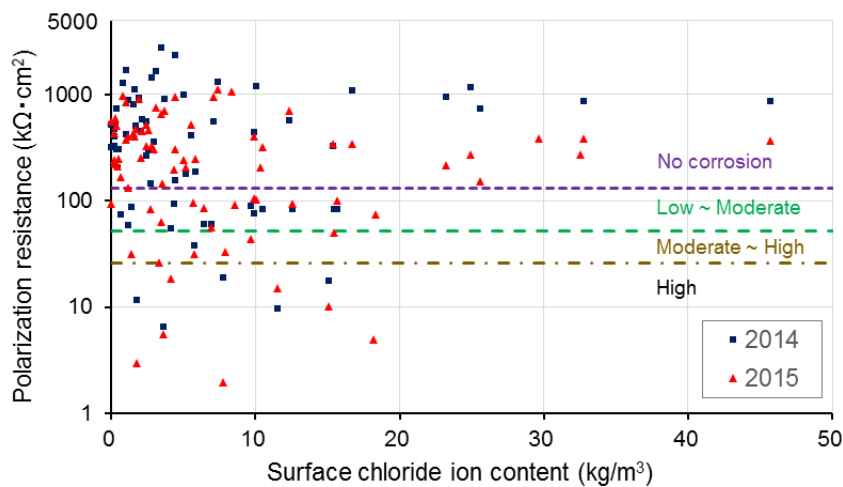
(b) Polarization resistance and surface chloride relationship

Figure 6.4 Surface chloride ion content and corrosion relationship

Although there were some variations, when the surface chloride ion content was larger than approximately 5 kg/m^3, many values of polarization resistance and half-cell potential were plotted on the corrosion zone. It indicated that the larger surface chloride ion corresponded to the possibility of higher corrosion rate. This value (5kg/m^3) of surface chloride ion was used as an index to evaluate the steel corrosion.

6.3.4 Classification and verification of steel corrosion

6.3.4.1 Classification of steel corrosion risk

From the above discussion, the surface moisture content of concrete is considered to correspond to the degree of water leakage and surface chloride ion content correlates to the degree of de-icing salt supply. However, the paths of water leakage in in-situ structures may change greatly during the service periods. Thereby, the degree of water leakage in the present time of measurement can differ with the degree of the leakage in the past time. On the other hand, the chloride ion content approximately corresponds to the degree of de-icing salt supply even if the supply of water leakage becomes small at the present and the accumulation of de-icing salt supply is large. Therefore, the degree of de-icing salt supply can be evaluated from the chloride ion content of concrete surface.

Figure 6.5 shows the relationship between surface moisture content (average value of each measured point of 2 years) and surface chloride ion content of concrete. Surface chloride ion content tended to increase with the increase of surface moisture content, although the variation was large. There were some areas where the surface moisture content was less than 6% and the chloride ion content of concrete surface was high. There was another exception where surface moisture content was high and chloride ion content was smaller than 5 kg/m^3. It can be explained that the remarkable change of the amount and paths of water leakage in the past and the present occurred in the above exception areas.

On the other hand, when both values of surface moisture and surface chloride ion contents were large, the degree of chloride penetration and water leakage were large. Thus, the possibility of the corrosion risk was relatively high. Conversely, corrosion risk was considered small when both values were small. Thus, the evaluation of corrosion risk can be examined based on the relationship between surface moisture content and surface chloride ion content in in-situ structures. From the results mentioned in sections 6.3.2 and 6.3.3, the threshold values of surface moisture and surface chloride ion contents were set at 6 % and 5 kg/m^3 for the evaluation, respectively. Corrosion risks are classified as L, MW, MC, H and the classification of corrosion risk is shown in **Figure 6.5**. Additionally, the number of measured areas corresponds to the corrosion risk classification is shown in **Table 6.4**.
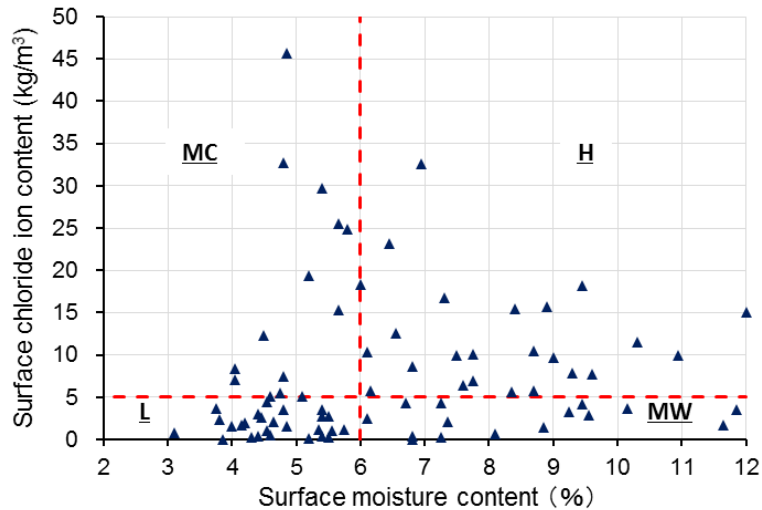
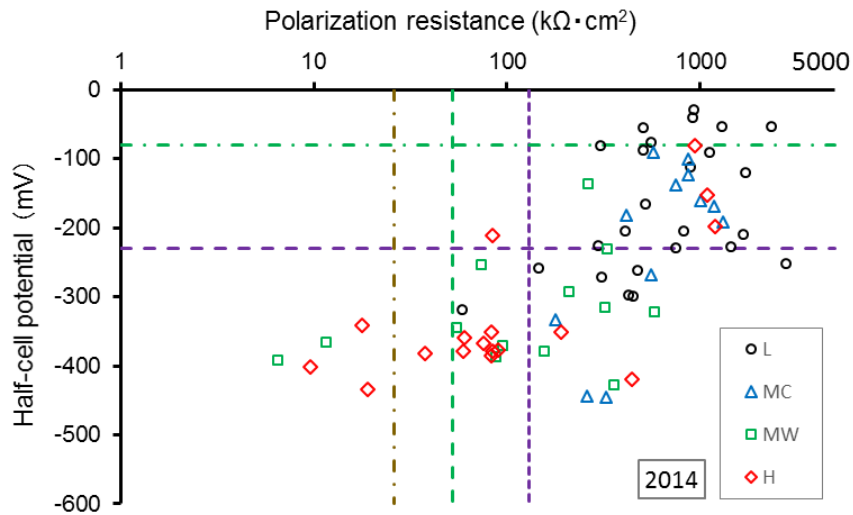**Figure 6.5** Corrosion risk classification based on surface moisture and surface chloride ion contents

Table 6.4 Corrosion risk classification

Risk	Surface moisture	Surface chloride ion	2014	2015	Total
L	< 6%	< 5kg/m^3	25	26	51
MW	≥ 6%	< 5kg/m^3	13	15	28
MC	< 6%	≥ 5kg/m^3	12	14	26
H	≥ 6%	≥ 5kg/m^3	17	24	41

6.3.4.2 Verification of the corrosion risk based on steel corrosion rate

In order to verify the evaluation of corrosion risk, the relationship between half-cell potential/polarization resistance and corrosion risk was discussed. This relationship for each measured year corresponding to the classification of corrosion risk is shown in **Figure 6.6**. The number of occurrences and the percentage for each corrosion rate corresponding to the corrosion risk are shown in **Figure 6.7**.

In corrosion risk L, the corrosion rate in most areas showed no corrosion zone and corrosion rate in a few areas showed low to moderate zones in both 2014 and 2015. On the other hand, in corrosion risk H, the corrosion in most areas (more than 70%) showed in the corrosion zone. Hence, the higher corrosion rate is likely to occur in the high corrosion risk H, whereas the low and/or no corrosion rate are likely to occur in the low corrosion risk L.

(a) Corrosion measurements in 2014
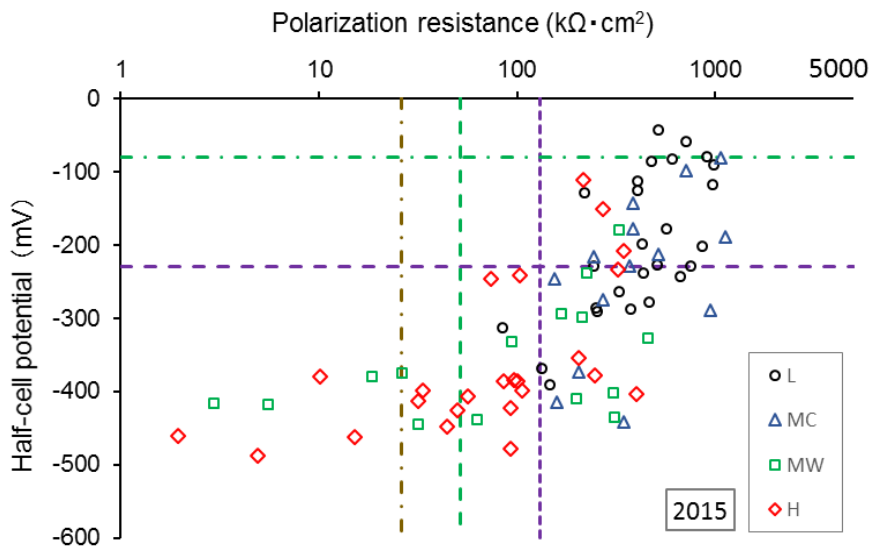
(b) Corrosion measurements in 2015

Figure 6.6 Corrosion risk classification based on electrochemical measurement

In the corrosion risk MC, chloride ion content of concrete surface was high and moisture content was relatively low, the corrosion rate in all areas showed in no corrosion zone in both years. In the corrosion risk MW, surface chloride ion was low and moisture content was relatively high, the corrosion rate of around a half of the area (more than 40%) showed in the corrosion zone. In other words, the high moisture content indicated that the influence of water leakage was large and the moisture content of concrete near the steel bar was kept in high moisture content. Therefore, it resulted in the occurrence and the progress of steel corrosion in the corrosion risk MW.

On the contrary, in corrosion risk MC, the corrosion rate could be suppressed due to lower moisture content of concrete near the steel bars although high content of chloride ion occurred.
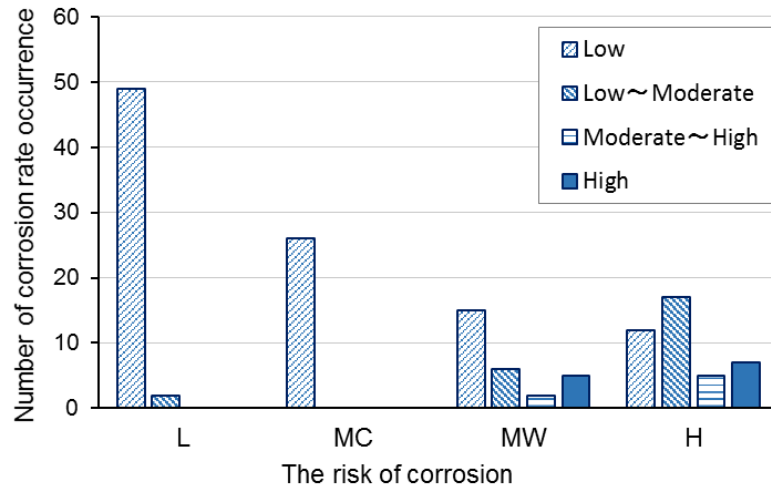
(a) Corrosion risk classification based on the number of corrosion rate occurrence
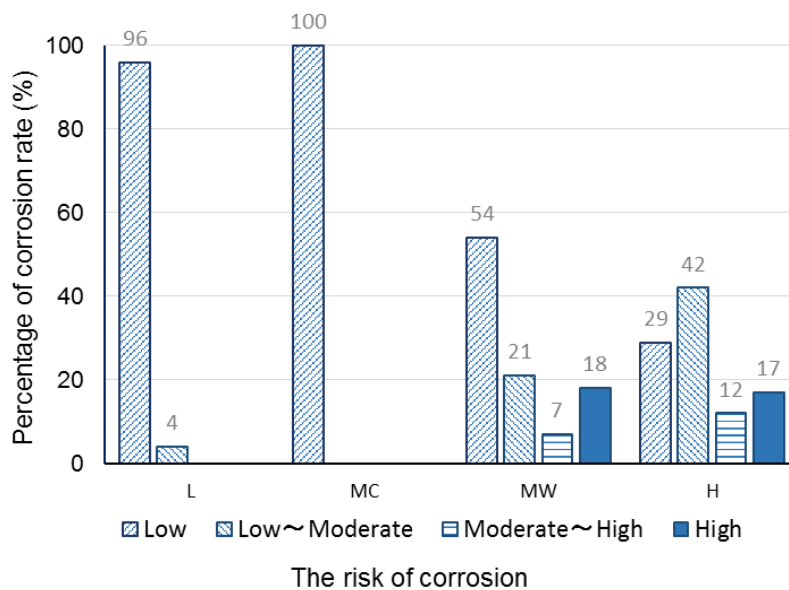
(b) Corrosion risk classification based on the percentage of corrosion rate occurrence

Figure 6.7 Verification of corrosion rate corresponds to the risk of corrosion

The relationship between corrosion risk and corrosion grade of steel bar that was judged from the visual observation of steel bar after chipping concrete was investigated. In addition, the chloride ion content at the concrete cover depth (from 80 to 100mm) was shown, in order to verify the evaluation of corrosion risk. The other corrosion risk was evaluated from chloride ion content at concrete cover depth.

Corrosion risk evaluated from surface moisture and surface chloride ion content values was compared to the corrosion risk (L', MC', MW', H') that evaluated from surface moisture and chloride ion content at concrete cover depth. The information to verify the evaluation of corrosion risk is shown in **Table 6.5**.

Table 6.5 Verification of corrosion risk

Abutment	Corrosion risk (Cl- on the surface)	Corrosion grade	Chloride ion content at cover depth (kg/m^3)	Corrosion risk (Cl- at cover depth)	Evaluation
A(U)	MW	I	0.63	MW'	O
A(D)	H	I	1.60	MW'	Δ
B(D)	MC	II	0.86	L'	O
C(D)	L	II	1.67	L'	O
C(U)	MC	III	2.03	MC'	O
D1(D)	L	I	0.34	L'	O
D2(D)	MW	II	3.38	H'	O
D3(D)	MC	I	0.25	L'	X
D4(D)	H	II	0.63	MW'	O
E(D-W)	L	I	0.16	L'	O
E(U)	L	I	0.32	L'	O
F(U-W)	MW	I	0.29	MW'	O

O: True X: False Δ: unclear

In the corrosion risk MC, the corrosion rate was negligible (no corrosion). However, corrosion grade of steel bar was grade II or III in 2 of 3 measured positions. It is considered that the corrosion progress in the past was large and the current progress is suppressed due to lower moisture content caused by the change of water leakage degree.

In the corrosion risk MW, the corrosion rate of around a half of measured areas was equal or lower than "low to moderate". However, it is noticeable that corrosion grade II occurred in the front wall of abutment D. Many cracks occurred in concrete structures affected by ASR expansion. Accordingly, these cracks can make water and chloride ion easy to penetrate into the concrete. Thus, it is considered that water and

oxygen supply near steel bar increase with the increase of crack density. This results in the promotion of occurrence of steel corrosion and corrosion rate in concrete even in low chloride ion content. Although the current corrosion rate in the corrosion risk MW is small, it is noted that the potential of steel corrosion may be high.

On the wing wall of corrosion risk MW, it showed the corrosion grade I. The influence of de-icing salt on steel corrosion in concrete may differ between the front wall and the wing wall. The de-icing salt supply on wing walls is relatively smaller than that on front walls, and wing walls are directly affected by rainwater and the surface chloride ion is washed away due to rainwater. From the results of chipping investigations on two wing walls, it may be recognized that both corrosion grade and the chloride ion content at cover depth are small. This difference between front wall and wing wall should be cleared in the future.

In the corrosion risk L, the corrosion rate at almost of measured areas was low. All abutment showed corrosion grade I and the chloride ion content was lower than 0.5 kg/m^3 except for abutment C(D). The evaluation of the corrosion risk corresponded to the result of corrosion grade and chloride ion content at cover depth.

In the corrosion risk H, the corrosion rate around a half of measured areas was larger than "low to moderate". On the other hand, at 30% of measured areas, the corrosion rate was low. In **Table 6.5**, there were only 2 abutments of corrosion risk H (Abutment A(D) and D4(D)). Abutment A(D) showed corrosion grade I but the chloride ion was 1.6 kg/m^3. Abutment D4(D) showed corrosion grade II, but chloride ion content was 0.63 kg/m^3. Both abutments had the possibility of steel corrosion. Thus, the evaluation of corrosion risk based on surface moisture content and chloride ion content of concrete surface has high validity.

Generally, the degree of water leakage varies considerably because it depends on some factors such as the condition of joint and drainage device, the addition of the bridge preventing device, etc. The influence of de-icing salts on this structure may be changed largely in the past and present. Therefore, it is noted that the evaluation of corrosion risk based on only surface moisture content and surface chloride ion contents entails some uncertainty. However, it was considered that surface chloride ion content reflected the situation in the past to some extent and it provided the wealth of information in the corrosion risk evaluation. In this study, the surface moisture content was also used to evaluate the corrosion risk with the surface

chloride ion. Hence, the surface moisture content is useful to recognize the degree of water leakage in the present. It is concluded that this evaluation method of corrosion risk is effective when concrete structures are affected by ASR and de-icing salts.

6.4 Conclusions

(1) From electrochemical corrosion measurement, half-cell potential and polarization resistance tended to decrease with the increase of the surface moisture content. On the surface chloride ion content measurement, the same tendency was observed.

(2) The evaluation of corrosion risk can be determined based on the relationship between surface moisture content and surface chloride ion content in the in-situ structures.

(3) The influence of de-icing salts on concrete structures may be changed largely in the past and present. Therefore, it is noted that the evaluation of corrosion risk based on only surface moisture content and surface chloride ion contents entails some uncertainty.

(4) The surface moisture content was also used to evaluate corrosion risk with the chloride ion content of concrete surface. It is considered that surface moisture content is useful to recognize the degree of water leakage in the present. This evaluation method of corrosion risk is effective when concrete structures are affected by ASR and de-icing salts.

References

Fujimura Yuki, Habuchi Takashi, Torii Kazuyuki, *Steel corrosion behavior of concrete structures influenced by ASR and sea water*, Concrete Engineering Annual Proceedings, Vol.31, No.1, pp. 1285-1290. 2009 (in Japanese)

Honjo Kiyoshi, Nakano Masahiro, Fujiwara Norio, Kuzume Kazuhiro, Maki Hironori, *Detailed investigation of steel bar in RC slab degraded by de-icing salts*, Repairing of the concrete structure, Reinforcement, Upgrade paper report, Vol.10 , pp. 51-56, October. 2010. (in Japanese)

Ibata Shiho, Yano Toshiki, Kubo Yoshimori, Hashizume Yasunori, *Estimate the influence of de-icing salts based on the monitoring results of structures affected by de-icing salts spraying*, Annual Concrete Engineering Proceedings, Vol.1, No.36, pp. 934 - 939, July. 2014. (in Japanese)

Kawamura, M., Shinghal, D., and Tsuji, Y., *Effects of ASR on corrosion of reinforcement in concrete under saline environment*, Proceedings of East Asia Alkali-Aggregate Reaction, Tottori, pp. 179-190, 1997.

Kikuchi Sota, Kubo Yoshimori, Kimura Hisato, Yanai Yoshihiro, Momiyama Yoshiyuki, *A Study of Surface Chloride Ion and Chloride Penetration Distribution of Concrete Structure under Sprinkling with De-icing Salts*, Upgrade Paper Report, Volume 16, October. 2016. (in Japanese)

Kubo Yoshimori, Yano Toshiki, Kikuchi Toru, Ishikawa Yuichi, *Study on the corrosion of reinforcing bars in ASR deteriorated structures affected by de-icing salts*, Repairing of Concrete Structures, Upgrade paper report, Vol.15, October. 2015. (in Japanese)

Yokoyama Kazuaki, Honjo Kiyoshi, Kuzume Katsuhiro, Fujiwara Norio, *Study on the elucidation of deterioration mechanism accompanied with the steel corrosion of RC deck on the road bridge*, Concrete Engineering Annual Proceedings, Vol.30, No.3, pp. 1687-1692, July. 2008. (in Japanese).

CHAPTER 7 CONCLUSIONS

Currently, many concrete structures have been deteriorating due to ASR and de-icing salts spraying. This study was performed to assess the current stage of concrete members and the effectiveness of countermeasures based on in-situ surveys and experiments. The main results of this study are concluded and summarized as follows.

The result of the steel corrosion occurrence in the ASR-deteriorated bridge abutments affected by de-icing salts indicates the larger of crack density and surface moisture content tend to increase chloride penetration, thus, the higher corrosion grade can be observed. Additionally, the progressing of cracks caused by ASR can promote much water, oxygen and chloride ion penetration. Hence, the steel bars can be corroded easier. Therefore, the countermeasures such as surface coatings, surface impregnation or even patching should be planned to prevent deteriorated factors such as water and chloride ion penetration.

The reinforced concrete specimens were conducted to evaluate the combined deterioration in comparison with single deterioration caused by ASR or chloride attack on the bridge deck slabs. In this experiment, the cracks occurred along the steel bars direction in the combined deterioration specimen were larger and more conspicuous than specimen affected by only ASR, and the cracks caused by only chloride attack possibility occurred later than specimens affected by ASR. From the ultrasonic propagation speed measurement, it can be confirmed that the horizontal cracks occurred in specimens due to ASR expansion. The FWD method was conducted to measure the center displacement of specimens and the result showed that the displacement of ASR or combined deterioration specimens was larger than that value of sound concrete specimen. Therefore, the FWD method can be applied to recognize whether or not degradation has occurred in concrete structures such as bridge deck slabs.

The patching materials method is suggested as a proper countermeasure for concrete structures deteriorated by ASR in the acceleration and deterioration stages. Thus, in this study, the experiment was conducted to assess the influence of ASR expansion on the patching materials and the interface between patching materials and ASR-deteriorated concrete. The result of this experiment showed that the patching material had contributed to restraining the expansion of the substrate concrete when the expansive strain was smaller than approximately 500×10^{-6}. However, it had a little effect on the confining expansion in the case of larger expansion. The adhesion test showed that all adhesive strength values were lower than 1.5 N/mm^2 and its value reduced slightly with the increase of expansion. Since all failure surfaces occurred in the substrate concrete, it is considered that the mechanical properties of patching material might be less affected by the expansion than that of substrate concrete. From the fluorescent observation and EPMA images, the integrity of the interface between substrate concrete and patching material was maintained even high level of expansion occurred, and it contributed to prevent the penetration of chloride ions.

Countermeasures for concrete structures deteriorated due to ASR with/without patching and combined with surface coating or crack injection methods had been performed. However, besides the effect of ASR, the concrete bridge structure is also affected by the water leakage that included a high concentration of chloride ion due to de-icing salts spraying. Therefore, the in-situ survey had been conducted to assess the effectiveness of these countermeasures when wheel guard structures were deteriorated due to combined deterioration of ASR and de-icing salts. The result of this in-situ survey showed that the cracks occurred on the surface of concrete, although the countermeasures had been applied and crack width in the patching material part was smaller than other parts that only applied the surface coating treatment. The steel corrosion had proceeded, although the content of chloride ion penetration was small and steel corrosion the patching material part was smaller than the surface coating treatment parts. In addition, the moisture content in the interior was relatively high while its content near the surface was lower due to the removal of the coating film. Hence, it is considered that the higher moisture content in concrete is favourable for the steel corrosion. This distribution of moisture content could affect remarkably due to the moisture supply from the backside of these structures.

The countermeasures of patching materials combined with surface coating or crack injection are considered to have a significant efficiency in repair and

maintenance of concrete structures deteriorated by ASR. In addition, these methods also prevented partly the penetration of chloride, moisture, and oxygen into concrete, thereby reducing the ability and the risk of steel corrosion caused by de-icing salts. However, the influence of water leakage from the backside of structures is considerable in the steel corrosion occurrence. Further studies are needed to evaluate the impact of this factor, hence, the proper countermeasures can be taken to prevent or minimize the combined deterioration of ASR and de-icing salts.

In this study, other in-situ measurements were conducted to evaluate the steel corrosion in ASR-deteriorated concrete affected by de-icing salts spraying. The corrosion measurement showed that the corrosion rate (half-cell potential and polarization resistance) tended to increase when the surface moisture and surface chloride ion contents increased. Furthermore, the evaluation of corrosion risk can be determined based on the relationship between surface moisture content and the chloride ion content of concrete surface in ASR-deteriorated concrete affected by de-icing salts. However, it entails some uncertainty due to the influence of de-icing salts on the structure may be changed largely in the past and present.

To summarize, the main results of this study have assessed the current stage of concrete members and the effectiveness of the countermeasures for some structures, which have deteriorated due to ASR and de-icing salts, of the road bridges located in the Hokuriku region. However, the scope of research is still limited due to few structures and specimens were conducted, and the mechanism of combined deterioration was complicated regarding specific concrete structures as well as the effect of many other factors. Therefore, further research will be necessary to perform in the future to have a deeper understanding of the combined deterioration mechanism and propose the proper countermeasures apply to ASR-deteriorated concrete structures affected by de-icing salts.